



Lawrence Berkeley Laboratory

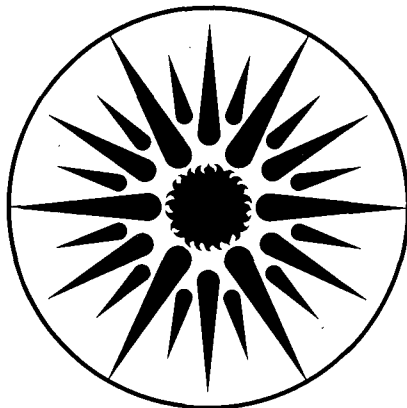
UNIVERSITY OF CALIFORNIA

ENERGY & ENVIRONMENT DIVISION

Exploratory Technology Research Program for Electrochemical Energy Storage: Annual Report for 1994

K. Kinoshita, Editor

September 1995



ENERGY & ENVIRONMENT
DIVISION

REFERENCE COPY
Does Not
Circulate

Bldg. 50 Library.

LBL-37665

Copy 1

DISCLAIMER

This document was prepared as an account of work sponsored by the United States Government. While this document is believed to contain correct information, neither the United States Government nor any agency thereof, nor the Regents of the University of California, nor any of their employees, makes any warranty, express or implied, or assumes any legal responsibility for the accuracy, completeness, or usefulness of any information, apparatus, product, or process disclosed, or represents that its use would not infringe privately owned rights. Reference herein to any specific commercial product, process, or service by its trade name, trademark, manufacturer, or otherwise, does not necessarily constitute or imply its endorsement, recommendation, or favoring by the United States Government or any agency thereof, or the Regents of the University of California. The views and opinions of authors expressed herein do not necessarily state or reflect those of the United States Government or any agency thereof or the Regents of the University of California.

LBL-37665

**EXPLORATORY TECHNOLOGY
RESEARCH PROGRAM
FOR
ELECTROCHEMICAL ENERGY STORAGE**

**ANNUAL REPORT
FOR 1994**

Energy & Environment Division
Lawrence Berkeley National Laboratory
University of California
Berkeley, California 94720

Edited by Kim Kinoshita, Technical Manager

September 1995

This work was supported by the Assistant Secretary for Energy Efficiency and Renewable Energy, Office of Transportation Technologies, Electric & Hybrid Propulsion Division of the U.S. Department of Energy under Contract No. DE-AC03-76SF00098.

CONTENTS

EXECUTIVE SUMMARY	v
I. INTRODUCTION	1
II. EXPLORATORY RESEARCH	
A. ADVANCED ZINC/NICKEL OXIDE CELLS	
Zn/NiOOH Cell Studies.....	2
B. SOLID-STATE CELLS	
Electrochemical Properties of Solid-State Sodium/Polymer Cells	4
Development of a Thin-Film Rechargeable Lithium Battery for Electric Vehicles	7
Room Temperature Sodium/Iron Chloride Battery Development.....	10
Na/SRPE Electric Vehicle Batteries	11
III. APPLIED SCIENCE RESEARCH	
A. ELECTRODE CHARACTERIZATION	
Surface Morphology of Metals in Electrodeposition/Carbon Electrochemistry.....	13
Battery Materials: Structure and Characterization.....	16
Fabrication and Testing of Carbon Electrodes as Lithium Intercalation Anodes.....	18
B. CORROSION PROCESSES IN HIGH-SPECIFIC-ENERGY CELLS	
Improved Container Electrode Coating for Na/S Battery Systems.....	21
C. COMPONENTS FOR AMBIENT-TEMPERATURE NONAQUEOUS CELLS	
Novel Lithium/Polymer-Electrolyte/Sulfur Cells.....	22
<i>In Situ</i> Spectroscopic Applications to the Study of Rechargeable Lithium Batteries.....	23
Polymer Electrolytes for Ambient Temperature Traction Batteries: Molecular Level Modeling for Conductivity Optimization.....	26
The Performance of New Materials for Polymer Electrolyte Batteries	28
Novel Polymer Electrolytes for Rechargeable Lithium Batteries.....	29
Novel Solid Polymer Electrolytes for Advanced Secondary Batteries	30
Sol-Gel Electrolytes in Lithium Batteries.....	32
New Cathode Materials.....	33
Development of High Energy Density Cathodes for Sodium/Polymer Cells.....	36
Synchrotron Radiation Studies of Structure, Rechargeability and Corrosion in Li/SPE/FeS ₂ Battery System	38
D. CROSS-CUTTING RESEARCH	
Analysis and Simulation of Electrochemical Systems.....	39
Heat Transport and Thermal Management in Advanced Batteries.....	41
Electrode Surface Layers	42
Electrode Kinetics and Electrocatalysis	43
Poisoning of Fuel Cell Electrocatalyst Surfaces: NMR Spectroscopic Studies	45
Effect of Electrocatalyst and Electrolyte Composition on Methanol/Air Fuel Cell Performance	47
IV. AIR SYSTEMS RESEARCH	
A. METAL/AIR CELL RESEARCH	
Novel Concepts for Oxygen Electrodes in Secondary Metal-Air Batteries	49
B. FUEL CELL RESEARCH	
Fuel Cells for Renewable Applications.....	51

EXECUTIVE SUMMARY

The U.S. Department of Energy's Office of Propulsion Systems provides support for an Electrochemical Energy Storage Program, that includes research and development (R&D) on advanced rechargeable batteries and fuel cells. A major goal of this program is to develop electrochemical power sources suitable for application in electric vehicles (EVs). The program centers on advanced systems that offer the potential for high performance and low life-cycle costs, both of which are necessary to permit significant penetration into commercial markets.

The DOE Electrochemical Energy Storage Program is divided into two projects: the Electric Vehicle Advanced Battery Systems (EVABS) Development Program and the Exploratory Technology Research (ETR) Program. The EVABS Program management responsibility has been assigned to Sandia National Laboratory (SNL), and the Lawrence Berkeley National Laboratory* (LBNL) is responsible for management of the ETR Program. The EVABS and ETR Programs include an integrated matrix of R&D efforts designed to advance progress on selected candidate electrochemical systems. The United States Advanced Battery Consortium (USABC), a tripartite undertaking between DOE, the U.S. automobile manufacturers and the Electric Power Research Institute (EPRI), was formed in 1991 to accelerate the development of advanced batteries for consumer EVs. The role of the ETR Program is to perform supporting research on the advanced battery systems under development by the USABC and EVABS Program, and to evaluate new systems with potentially superior performance, durability and/or cost characteristics. The specific goal of the ETR Program is to identify the most promising electrochemical technologies and transfer them to the USABC, the battery industry and/or the EVABS Program for further development and scale-up. This report summarizes the research, financial and management activities relevant to the ETR Program in CY 1994. This is a continuing program, and reports for prior years have been published; they are listed at the end of this Executive Summary.

The general R&D areas addressed by the program include identification of new electrochemical couples for advanced batteries, determination of technical feasibility of the new couples, improvements in battery components and materials, establishment of engineering principles applicable to electrochemical energy storage and conversion, and the development of air-system (fuel cell, metal/air) technology for transportation applications. Major emphasis is given to applied research which will lead to superior performance and lower life-cycle costs.

The ETR Program is divided into three major program elements: Exploratory Research, Applied Science Research, and Air Systems Research. Highlights of each program element are summarized according to the appropriate battery system or electrochemical research area.

* Participants in the ETR Program include the following LBL scientists: E. Cairns, J. Evans, K. Kinoshita, F. McLarnon and J. Newman of the Energy and Environment Division; and L. DeJonghe, P. Ross and C. Tobias of the Materials Science Division.

EXPLORATORY RESEARCH

The objectives of this program element are to identify, evaluate and initiate development of new electrochemical couples with the potential to meet or exceed advanced battery and electrochemical performance goals. Research was conducted on new versions of the Zn/NiOOH cell, novel Na cells that contain polymer or molten-salt electrolytes, and an all-solid state Li/Mn oxide cell. Each of these cells is considered to be an attractive candidate for EV applications, and should provide high performance at ambient or near-ambient temperatures. A Zn/NiOOH battery would exhibit higher performance and lower costs, compared to the MH/NiOOH battery; and a Na/polymer battery would lower cost, compared to a Li/polymer battery.

- From cycling tests in 1.35-Ah Zn/KOH/NiOOH cells, LBNL concluded that the 4.5 M KOH – 1.8 M KF – 1.8 M K₂CO₃ electrolyte is considered to be near-optimal, and is being evaluated in larger cells under sponsorship of the DOE Laboratory Technology Transfer Program.
- LBNL developed a new method of measuring transference numbers in polymer electrolytes using straightforward electrochemical techniques, and a rigorous theoretical treatment of the results. The Na-ion transference number in the PEO-NaCF₃SO₃ system was found to decrease with increasing salt concentration.
- Oak Ridge National Laboratory (ORNL) has fabricated all-solid-state Li/Li_xMn₂O₄ cells that exhibited good performance with less than 0.05% capacity loss per cycle after hundreds of cycles when discharged at 20–40 mA/cm² to 2–3 volts (~C/1). Efforts are underway to fabricate thicker Mn oxide electrodes to improve the specific energy of the cell.
- Georgia Institute of Technology has achieved sodium plating and stripping with 94% coulombic efficiency at current densities to 25 mA/cm² in an electrolyte that contains methyl-ethyl imidazolium chloride/aluminum chloride buffered with sodium chloride.
- PolyPlus Battery Co. achieved 20 cycles at 100 Wh/kg with Na/organosulfur (Na/SRPE) cells at 90°C. The Na electrode was prone to shorting during the charge cycles, and this charging instability is attributed to the difficulty in maintaining a contamination-free Na/polyethylene oxide (PEO) interface.

APPLIED SCIENCE RESEARCH

The objectives of this program element are to provide and establish scientific and engineering principles applicable to batteries and electrochemical systems; and to identify, characterize and improve materials and components for use in batteries and electrochemical systems. Projects in this element provide research that supports a wide range of battery systems — alkaline, metal/air, flow, solid-electrolyte and nonaqueous. Other cross-cutting research efforts are directed at improving the

understanding of electrochemical engineering principles, minimizing corrosion of battery components, analyzing the surfaces of electrodes, and electrocatalysis.

Electrode Characterization studies are an important research element for the successful development of rechargeable electrodes for advanced secondary batteries. Efforts are underway to determine the role of surface morphology on mass transport which may affect the morphology of electrodeposits and to evaluate the performance of cells utilizing Li intercalation electrodes. Advanced spectroscopic techniques are utilized to investigate the chemical state of electrode materials during charge/discharge cycling.

- Analysis of published data by LBNL indicates that the intercalation of Li is lower with carbons that have a $d(002)$ spacing of about 0.345 nm, than with materials having higher or lower d -spacing.
- Brookhaven National Laboratory (BNL) has used extended X-ray absorption fine structure (EXAFS) and X-ray absorption near-edge spectroscopy (XANES) to study nickel oxide electrodes that were cycled in Zn/NiOOH cells. EXAFS showed no specific interaction of the zincate with $\text{Ni}(\text{OH})_2$. Ni EXAFS for a nickel oxide electrode (with sintered plaque) after cycling indicate that most of the sintered plaque has corroded to form $\beta\text{-Ni}(\text{OH})_2$.
- Lawrence Livermore National Laboratory (LLNL) observed that electrodes fabricated from various Lonza graphites yielded Li intercalation capacities that range from 320 to 365 mAh/g (equivalent to x in Li_xC_6 from 0.85 to 0.95), approaching the theoretical value of 372 mAh/g corresponding to LiC_6 . The graphite powders with particle diameter in the range of 6-44 μm showed no Li diffusion limitation to deintercalation at rates from $C/2$ to $C/60$.
- Studies at LBNL on the coalescence of electrolytic gas bubbles showed that the initial velocity of the interface joining two bubbles depends on the bubble size and surface tension but not on the electrolyte viscosity.

Corrosion Processes in High-Specific-Energy Cells are under investigation, and the aim is to develop low-cost container and current-collector materials for use in nonaqueous, alkali/sulfur and molten-salt cells.

- The Environmental Research Institute of Michigan (ERIM) has prepared TiN-coated Al containment materials, and two cells using these coatings produced by commercial reactive ion-plating have achieved over 300 cycles on accelerated charge/discharge cycles (at a rate of $\sim 2/\text{day}$) at Silent Power Ltd., Salt Lake City, UT.

Components for Ambient-Temperature Nonaqueous Cells, particularly metal/electrolyte combinations that improve the rechargeability of these cells, are under investigation.

- LBNL has initiated a new project to investigate the viability of Li/polymer electrolyte/sulfur cells for EV applications. Preliminary cycling tests of small cells indicate that the utilization of the sulfur electrode needs to be improved.

- Case Western Reserve University (CWRU) designed and constructed a versatile, variable temperature, electrochemical cell for conducting *in situ* attenuated total reflection-Fourier transform infrared spectroscopic (ATR-FTIR) experiments under reduced pressure. The results with Li/PEO(LiAsF₆) suggest that under the experimental conditions selected for these studies, and to the level of sensitivity of this technique, PEO(LiAsF₆) does not react with metallic Li.
- Northwestern University (NWU) has synthesized polymer electrolytes based on aluminosilicate-polyether hybrid electrolytes, (amorphous PEO)₂₅LiTf and (amorphous PEO)₃₈Li[Al(OSiEt₃)₄], which yielded 135 mAh/g active cathode material in Li/Li_xMn₂O₄ cells.
- NWU showed conclusively by molecular dynamics simulation that in polymer/salt electrolytes of the stoichiometry usually measured, there are very few free ions, and that the conductivity is fixed both by the segmental relaxation of the polymer host (the renewal time) and by the number of effectively free ions.
- CWRU successfully sulfonated a polybenzimidazole (PBI) to obtain 2.1 to 2.2 sulfonic acid groups per PBI unit.
- The University of Dayton has successfully prepared a novel liquid crystalline monomer, 4-[11-acryloylundecan-1yl)oxy]-4'-(4'-carboxybenzo-15-crown-5)biphenyl (ACB), by a four-step synthetic route. Studies are underway to prepare aligned, doped polymeric films with ACB that contain crown ethers which could have a fundamentally different mode of ion transport than those currently under investigation.
- Rutgers University identified alumina-containing formulations that showed improved thermodynamic stability. A formulation containing 14 mol% alumina had the highest ionic conductivity at 250°C – 4.7×10^{-6} S/cm.
- The State University of New York (Binghamton) has produced hexagonal Mo oxides by a hydrothermal method at 150-200°C which has a greater capacity for Li intercalation than the normal MoO₃ phase.
- SRI International cycled a Na/PEO₃NaTf/polyorganopolydisulfide (polyHTB) cell and achieved a cathode utilization of 164 mAh/g, with an energy density of 260 Wh/kg (C/10 rate) at 95°C.
- Southern University has built an electrochemical system for *in situ* EXAFS studies of Li/FeS₂ cells.

Cross-Cutting Research is carried out to develop mathematical models of electrochemical systems and to address fundamental problems in electrocatalysis and current-density distribution; solutions will lead to improved electrode structures and performance in batteries and fuel cells.

- LBNL has developed the following models: (i) a model which describes the impedance response of a rechargeable Li battery at open circuit; (ii) the metal hydride/NiOOH battery which has been modeled in both one-dimensional and full two-dimensional form; and (iii) a model which predicts the behavior of electrochemical double layer capacitors during operating conditions. The effect of side reactions, which have a pronounced impact on the cycling behavior, was included in the capacitor model.

- Mathematical modeling of heat transport in Li/polymer batteries at LBNL revealed that the major resistance to heat transport in a Li/polymer-electrolyte battery is the polymer electrolyte.
- A newly developed technique at LBNL for low-energy ion implantation known as Metal Plasma Immersion Ion Implantation (MPIII) was used to implant Au, Pb, Ta, Ti, W and Ti₄O₇ in nickel oxide electrodes. Tests showed that the overpotential for O₂ evolution at the surface of a Ti₄O₇-implanted Ni electrode is increased by 50–105 mV, compared with electrodes implanted with other elements.
- LBNL has found that the property of Ru atoms to nucleate oxygen-containing species at low potentials produced a strong enhancement in the catalytic activity of sputter-cleaned Pt-Ru alloy electrodes compared to pure Pt, thereby supporting the concept of the bifunctional character of the oxidation process of these alloys.
- LBNL has designed and fabricated fuel cells with 20-cm² electrodes. Studies of the direct electrochemical oxidation of methanol and hydrocarbon fuels in liquid alkali carbonate and solid polymer electrolytes (SPE), respectively, are underway.

AIR SYSTEMS RESEARCH

The objectives of this program element are to identify, characterize and improve materials for air electrodes; and to identify, evaluate and initiate development of metal/air battery systems and fuel-cell technology for transportation applications.

Metal/Air Cell Research projects address bifunctional air electrodes, that are needed for electrically rechargeable metal/air (Zn/air, Fe/air) cells; and novel alkaline Zn electrode structures, that could be used in either electrically recharged or mechanically recharged cell configurations.

- Eltech Research Corporation achieved 145 cycles with electrodes containing graphitized carbon black (Monarch 120) for the support and La_{0.6}Ca_{0.4}CoO₃ as electrocatalysts in 35 wt% KOH at room temperature.

Fuel Cell Research at Los Alamos National Laboratory (LANL) includes research in several areas of electrochemistry, theoretical studies, fuel-cell testing, fuel processing, and membrane characterization. Major achievements of the fuel-cell program during 1994 are listed below:

- LANL obtained for the first time, limiting currents significantly in excess of 2 A/cm² in H₂/air proton-exchange membrane (PEM) fuel cells under ordinary operating conditions.
- LANL determined by nuclear magnetic resonance (NMR) that the diffusion coefficient of methanol in Nafion membranes is only a factor of 2–3 smaller than in aqueous solutions, and this is an important factor contributing to the sizable cross-over rates observed.
- LANL has experimentally established that with a cathode of low Pt loading (0.4 mg/cm²), the cathode loss caused by methanol cross-over could easily reach 100 mV.

MANAGEMENT ACTIVITIES

During 1994, LBNL managed 17 subcontracts and conducted a vigorous research program in electrochemical energy storage. LBNL staff members attended project review meetings, made site visits to subcontractors, and participated in technical management of various ETR projects. LBNL staff members also participated in the following reviews, meetings, and workshops:

- 29th IECEC Planning Meeting, Monterey, CA, January 31, 1994
- EPRI/Georgia Tech Battery Review Meeting, Atlanta, GA, March 8, 1994
- Conference on "Additive for Supporting Electrolyte Solutions for Electrochemical Power Supplied," Sandia National Laboratories, Albuquerque, NM, March 23, 1994.
- DOE Direct Methanol Fuel Cell Review Meeting, Baltimore, MD, April 26-27, 1994
- 7th International Lithium Battery Meeting, Boston, MA, May 15-20, 1994
- 185th Meeting of the Electrochemical Society, San Francisco, CA, May 22-27, 1994
- 4th International Symposium on Polymer Electrolytes, Newport, RI, June 20-23, 1994
- IAPG Chemical Working Group Meeting, Washington, D.C., June 28-30, 1994
- Vice President's Automotive Technology Symposium #2, Washington, D.C., July 27, 1994
- 29th IECEC, Monterey, CA, August 7-11, 1994
- PEM Fuel Cells for Transportation Meeting, Washington, D.C., September 20, 1994
- 186th Meeting of the Electrochemical Society, Miami, FL, October 9-14, 1994
- Annual Automotive Technology Development Contractors' Coordination Meeting, Dearborn, MI, October 24-27, 1994.
- Annual AIChE Meeting, San Francisco, CA November 14-17, 1994
- 1994 Fuel Cell Seminar, San Diego CA, November 28 - December 1, 1994
- Twelfth International Electric Vehicle Symposium, Anaheim, CA, December 5-8, 1994

ACKNOWLEDGMENT

This work was supported by the Assistant Secretary for Energy Efficiency and Renewable Energy, Office of Propulsion Systems, Energy & Hybrid Propulsion Division of the U.S. Department of Energy under Contract No. DE-AC03-76SF00098. The support from DOE and the contributions by the participants in the ETR Program are acknowledged. The assistance of Ms. Susan Lauer for coordinating the publication of this report and Mr. Garth Burns for providing the financial data are gratefully acknowledged.

ANNUAL REPORTS

1. Exploratory Technology Research Program for Electrochemical Energy Storage – Annual Report for 1993, LBL-35567 (September 1994).
2. Exploratory Technology Research Program for Electrochemical Energy Storage – Annual Report for 1992, LBL-34081 (October 1993).
3. Exploratory Technology Research Program for Electrochemical Energy Storage – Annual Report for 1991, LBL-32212 (June 1992).
4. Technology Base Research Project for Electrochemical Energy Storage – Annual Report for 1990, LBL-30846 (June 1991).
5. Technology Base Research Project for Electrochemical Energy Storage – Annual Report for 1989, LBL-29155 (May 1990).
6. Technology Base Research Project for Electrochemical Energy Storage – Annual Report for 1988, LBL-27037 (May 1989).
7. Technology Base Research Project for Electrochemical Energy Storage – Annual Report for 1987, LBL-25507 (July 1988).
8. Technology Base Research Project for Electrochemical Energy Storage – Annual Report for 1986, LBL-23495 (July 1987).
9. Technology Base Research Project for Electrochemical Energy Storage – Annual Report for 1985, LBL-21342 (July 1986).
10. Technology Base Research Project for Electrochemical Energy Storage – Annual Report for 1984, LBL-19545 (May 1985).
11. Annual Report for 1983 – Technology Base Research Project for Electrochemical Energy Storage, LBL-17742 (May 1984).
12. Technology Base Research Project for Electrochemical Energy Storage – Annual Report for 1982, LBL-15992 (May 1983).
13. Technology Base Research Project for Electrochemical Energy Storage – Report for 1981, LBL-14305 (June 1982).
14. Applied Battery and Electrochemical Research Program Report for 1981, LBL-14304 (June 1982).
15. Applied Battery and Electrochemical Research Program Report for Fiscal Year 1980, LBL-12514 (April 1981).

LIST OF ACRONYMS

AES	Auger electron spectroscopy
ATR-FTIR	attenuated total reflection-Fourier transform infrared spectroscopy
BIEM	Boundary Integral Element Method
BNL	Brookhaven National Laboratory
CRADA	Cooperative Research and Development Agreement
CV	cyclic voltammetry
CWRU	Case Western Reserve University
DME	dimethoxyethane
DMFC	direct methanol fuel cell
DOD	depth of discharge
DOE	Department of Energy
DSC	differential scanning calorimetry
DSP	digital signal processing
DST	Dynamic Stress Test
ECC	environment-controlled chamber
EIS	electrochemical impedance spectroscopy
EMF	equilibrium electromotive force
EPRI	Electric Power Research Institute
ERC	Energy Research Corporation
ERIM	Environmental Research Institute of Michigan
ETR	Exploratory Technology Research
EV	electric vehicle
EVABS	Electric Vehicle Advanced Battery Systems
EXAFS	extended X-ray absorption fine structure
FTIR	Fourier transform infrared spectroscopy
HOPG	highly ordered pyrolytic graphite
HREM	high-resolution electron microscopy
HTB	hexathiobenzene
IECEC	Intersociety Energy Conversion Engineering Conference
IRE	internal-reflection element
ISE	International Society of Electrochemistry
LANL	Los Alamos National Laboratory

LBNL	Lawrence Berkeley National Laboratory
LEED	low energy electron diffraction
LEIS	low energy ion scattering
LLNL	Lawrence Livermore National Laboratory
M&E	membrane and electrode
MD	molecular dynamic
MPIII	Metal Plasma Immersion Ion Implantation
NEXAFS	near-edge X-ray absorption fine structure
NMR	nuclear magnetic resonance
NWU	Northwestern University
ORNL	Oak Ridge National Laboratory
PBI	polybenzimidazole
PDS	photothermal deflection spectroscopy
PEFC	polymer electrolyte fuel cells
PEM	proton-exchange membrane
PEO	poly(ethylene oxide)
PFSA	perfluorinated sulfuric acid
PTFE	polytetrafluoroethylene
PVDF	polyvinylidene difluoride
SEI	solid electrolyte interface
SEM	scanning electron microscopy
SNL	Sandia National Laboratories
SPAIRS	single-potential alteration infrared spectroscopy
SPE	solid polymer electrolyte
SPEFC	solid polymer electrolyte fuel cell
SRPE	solid redox polymerization electrode
TEM	transmission electron microscopy
TEOS	tetraethyl orthosilicate
TMA	tetramethyl ammonium
UHV	ultrahigh vacuum
USABC	United States Advanced Battery Consortium
XANES	X-ray absorption near-edge spectroscopy
XAS	X-ray absorption spectroscopy

SUBCONTRACTOR FINANCIAL DATA - CY 1994

Subcontractor	Principal Investigator	Project	Contract Value (K\$)	Term (months)	Expiration Date	Status in CY 1994*
<u>EXPLORATORY RESEARCH</u>						
Solid-State Cells						
Oak Ridge National Laboratory	J. Bates	Rechargeable Li Batteries	150	18	9-95	C
PolyPlus Battery Company	M.-Y. Chu	Na/SRPE EV Batteries	185	12	12-95	T
<u>APPLIED SCIENCE RESEARCH</u>						
Lawrence Berkeley National Laboratory	E. Cairns, L. DeJonghe, J. Evans, K. Kinoshita, F. McLarnon, J. Newman, P. Ross and C. Tobias	Electrochemical Energy Storage	1990	12	9-95	C
Electrode Characterization						
Brookhaven National Laboratory	J. McBreen	Battery Materials	95	12	10-95	C
Lawrence Livermore National Lab.	R. Pekala	Li-Ion Battery Testing	55	12	9-95	C
Corrosion Processes in High-Specific Energy Cells						
ERIM	T. Hunt	Secondary Batteries	100	13	1-94	T
Components for Ambient-Temperature Nonaqueous Cells						
Case Western Reserve University	D. Scherson	<i>In Situ</i> Studies	125	12	11-95	C
Northwestern University	M. Ratner	Polymer Electrolytes	145	12	3-96	C
Northwestern University	D. Shriver	Polymer Electrolytes	113	12	3-96	C
Case Western Reserve University	M. Litt	Polymer Electrolytes	166	12	1-96	T
University of Dayton	G. Glasgow	Polymer Electrolytes	99	12	2-96	C
Rutgers University	L. Klein	Sol-Gel Electrolytes	95	12	6-95	T
SUNY at Binghamton	S. Whittingham	Cathode Materials	73	12	2-96	C
SRI International	S. Smedley	Na/Polymer Cells	152	12	1-96	C
Southern University	R. Bobba	LiFeS ₂ Battery System	98	12	9-95	C
<u>AIR SYSTEMS RESEARCH</u>						
Metal/Air Cell Research						
Eltech Research Corporation	E. Rudd	Oxygen Electrodes	104	18	3-95	T
Fuel Cell R&D						
Los Alamos National Laboratory	S. Gottesfeld	Fuel Cell R&D	1200	12	12-95	C

* C = continuing, T = terminating

I. INTRODUCTION

This report summarizes the progress made by the Exploratory Technology Research (ETR) Program for Electrochemical Energy Storage during calendar year 1994. The primary objective of the ETR Program, which is sponsored by the U.S. Department of Energy (DOE) and managed by Lawrence Berkeley National Laboratory (LBNL), is to identify electrochemical technologies that can satisfy stringent performance, durability and economic requirements for electric vehicles (EVs). The ultimate goal is to transfer the most-promising electrochemical technologies to the private sector or to another DOE program (*e.g.*, SNL's Electric Vehicle Advanced Battery Systems Development Program, EVABS) for further development and scale-up.

Besides LBNL, which has overall responsibility for the ETR Program, LANL, LLNL, ORNL and BNL have participated in the ETR

Program by providing key research support in several of the program elements. The ETR Program consists of three major elements:

Exploratory Research

Applied Science Research

Air Systems Research

The objectives and the specific battery and electrochemical systems addressed by each program element are discussed in the following sections, which also include technical summaries that relate to the individual programs. Financial information that relates to the various programs and a description of the management activities for the ETR Program are described in the Executive Summary.

II. EXPLORATORY RESEARCH

The major thrust of this program element is to evaluate promising electrochemical couples for advanced batteries for EVs. Exploratory research was carried out on Zn/NiOOH and Na/polymer cells, and novel components for various versions of these cells were also investigated, as described in the Applied Science section of this report.

A. ADVANCED ZINC/NICKEL OXIDE CELLS

New approaches to extend the cycle life of Zn/NiOOH cells by modifying the electrolyte composition are underway. There is a strong incentive to develop a long-lived Zn/NiOOH battery, because it would exhibit superior performance and lower life-cycle costs, compared to Cd/NiOOH and MH/NiOOH batteries.

Zn/NiOOH Cell Studies

Elton J. Cairns and Frank R. McLarnon

90-2024, Lawrence Berkeley National Laboratory, Berkeley CA 94720

(510) 486-4636; fax: (510) 486-4260

Objectives

- Investigate the behavior of Zn electrodes in alkaline Zn/NiOOH cells and improve their lifetime and performance.
- Improve NiOOH electrode performance without compromising the lifetime of the Zn electrode.

Approach

- Determine the performance and cycle life of alkaline Zn/NiOOH cells using realistic cell components and operating conditions.
- Utilize analytical instruments such as X-ray diffraction analysis and XAS to understand changes to cell components resulting from charge/discharge cycling.

Accomplishment

- Cycling tests in 1.35-Ah Zn/KOH/NiOOH cells concluded that the 4.5 M KOH-1.8 M KF-1.8 M K₂CO₃ electrolyte is considered to be near-optimal and is recommended for evaluation in larger cells.

Future Directions

- A CRADA was established with Energy Research Corporation (ERC) to further technology transfer.
 - LBNL will provide research support by testing smaller-scale cells using the ERC lightweight roll-bonded NiOOH electrodes, supported by the DOE Laboratory Technology Transfer Program.
-

The purpose of this project is to investigate the behavior of Zn electrodes in alkaline Zn/NiOOH cells to improve their lifetime and performance. Earlier work at LBNL demonstrated that KOH-KF-K₂CO₃ electrolytes greatly extend the cycle life of 1.35-Ah Zn/NiOOH cells. The rate of Zn-

electrode shape change is much slower in these cells, and cell cycle life is increased to 500-800 deep-discharge cycles, compared to 100-200 cycles in traditional 7 M KOH - 0.5 M LiOH electrolytes. Zn/NiOOH cells employing these novel electrolytes now tend to be life-limited and

performance-limited by the NiOOH electrode rather than the Zn electrode.

It is projected that the Zn/NiOOH battery can meet all of the mid-term performance and cost goals set by the U.S. Advanced Battery Consortium (USABC) for EV batteries, however prior versions of Zn/NiOOH batteries have exhibited lifetimes of only 100-200 deep discharge cycles. The life-limiting factor has been the rapid redistribution of active material (known as shape change) on the Zn electrode caused by the high solubility of Zn species in the 7 M KOH electrolyte that was used. We have demonstrated that this shape-change problem can be largely eliminated by using electrolytes that have low Zn species solubility. Electrolytes with 3-5 M KOH concentrations supplemented by the addition of F⁻ and CO₃²⁻ anions can extend the cycle-life of Zn/NiOOH cells to 500-600 cycles before the cells lose 40% of their initial capacities. These results were obtained in cells using an electrolyte consisting of 3.2 M KOH, 1.8 M KF and 1.8 M K₂CO₃. Our tests also demonstrated that these cells can recover from severe overcharge and over-discharge excursions. Furthermore, they have been successfully discharged using the USABC Dynamic Stress Test and the USABC Peak Power Test.

Additional cell cycle-life testing using electrolytes with a range of KOH and anion concentrations have been carried out to determine the functional limits of this class of electrolytes. Three 1.35-Ah cells were prepared with fixed anion concentrations of 1.8 M KF and 1.8 M K₂CO₃, while the KOH concentration was varied. Cells were cycled at 100% DOD until 20% of the initial cell capacity was lost. The cell with 5.5 M KOH reached 220 cycles, the cell with 4.5 M KOH reached 420 cycles and the cell with 3.5 M KOH reached 385 cycles. Thus the 4.5 M KOH - 1.8 M KF - 1.8 M K₂CO₃ electrolyte is considered to be near-optimal and is recommended for evaluation in larger cells. To determine if very low concentrations of anions would be effective a cell was tested with 4.5 M KOH - 0.1 M KF - 0.1 M K₂CO₃ electrolyte; it lost 20% of its capacity after only 15 cycles, which indicates that large F⁻ and CO₃²⁻ anion concentrations are needed. A cell with 2.5 M KOH - 5 M KF - 1.5 M K₂CO₃ electrolyte lost 20% of its capacity after 60 cycles, and another cell containing 3.5 M KOH - 3.2 M KF electrolyte achieved

180 cycles. These results indicate that the inclusion of significant amounts of OH⁻ and CO₃²⁻ ions in the electrolyte is important.

Conductivities of these electrolytes and others were measured at 25°C using a specially designed cell. It was found that pure aqueous KOH electrolyte exhibits a conductivity maximum at ~5.7 M, and the conductivity of 4.5 M KOH electrolyte is ~90% of this maximum value. The addition of F⁻ and/or CO₃²⁻ anions to 3.2 and 4.5 M KOH electrolytes substantially decreases the ionic conductivity, contrary to our expectations. Saturation of the electrolyte with ZnO further reduces conductivity by complexing free OH⁻ ions. The exact manner in which the presence of these anions benefit the cell is not clearly understood. They may partially passivate the Zn electrode surface, or otherwise alter the kinetics of Zn dissolution and deposition, thereby modifying the current density distribution and impeding shape change.

A CRADA has been initiated with the Energy Research Corporation (ERC) of Danbury, CT. Using the LBNL class of electrolyte, ERC will develop 15-Ah and 150-Ah sealed cells, while LBNL will provide research support by testing smaller-scale cells using the ERC lightweight roll-bonded NiOOH electrodes.

PUBLICATIONS

- Plivelich, R.F., F.R. McLarnon and E.J. Cairns, "Nickel Hydroxide Electrodes in Reduced-Alkalinity Electrolytes," *J. Appl. Electrochem.* 25, 433 (1995 April 1994).
- Taucher, W., T.C. Adler, F.R. McLarnon and E.J. Cairns, "Lightweight Nickel Electrodes for Zinc/Nickel Oxide Cells," Paper presented at the 45th Meeting of the International Society of Electrochemistry, Porto, Portugal, August 1994.
- Taucher, W., T.C. Adler, F.R. McLarnon and E.J. Cairns, "Development of Lightweight Nickel Electrodes for Zinc/Nickel Oxide Batteries," Paper No. 132, 186th Meeting of the Electrochemical Society, Miami Beach, FL, October 1994.

B. SOLID-STATE CELLS

Efforts are underway to develop all-solid-state cells. The studies focus on demonstrating the viability of a sodium/sodium-alloy negative or a lithium negative and a metal oxide positive or an organosulfur positive in a rechargeable cell. In addition, the feasibility of an ambient-temperature molten-salt electrolyte was investigated.

Electrochemical Properties of Solid-State Sodium/Polymer Cells

Lutgard C. De Jonghe

62-203, Lawrence Berkeley National Laboratory, Berkeley CA 94720

(510) 486-6138, fax: (510) 486-4881

Objectives

- Investigate the viability of all-solid-state cells based on a Na or Na-alloy negative electrode, polymeric electrolytes, and a metal oxide positive electrode for EV applications.
- Develop a suitable cathode material for use in Na/polymer cells.

Approach

- Synthesize and characterize manganese oxides for use as a cathode in Na/polymer cells.
- Employ ac and dc techniques (*e.g.*, galvanostatic charging and discharging, four-probe techniques, impedance spectroscopy and pulse testing) to characterize solid state batteries, as well as the properties of the individual components and interfaces.

Accomplishment

- The most promising manganese oxide found so far for Na/polymer cells is $\text{Na}_{0.44}\text{MnO}_2$, first synthesized by Parant and Hagenmuller in 1971. Tests on Na/polymer cells with $\text{Na}_{0.44}\text{MnO}_2$ cathodes indicate that this material can insert 0.55 Na/Mn over a voltage range of 3.4-2.0 V at 0.1 mA/cm² (x ranges from 0.2-0.75 in Na_xMnO_2), corresponding to a capacity of 160 mAh/g, a theoretical specific energy of 440 Wh/kg and a theoretical energy density of 1450 Wh/L.

Future Direction

- Further research in this laboratory will be directed towards 1) continuation of polymer electrolyte studies including both transport-property measurements and thermal analysis, 2) use and testing of new Na salts such as $\text{NaN}(\text{CF}_3\text{SO}_2)_2$ in cells, 3) improvement in the understanding of the kinetics and thermodynamics of intercalation processes in metal oxides, and 4) Na/polymer electrolyte interface studies.
-

The objective of this project is to investigate the viability of all-solid-state cells based on Na or Na-alloy negative electrodes, polymeric electrolytes, and metal oxide positive electrodes. Emphasis is placed on developing a suitable cathode material not only in terms of performance but also in terms of cost and environmental impact. Fundamental investigations of bulk- and thin-film elastomeric electrolytes furnish information on the electrochemical and mechanical properties of these polymers, and provide the basis for advanced design of batteries, as well. Characterization of

the various interfaces in solid polymer batteries is crucial to the successful development of these advanced systems. ac and dc techniques (*e.g.*, galvanostatic charging and discharging, four-probe techniques, impedance spectroscopy and pulse testing) are used to characterize these solid-state batteries as well as the properties of the individual components and interfaces.

A full set of transport property measurements for the poly(ethylene oxide)-sodium triflate (P(EO)- NaCF_3SO_3) system was completed this year. Especially noteworthy was the development

of a new method of measuring transference numbers in polymer electrolytes using straightforward electrochemical techniques, and a rigorous theoretical treatment of the results (performed in conjunction with M. Doyle and J. Newman of the Chemical Engineering Department at U. C. Berkeley). To obtain t_+^0 , two types of experiments are carried out. First, junction potentials are determined from concentration cells, and are used to relate cell electromotive forces (EMFs) to concentration gradients. In concentrated polymer electrolytes, these values are related both to t_+^0 and salt activity coefficients, which are generally not well-known. An additional experiment is required in order to separate the transference numbers from the activity coefficients. Na/P(EO)_nCF₃SO₃/Na cells are polarized galvanostatically for a length of time (t_i) and the open circuit voltage difference measured immediately after the current is turned off. A plot of this value versus $It_i^{1/2}$ allows the transference number to be calculated from the slope, according to equation 1.

$$\Delta\Phi = \frac{4t_+^0}{c_\infty F(\pi D)^{1/2}} \frac{dU}{d \ln c} (It_i^{1/2}) \quad 1)$$

Data for the PEO-NaCF₃SO₃ system was found to fit equation 1 well, and allowed determination of transference numbers for a wide range of concentrations. These experiments are much easier to carry out than the Hittorf method, which requires extremely precise weighing of polymer electrolyte segments carefully extracted from polarized cells. The PEO-NaCF₃SO₃ system was found to have non-unity t_+^0 values which decrease with increasing salt concentration (Fig. 1).

Bulk conductivity and salt diffusion coefficients were measured by AC impedance and a restricted diffusion method, respectively. For the latter method, Na/P(EO)_nCF₃SO₃/Na cells are galvanostatically polarized. After the current is shut off, the cells are allowed to relax, and the open circuit voltage is monitored as a function of time. At long times, equation 2 holds true:

$$\ln \Delta\Phi = \frac{\pi^2 D}{L^2} t + A_1 \quad 2)$$

(where L is the electrolyte thickness and A₁ is a constant). The highest diffusion coefficients are obtained for P(EO)₂₀₋₄₀NaCF₃SO₃ and the highest conductivity for P(EO)₂₀NaCF₃SO₃.

The diffusion coefficient, conductivity and transference numbers strongly suggest that better cell performance should be obtained when a composition of P(EO)₂₀NaCF₃SO₃ is used, rather than the P(EO)₈NaCF₃SO₃ that had been used previously. By comparing Na/Na_xCoO₂ and Na/Na_xMnO₂ cells with the two different electrolyte compositions, it was possible to show this. In both cases, better utilization at higher rates (for electrode area capacities of 0.5-1 mAh/cm²) was observed when P(EO)₂₀NaCF₃SO₃ was used as the electrolyte. It is clear that premature cell polarization due to high salt concentration gradients (and possibly salt precipitation) occurs when P(EO)₈NaCF₃SO₃ is used. Interestingly, improved cycle lives were also observed for Na/PEO/Na_xMnO₂ cells with the lower salt concentrations (from 60 cycles at 0.1 mA/cm² to 50% DOD or better, to 150 cycles at 0.1-0.5 mA/cm² to 50% DOD or better).

Although the use of more-dilute electrolytes approximately doubled the rate capability of Na/Na_xMnO₂ cells, Na/Na_xCoO₂ cells can still consistently be discharged at higher current densities (e.g., when 0.5 mAh/cm² electrodes are used, 100% DOD is obtained at 0.5-1 mA/cm² for the latter, but is only obtained at about 0.2 mA/cm² for the former). Because the physical properties of the two metal oxides are similar (e.g., particle size, particle size distribution, surface area, levels of impurities, etc.) and the method of fabrication of composite electrodes is the same, this difference can, most likely, be attributed to lower rates of Na ion diffusion in the manganese oxide (or, possibly, different wetting properties). If so, further improvements in this material can be brought about by increasing the surface area and decreasing the particle size.

Capacity fading is consistently seen in all of the sodium/polymer cells tested so far. Coulombic inefficiencies upon cell charge indicate that a parasitic reaction is occurring, either corrosion at the current collectors or electrolyte oxidation. (The sodium/polymer interface has been ruled out as a significant factor, based upon four-probe DC measurements and half-cell cycling studies). Because Na_xCoO₂ is highly oxidizing in its fully charged state (over 4 V vs. Na), it is not unreasonable to suspect that electrolyte oxidation is occurring. Na_xMnO₂ is less oxidizing in the fully charged state (3.45 V vs. Na), however. Slow electrochemical potential spectroscopy experiments on Na/Na_xMnO₂ cells confirm the excellent reversibility of the intercalation process (Fig. 2), but show that a non-diffusive irreversible process

occurs as low as 3.3 V vs. Na. This may be due to impurities, such as water, in the electrolyte, or corrosion at current collector interfaces, but requires more study. Use of Na salts with better oxidative stability (e.g., NaClO_4), or that allow lower temperature operation (e.g., $\text{NaN}(\text{CF}_3\text{SO}_3)_2$), should decrease electrolyte degradation and/or corrosion and result in improved cycle life. $\text{NaN}(\text{CF}_3\text{SO}_3)_2$ has now been successfully synthesized in a pure form in this laboratory and will be evaluated shortly.

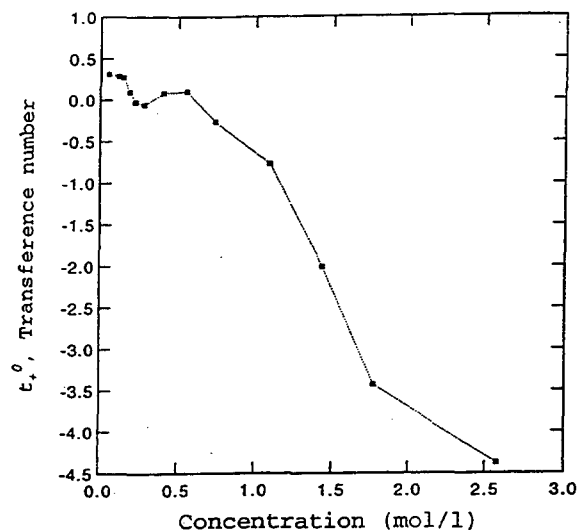


Figure 1. Transference number of the Na ion in $\text{P}(\text{EO})_n\text{NaCF}_3\text{SO}_3$ solutions at 85°C . The method of measurement is described in the text.

PUBLICATIONS

Doeff, M.M., M. Peng, Y. Ma and L.C. De Jonghe, "Orthorhombic Na_xMnO_2 as a Cathode Material for Secondary Sodium and Lithium Polymer Batteries," *J. Electrochem. Soc.* **141**, L145 (1994).

Lampert, C.M., S.J. Visco, M.M. Doeff, Y. Ma, Y. He and J.C. Giron, "Characteristics of Laminated Electrochromic Devices using Polyorganodisulfide Electrodes," *Solar Energy Mat. and Solar Energy* **33**, 91 (1994).

Visco, S.J., L.C. De Jonghe and M. Ue, "A New Trend on Electroactive Polymer Research. 2. A New Concept of Energy Storage Material - Disulfide Polymer," *Denki Kagaku* **62**, 300, (1994).

Doeff, M.M., S.J. Visco, Y. Ma, M. Peng, L. Ding and L.C. De Jonghe, "Thin Film Solid State Sodium Batteries for Electric Vehicles," LBL-35743, June 1994.

Doeff, M.M., Y. Ma, M. Peng, L. Ding and L.C. De Jonghe, "New Sodium Batteries with Polymer Electrolytes," The Twelfth International Electric Vehicle Symposium, Anaheim, CA, December 1994, Vol. 2, p. 580.

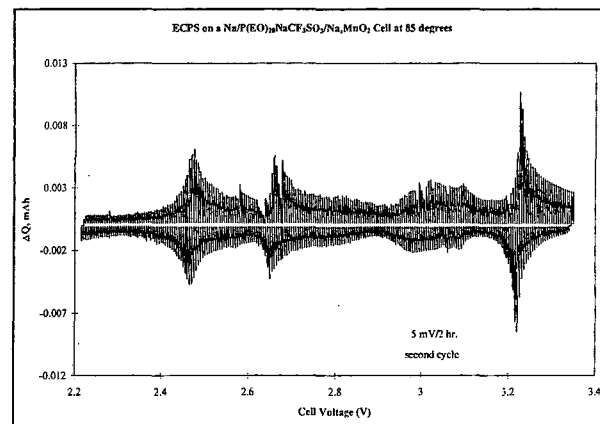


Figure 2. Electrochemical potential spectroscopy of a $\text{Na}/\text{P}(\text{EO})_{20}\text{NaCF}_3\text{SO}_3$ cell at 85°C . The potential was incrementally stepped 5 mV, and the current allowed to decay to 1/100th of the initial value between steps. Note the excellent reversibility of the intercalation process, except at high voltages upon charge where an irreversible oxidation of electrolyte takes place.

Development of a Thin-Film Rechargeable Lithium Battery for Electric Vehicles

John B. Bates

MS 6030, Oak Ridge National Laboratory, P.O. Box 2008, Oak Ridge TN 37830-6030

(615) 574-6280, fax: (615) 574-4143

Objectives

- Identify methods for depositing at temperatures below 180°C acceptable thin-film Li/Li_xMn₂O₄ cathodes for rechargeable thin-film Li batteries.
- Develop solid-state Li-Li_xMn₂O₄ rechargeable batteries for EV applications that meet or exceed the long-term goals of the USABC.

Approach

- Fabricate Li/Li_xMn₂O₄ cathodes at temperatures below 180°C by rf magnetron sputtering using different process variables and substrate bias.
- Fabricate and test 4 V thin-film solid-state Li cells with Li_xMn₂O₄ (x<1) cathodes.
- Fabricate and test hybrid cells consisting of bulk processed LiMn₂O₄ cathode plates, a thin Lipon electrolyte film and a thick Li anode film.

Accomplishment

- Li-Li_xMn₂O₄ cells exhibited good performance with less than 0.05% capacity loss per cycle after hundreds of cycles when discharged at 20-40 mA/cm² to 2-3 volts (~C/1).

Future Direction

- Fabricate cells that are based on a thick-film composite cathode (100-1000 μm) coupled with the thin-film Lipon electrolyte by various techniques such as screen printing, electrophoretic deposition and tape casting.
-

Research during the past year has focused on the synthesis of thin-film LiMn₂O₄ cathodes that can sustain high current densities. A low-temperature process for cathode film growth is desired as this will permit deposition on underlying Li layers or on substrate materials with lower melting temperatures. The performance of cells fabricated with amorphous LiMn₂O₄ cathodes, which can be deposited at near ambient temperatures, has been compared with cells containing well-crystallized spinel cathode films prepared at high temperatures (700-800°C).

The thin-film cells were fabricated on alumina substrates by successive film depositions of: *i*) Ni or Pt current collectors, *ii*) the LiMn₂O₄ cathode by magnetron sputtering or evaporation, *iii*) the lithium phosphorous oxynitride (Lipon) electrolyte by rf magnetron sputtering of Li₃PO₄ in N₂, *iv*) an evaporated Li metal anode, and *v*) a protective multilayer coating if the cell was to be exposed to

the air. The cells were subjected to constant current cycling at different discharge current densities. Impedance measurements were made at various stages of cycling in order to determine the sources of cell polarization. In all cases with cathodes thicker than 0.1 μm, Li transport in the cathode limits the current density during cell discharge.

The crystalline LiMn₂O₄ cathode films were prepared by electron-beam evaporation of LiMn₂O₄ followed by a post-deposition anneal at 700-800°C in O₂. Magnetron sputtering was investigated as a possible technique to form LiMn₂O₄ films at much lower temperatures. A wide range of sputtering conditions have been investigated, including depositions with substrate temperatures up to 230°C, various Ar + O₂ sputter gas mixtures and total gas pressures of 5-20 mTorr, and substrates with floating or an applied ± dc potential. While all of the films were amorphous to X-rays, these conditions were found to give significant variations

in the properties of the films. The processing conditions have been optimized for both the evaporated/annealed and the sputter-deposited cathodes to give cells with high specific powers and energies.

Some examples of low-current discharge curves for the crystalline and amorphous LiMn_2O_4 cathodes prepared at the different temperatures are shown in Figure 3. The capacities are comparable if the cells are discharged to about 2.5 V. However, if limited to the 4.5-3.8 V range, the capacity of the sputter deposited cathodes is smaller than that of the crystalline materials.

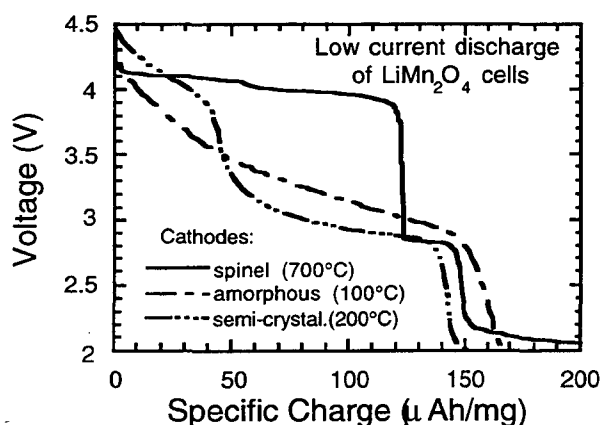


Figure 3. Low-current discharge curves for thin-film cells with various LiMn_2O_4 cathode films. A specific charge of 148 mAh/mg corresponds to 1 Li^+ per Mn_2O_4 .

Discharge of the cells at higher current densities decreases the useful capacity of the cells due to polarization. The polarization losses for the different cathodes and different cathode thicknesses are readily compared in the form of a Ragone plot as shown in Figure 4. This plot shows the superior Li transport rates for the crystalline compared to the amorphous LiMn_2O_4 cathodes. In both types of cells, the polarization loss is due to slow Li^+ ion diffusion in the cathodes, but the Li diffusivity is about two orders of magnitude lower in the amorphous material than in the crystalline form.

The best results obtained to date with sputter deposited cathodes of moderate film thicknesses are shown in Figure 4. These were deposited at 5 mTorr total Ar + O_2 pressure onto an unheated substrate at $\sim 100^\circ\text{C}$ with a +5 V dc substrate bias.

Measurements of cells with cathodes sputter deposited onto a substrate heated to 200°C are being repeated as ac impedance results indicate that the high cell resistance originally attributed to the LiMn_2O_4 cathode may in fact have been due to a reaction layer at the current collector. We expect the cell performance for the 200°C deposited cathodes to be between that of the crystalline-spinel cathodes and the amorphous cathodes deposited at $\sim 100^\circ\text{C}$.

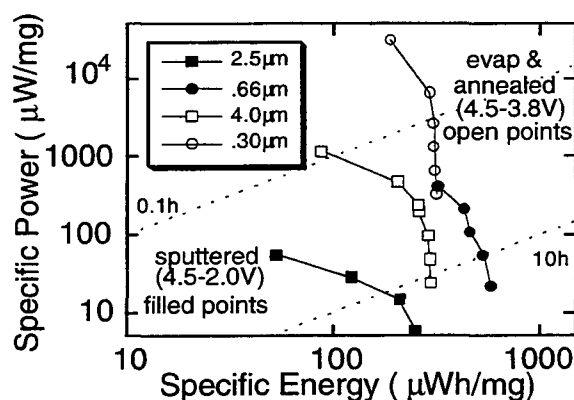


Figure 4. Specific power and specific energy measured for selected cells with moderate to thick cathodes fabricated using a sputter source (filled points) or an e-beam evaporation source followed by a high-temperature anneal (open points).

Representative cells have been tested by continuous cycling. Generally, the cells exhibited good performance with less than 0.05% capacity loss per cycle after hundreds of cycles when discharged at 20-40 mA/cm^2 to 2-3 volts ($\sim C/1$). Some results suggest that the capacity loss per cycle may be more severe for thicker cathodes. This observation is under further examination. An example of the cycling behavior of a cell with an amorphous cathode tested at room temperature and elevated temperatures is shown in Figure 5. The high-temperature operation of the cell did not adversely affect the cell performance. As a consequence of cell polarization, the capacity for these cycling conditions is very sensitive to the temperature and the erratic fluctuations in the results correlate with changes in the room temperature.

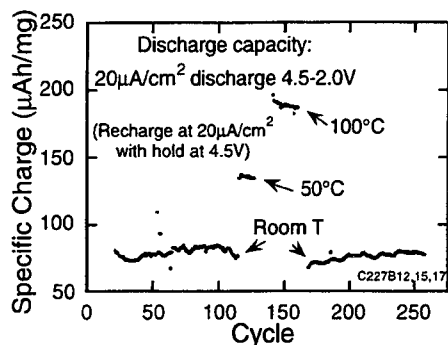


Figure 5. Cycle life of a cell with a sputter deposited LiMn_2O_4 cathode at room temperature and at elevated temperatures.

One approach for achieving the higher Li diffusivities is to operate the thin-film cells at elevated temperatures. High-temperature cell testing has been initiated recently. A set of constant current discharge curves measured at 100°C for a cell with a $2.5\text{-}\mu\text{m}$ -thick amorphous cathode is shown in Figure 6. The cell operation appears to be stable at these temperatures, although long-term testing will be needed to evaluate the cycle life.

Several new techniques for fabricating higher rate LiMn_2O_4 cathodes are being explored. One possible method to enhance the crystallinity of the growing sputtered or evaporated LiMn_2O_4 films while minimizing the heat load to the substrate and the underlying battery films is by pulse heating of the surface. Initial investigations will

involve pulsed laser heating of the surface of the growing films.

Future research will place more emphasis on the fabrication of hybrid cells that are based on a thick-film composite cathode ($100\text{-}1000\ \mu\text{m}$) coupled with the thin-film Lipon electrolyte. This approach will pose a new set of materials and processing challenges. The formation of a composite is the most likely means to greatly enhance the Li transport cathode beyond that of the pure crystalline spinel material. Possible inorganic electrolytes that might be used in the composite cathode include a $\text{LiSiO}_4\text{:Li}_3\text{PO}_4$ solid solution or LiI. Various techniques to form the composite layer being considered include screen printing, electrophoretic deposition and tape casting.

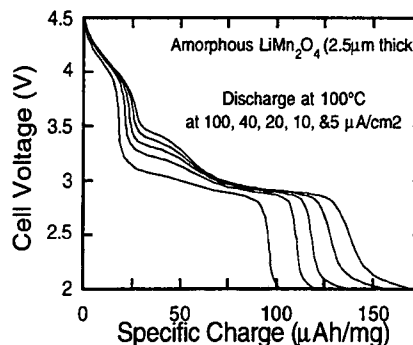


Figure 6. Constant current discharge curves for a thin-film cell operating at 100°C .

Room Temperature Sodium/Iron Chloride Battery Development *

Jack Winnick

School of Chemical Engineering, Georgia Institute of Technology, 778 Atlantic Ave., NW, Atlanta, GA 30332-0100;
(404) 894 2839, fax: (404) 894 2866

Objectives

- To synthesize and characterize new room-temperature electrolytes that contain organic salts to provide improved Na-ion transport.
- To develop advanced Na/metal chloride batteries that operate at ambient temperatures.

Approach

- Evaluate room-temperature molten salt electrolytes containing Na ions along with a solid Na anode and metal/metal chloride cathode.

Accomplishments

- Sodium plating/stripping has been achieved with 94% coulombic efficiency at current densities to 25 mA/cm².
- The effect of protons on the room-temperature chloroaluminate melt has been quantified, and stable open-circuit voltages have been achieved with solid Na in contact with the chloroaluminate melt.

Future Directions

- Identify new organic cations that yield higher coulombic efficiency and greater stability to elemental Na.
 - Conduct tests in cells with minimal electrolyte and with new cathode materials.
-

The Na-metal chloride battery has relatively high energy density, but the high operating temperature, ~250°C, and the need for a solid, Na-ion conducting electrolyte are drawbacks. This project seeks to eliminate both by using a room-temperature electrolyte containing Na ions which will be compatible with a metallic Na negative and metal/metal chloride positive. The theoretical energy density of such a battery is about 760 Wh/kg.

The first goal has been to identify an electrolyte which is compatible with metallic Na, recognizing that such compatibility is not observed with the high-temperature NaCl-AlCl₃ melt. However, highly efficient stripping and plating, as well as resistance of metallic Na to continued attack has been observed in the melt at room temperature. This melt consists of methyl-ethyl imidazolium chloride/aluminum chloride buffered with sodium chloride. The key to stability is the addition of protons in the form of HCl, which is apparently not consumed during the plating or

stripping. There is a minimum HCl pressure to accomplish the >90% efficiency so far achieved (*i.e.*, 6 μm Hg). Below this limit, the Na is rapidly consumed after plating, showing no stripping peak; above it, high coulombic efficiency is seen, but with no further advantage of higher HCl pressures.

The second goal is to identify an appropriate cathode material. Initial attempts with Fe showed that little reduction of ferrous chloride to Fe is achieved below -0.5 V (relative to Al/Al⁺³); this would yield a rather low cell voltage, since the Na/Na ion couple is -2.1 V.

A full cell has been tested in two configurations: - *i*) a cylindrical configuration, vertically oriented, submerged in electrolyte; and *ii*) a thin, flat-plate design 0.87 cm² in area, horizontally oriented, containing just enough electrolyte (~0.2 g) to wet a thin (0.5 mm glass-fiber mat) separator. Each design was contained in a sealed glass cell that could be purged with HCl. As anticipated from the half-cell study, the open-circuit voltage is only about 1.5 V. However, cycle performance starting

from charged (sodium/ferrous chloride) or uncharged (nickel substrate/iron) states was obtained, albeit with low efficiency. Most impressive was the ability to charge the thin, flat-cell arrangement with depletion of almost all of the Na ions in the melt, both dissolved and colloidal, or about 18 C of charge. The cell was able

to sit in the charged state for up to 36 h before discharge.

* This project is funded by EPRI under a collaborative agreement with DOE to sponsor exploratory research on advanced batteries for transportation applications.

Na/SRPE Electric Vehicle Batteries

May-Ying Chu

*PolyPlus Battery Company, Inc., 2431 Fifth Street, Suite B, Berkeley CA 94710
(510) 841-7242, fax: (510) 841-4313*

Objectives

- Demonstrate cycling capability of cells containing Na negative and organosulfur-based positive electrodes.
- Develop a low-cost high-performance Na/polymer cell that utilizes an organosulfur-based positive electrode.

Approach

- Fabricate Na/PEO/SRPE cells with various cathode and separator compositions, and test cells for maximum discharge, power capabilities and cycling behavior.
- Test stability of electrode interfaces with ac impedance.

Accomplishments

- Na/PEO/SRPE cells have been constructed and evaluated.
- Maximum single discharge of 450 Wh/kg of cathode *vs.* Na and peak power of 800 W/kg of cathode *vs.* Na have been demonstrated.
- Limited cycling of 5 cycles above 250 Wh/kg for the cathode *vs.* Na and 20 cycles above 100 Wh/kg for the cathode *vs.* Na were achieved.
- Initial evaluation by ac impedance demonstrated the stability of the Na/PEO interface after temperature excursions above the melting point of Na.

Future Directions

- Formulate cell construction and composition to increase cycling performance.
- Use low levels of alloying elements and develop single-ion conductor for polymer electrolyte to maintain a stable Na/PEO interface.
- Develop ac impedance signature testing to predict subsequent cell performance.

The objective of this work is to evaluate Na and organosulfur (SRPE) electrodes in secondary cells which provide a low-cost high-performance alternative battery for EV applications. This evaluation included the determination of maximum

accessible capacity in a single discharge, peak power capability, and cycling behavior. Cell engineering and optimization has not yet been considered.

Standardized methods of cell assembly were used to produce cells with consistent performance. Cathode and electrolyte films were made by casting using acetonitrile as a solvent. The active electrode areas were either 4 or 12 cm², with electrode capacities ranging from 2 to 9 mAh. The cathode and electrolyte films were dried at 110°C under vacuum for 12-24 h to minimize residual moisture. High-purity Na ingots were purified by reaction in the molten state (350°C) with titanium sponge to remove oxygen. The molten Na was cast directly into stainless steel holders. After cooling, the Na formed a clean bond with the stainless current collector which minimized electrical contact problems. The cell was assembled, compressed lightly, and heated to 90°C overnight to promote good contact between the films. The cells were evaluated at 90°C at current densities between 25-125 mA/cm² (~C/10-C/4). These low current densities were used to minimize shorting problems during recharge. Generally, the cells were discharged to 1.6 V and recharged to either 2.9 V or to a charge capacity which was 5% in excess of the previous discharge. The peak power was evaluated by discharging the cells to a cutoff voltage of 1.0 V, at current densities up to 3.0 mA/cm², for a duration of ~30 sec.

A number of cells were made with either the X1(dimercaptiothiadiazole) or X8(ethane dithiol) polymer with different salts including NaTf (sodium triflate), NaClO₄, NaBF₄, NaPF₆, LiClO₄, and LiDTf (lithium ditriflate). The initial optimization of the cathode composition showed that the best cell performance was obtained with cathode films that had an approximate composition of 50 wt% X8 polymer, 8% carbon black, 2% dispersant, and a PEO to LiDTf mole ratio of 20:1. The electrolyte composition was (PEO)₈ LiDTf. Sodium-ditriflate was not available. In general, the better performances correlated with the use of supporting salts that were known to yield the lowest glass transition temperature with PEO.

From the measurements of the maximum accessible capacity of the laboratory cells, discharge capacities as high as 450 Wh/kg of cathode *vs.* Na at a mean cell voltage of 1.8 V (250 mAh/g of cathode or 500 mAh/g of active material) were obtained. Peak power, determined by setting increasing discharge current densities to a cut-off voltage of 1.0 V showed peak power to 800 W/kg of cathode *vs.* Na. While these are attractive numbers, similar performance could not be maintained in a cycling mode, to date.

Limited cyclability was demonstrated in cells cycled at 90°C: 5 full cycles have been obtained at 250 Wh/kg of cathode *vs.* Na and about 20 cycles at a reduced performance of 100 Wh/kg. The Na electrodes were prone to shorting during the charge cycles, and this charging instability is attributed to the difficulty in maintaining a contamination-free Na/PEO interface. Additional steps are underway to reduce contamination from the glove box environment by enclosing the tests cells in hermetic containers. Another problem with the Na/PEO interface was thought to be associated with the fraction of the thiols reaching the Na/PEO interface after some time of operation. In contrast to Li-based electrodes, Na does not appear to form a solid electrolyte interface (SEI) layer to protect the Na from attack. An important aspect of future work must be to develop methods to protect the Na/PEO interface, which include the use of alloying the Na or the use of a single ion conductor.

Studies were undertaken to assess the stability of various interfaces in Na/PEO/ SRPE cells. The configuration of the test cells were positive-positive cells (SRPE/PEO/SRPE) and negative-negative cells (Na/PEO/Na) which were characterized by ac impedance. The bulk and interfacial properties of these components were measured with a high precision (16-bit) digital signal processing (DSP) data acquisition card interfaced with a 486 personal computer. The accuracy of the impedance measurements was better than 0.05% over a frequency range of 0.1 mHz to 22 kHz. The SRPE/PEO interface was found to be very stable under all cycling conditions. Additionally, no increase in impedance was measured on the Na/PEO interface after extensive hold time at 90°C. Full cells with additional reference electrodes are being constructed to measure the impedance of the cell at various stages of cycling. Tests were also performed to evaluate the effects on the Na/PEO interface with temperature excursions above the melting point of Na. After 20 min at 110°C, no evidence of interface deterioration or catastrophic shorting was found. This indicates that accidental cell overheating to above the melting point of Na may be tolerated.

In conclusion, the initial work has indicated that while significant development is needed, particularly in the protection of the Na/PEO interface, the accessible capacity and power of the Na/PEO/SRPE system measured to date has yielded encouraging results.

III. APPLIED SCIENCE RESEARCH

The objectives of this program element are to provide and establish scientific and engineering principles applicable to batteries and electrochemical systems; and to identify, characterize and improve materials and components for use in batteries and electrochemical systems. Projects in this element provide research that supports a wide range of battery systems: alkaline, flow, molten salt, nonaqueous and solid-electrolyte. Other projects are directed at research on improving the understanding of electrochemical engineering principles, corrosion of battery components, surface analysis of electrodes, and electrocatalysis.

A. ELECTRODE CHARACTERIZATION

Characterization of electrode morphology and chemical composition are important for the successful development of rechargeable electrodes for advanced secondary batteries. Efforts are underway to utilize advanced microfabrication techniques and spectroscopy to characterize electrode properties.

Surface Morphology of Metals in Electrodeposition/Carbon Electrochemistry

Kim Kinoshita and Charles W. Tobias

90-2024, Lawrence Berkeley National Laboratory, Berkeley CA 94720

(510) 486-7389, fax: (510) 486-4260

Objectives

- Develop a pragmatic understanding of the component processes and their interactions in the macrocrystallization of metals, necessary for the design and optimization of rechargeable galvanic cells.
- Investigate the role of electric field and solution-side mass transport in the electrocrystallization of metals and the physical processes involved in the evolution of gases at electrodes, with emphasis on their effect on ohmic resistance and mass transfer.
- Identify the critical parameters that control the reversible intercalation of Li in carbonaceous materials and determine their maximum capacity for Li intercalation.

Approach

- Apply mathematical modeling and experimental studies to understand mass transport phenomena involving small protrusions in a hydrodynamic flow field and the dynamics of gas bubble coalescence.
- Couple electrochemical studies with physical measurements to correlate the relationship between the physicochemical properties of carbonaceous materials and their ability to intercalate Li.

Accomplishments

- Mathematical models that uses the BIEM and FIDAP were analyzed to understand the hydrodynamics of flow over protrusions. The flow trajectories around an axisymmetric, hemispherical protrusion computed from BIEM compared favorably to those generated by FIDAP in the range of $0 < Re < 1$.
- Observation of the coalescence of electrolytic gas bubbles showed that the initial velocity of the interface joining two bubbles depends on the bubble size and surface tension but not on the electrolyte viscosity.
- Analysis of existing data suggests that the mechanism and capacity for intercalation of Li may differ between the highly ordered graphites and the less-ordered carbons. Analysis of published data indicates that the intercalation of Li is lower with carbons that have a $d(002)$ spacing of about 0.345 nm than with materials having higher or lower d -spacing.

Future Directions

- Extend numerical modeling using FIDAP to study mass transport for flows in the turbulent region.
 - Evaluate the dynamics of bubble phenomena in electrolytic gas evolution to understand coalescence behavior and its impact on the hydrodynamics and mass transfer in gas-evolving systems.
 - Analyze carbonaceous materials by Raman spectroscopy, transmission electron microscopy (TEM) and X-ray diffraction analysis to determine the relationship between the physical properties and the intercalation of Li.
-

The objective of this project is to develop a pragmatic understanding of the component processes and their interactions in the macrocrystallization of metals necessary for the design and optimization of rechargeable galvanic cells. A new effort has been initiated to identify the critical parameters that control the reversible intercalation of Li in carbonaceous materials and to determine their maximum capacity for Li intercalation. This project involves investigations of *i*) the role of electric field and solution-side mass transport in the electrocrystallization of metals: mechanisms of initiation, growth and propagation of imperfections and development of surface textures; *ii*) the characterization of the physical processes involved in the evolution of gases at electrodes, with emphasis on their effect on ohmic resistance and mass transfer; and *iii*) the role of physicochemical properties of carbonaceous materials on their ability to reversibly intercalate Li. This latter effort is coordinated with the research conducted at LLNL to evaluate the intercalation of Li in carbonaceous materials for rechargeable Li batteries (see discussion in "Fabrication and Testing of Carbon Electrodes as Lithium Intercalation Anodes" - Pekala, LLNL).

Surface Morphology of Metals in Electrodeposition. Numerical solutions using the Boundary Integral Element Method (BIEM) of the Navier-Stokes equations at $Re = 0$ for flow over an axisymmetric, hemispherical protrusion were extended to include flow trajectories. From this analysis, a vortex region of ~20% of the radius of the hemisphere was found to exist immediately in front of and behind the protrusion. This vortex region could not be resolved accurately until the code was further refined to include the Green's function at the wall. The flow trajectories and the shear stress at the wall were also computed using the commercially available finite element package called FIDAP in the range of $0 < Re < 10$. Unlike the BIEM, FIDAP can account for non-linear flow effects (*i.e.*, $Re > 0$) and can be used to solve the mass conservation equations for up to 11 species in solution. However, the mesh in FIDAP must be

three-dimensional, and the mesh required by the BIEM is only one-dimensional. Hence, changing the mesh to study different protrusion geometries is easier with the BIEM, and greater resolution of the flow pattern is possible. The trajectories from the BIEM compared favorably to flow trajectories generated by FIDAP in the range of $0 < Re < 1$, but deviations became more noticeable in the range of $1 < Re < 10$. The shear stress at the wall that was obtained by BIEM and FIDAP was also compared. FIDAP predicted higher shear rates at the top of the hemisphere than by BIEM, but the results were within 10% deviation. This deviation is to be expected since the flow volume is constricted for the finite element method, but the flow extends to infinity for the BIEM solution.

Two segmented, Pt microelectrodes were completed in the Microfabrication Laboratory of Electrical Engineering & Computer Sciences Department on the Berkeley campus. One has a 50- μm diameter, 316 stainless steel and hemispherical protrusion grafted to the electrode surface. It is surrounded by 22 microelectrodes (50- μm square) arranged in a cross pattern around the protrusion. The electrodes can be inserted into the previously designed flow cell. The flow cell can be rotated on the axis of symmetry of the protrusion so that mass transfer information can be obtained 360° around the protrusion. Mass transport coefficients will be measured in both the laminar and turbulent regimes in the range of $0 < Re < 4000$ with a redox couple. The other microelectrode has no protrusion and will serve as a baseline for testing the system in the same Reynolds number range.

For the study of coalescence between electrolytically generated gas bubbles, a laser projection apparatus developed in this laboratory was employed. The fast movement of the interface associated with the coalescence and separation from the surface of two electrolytically generated bubbles, each 0.015-0.1 cm diameter, is recorded by a photodiode array with a resolution of 10^{-5} sec. The system includes a high-speed laser-illuminated photodetector array and associated data acquisition system, a 1-W Ar laser, precisely

positioned and focused lenses, and a video microscope monitor and recorder for accurate electrode positioning and bubble size measurement (to ± 0.001 cm). The electrolysis apparatus built for this purpose is a small (20 ml) cell which contains two opposing microelectrodes on which identical or dissimilar gases may be electrolytically generated at slow, controlled rates. Refinements have been made to the system to extend the range of the experiments from 0.025-0.1 cm to 0.01-0.1 cm diameter bubbles and to improve the accuracy and reproducibility of the coalescence measurements. These changes include an improved cell design which allows close approach of the video microscope and a refined lens placement technique which reduces diffraction and improves resolution. In the experiments, bubble size, electrolyte viscosity and surface tension are varied independently. The position of the saddle point at the interface between the two bubbles is recorded as a function of time starting with the rupture of the interfacial film between the equal-size bubbles. The initial velocity of the interface, the relative degree to which the initial recoil overshoots the equilibrium spherical position, the period and damping rate of the oblate/prolate oscillations, and the buoyant float velocity of the resultant bubble are determined using the data for the change in position with time. The results to date show the following: the initial velocity of the interface depends on the bubble size and surface tension but not on the electrolyte viscosity; overshoot is limited by viscous forces but not by surface forces; the oscillation period is longer for larger sizes and lower surface tensions but does not vary with viscosity; damping is faster for smaller sizes and higher viscosities but does not vary with surface tension; and finally, the float velocity of the resultant bubble is higher when viscosity and surface tension are lower. The results agree qualitatively with theories that model the initial motion as a ruptured film and the oscillations as surface tension forced harmonic motion damped by viscous forces.

Carbon Electrochemistry. Studies on the intercalation of Li in carbonaceous materials were conducted in collaboration with LLNL. Samples obtained from commercial vendors, as well as several that were synthesized in-house, were investigated. A systematic study of the physical properties was undertaken utilizing electron

microscopy (facilities at the National Center for Electron Microscopy) and X-ray diffraction analysis at LBNL. These carbons were fabricated into electrode structures and the electrochemical intercalation of Li in nonaqueous electrolytes was studied at LLNL. Synthetic graphites with d(002) spacing of 0.3354 nm, obtained from Lonza, yielded the theoretical capacity for Li intercalation (LiC_6), whereas non-graphitized carbonaceous materials were able to intercalate only about 50% of the theoretical amount. However, petroleum coke that was doped with phosphorus showed enhanced Li intercalation. Carbon black which was heat treated to form a graphitic structure, with a d(002) spacing of 0.344 nm, did not intercalate as much Li as the initial sample. This result appears to contradict the findings with the synthetic graphites. However, other studies indicate that the graphitic layer on the carbon black particles inhibits Li intercalation. A closer analysis of the intercalation mechanism is underway, and suggests that the mechanism may differ between the highly ordered graphites and the less ordered carbons. Initial analysis of published data indicates that the intercalation of Li is lower with carbons that have a d(002) spacing of about 0.345 nm than with materials having higher or lower d-spacing. This finding suggests that the mechanism for Li intercalation may differ with graphitic materials, $d(002) < 0.345$ nm and with the disordered carbons, $d(002) > 0.345$ nm.

PUBLICATIONS

- Egan, E.W. and C.W. Tobias, "Measurement of Interfacial Re-equilibration During Hydrogen Bubble Coalescence," *J. Electrochem. Soc.* **141**, 1118 (1994).
- Sutija, D.P., R.H. Muller and C.W. Tobias, "On the Emergence and Spacing of Zinc Striations. I. Determination of Preferred Striation Frequency," *J. Electrochem. Soc.* **141**, 1477 (1994).
- Tran, T., J. Feikert, S. Mayer, X. Song and K. Kinoshita, "Carbonaceous Materials as Lithium Intercalation Anodes," Paper No. 88, 186th Meeting of the Electrochemical Society, Miami, FL, October 1994.

Battery Materials: Structure and Characterization

James McBreen

Brookhaven National Laboratory, DAS-Bldg. 480, P.O. Box 5000, Upton NY 11973-5000

(516) 282-4513, fax: (516) 282-4071

Objective

- Elucidate the molecular aspects of battery materials and processes by *in situ* synchrotron X-ray techniques.

Approach

- Apply *in situ* EXAFS to obtain chemical information on zincate electrolytes.
- Use *ex situ* EXAFS to study cycled nickel oxide electrodes from zinc/nickel oxide cells and lithium manganese oxides.

Accomplishments

- XAS studies indicate that corrosion of the Ni plaque is the failure mode for sintered nickel oxide electrodes.
- No chemical interaction between zincate and Ni(OH)₂ was observed by XAS. Decreases in nickel oxide electrode capacity in zinc/nickel oxide cells are most likely due to pore plugging by ZnO.

Future Directions

- Complete XAS studies of zincate electrolytes including supersaturated solutions.
 - Continue XAS studies of additives in Zn electrodes.
 - Use XAS to determine the existence of Ni⁴⁺ in charged Ni(OH)₂ electrodes.
-

The objective of this research is to elucidate the molecular aspects of materials and electrode processes in batteries and to use this information to develop electrode and electrolyte structures with good performance and long life. Work during the year included EXAFS studies of Ni, Co and Zn in cycled nickel oxide electrodes and zincate electrolytes.

EXAFS Studies of Nickel Oxide Electrodes. X-ray absorption spectroscopy (XAS) measurements were made on fresh nickel oxide electrodes and electrodes that had been cycled for 20,000 cycles. The electrodes, prepared by the Pickett method contained Co. Figure 7 shows a comparison of the Fourier transforms of the Ni EXAFS for the uncycled electrode and the electrode after cycling. The spectra for the uncycled electrode are very complicated since they contain contributions from the Ni in the sintered plaque and the Ni in the active material (β -Ni(OH)₂). The respective assignments for peaks A and C are the first Ni-O shell and the first Ni-Ni shell of β -Ni(OH)₂.

Peak B can be assigned to the first Ni-Ni shell of Ni. The second Ni-Ni shell of Ni overlaps peak C. The results for the cycled material indicate that most of the sintered plaque has corroded to form β -Ni(OH)₂. The small remnant of peak B, the shoulder at 0.2 nm indicates that <10% of the sintered plaque is left. However, X-ray diffraction of the cycled material gave a very clear Ni pattern because the residual plaque is the only crystalline material left. The Ni(OH)₂ corrosion product in the cycled plates is amorphous and does not contribute to the diffraction pattern. XAS, which probes short-range order, weighs both crystalline and amorphous phases equally and highlights the corrosion of the plaque and its contribution to capacity loss on cycling.

The Co EXAFS spectra for the uncycled electrode are very simple and resemble that for hydrated Co²⁺ ions. There is no evidence of Co in the Ni(OH)₂ lattice. In the case of the cycled electrode the Fourier transform has many characteristics that are similar but not identical to

that for Ni(OH)_2 . The XANES features indicate that the Co exists as Co(II) in the uncycled electrode and as Co(III) after the first charge. It is not reduced to Co(II) when the NiOOH is discharged. The results indicate that in the as-prepared electrode the Co exists as a Co(II) species on the surface of the Ni(OH)_2 . After cycling it is either incorporated in the Ni(OH)_2 lattice or it forms a new phase.

There is still some controversy as to whether zincate species interact with Ni(OH)_2 or NiOOH . Also zincate has been deemed to be either an electrode poison or a beneficial additive. There are several claims for the latter in the recent Japanese patent literature. *In situ* EXAFS studies were done on non-sintered nickel oxide electrodes, with and without Co additions in a zincate electrolyte. The EXAFS studies were done at both the Zn and Ni K edges at the end of the formation charge in 8.4 M KOH + 0.74 M ZnO. Analysis of the data indicated no specific interaction of the zincate with the Ni(OH)_2 . It is well known that large amounts of Zn can be incorporated in the nickel hydroxide electrode during cycling. The evidence so far is that the Zn does not react chemically with the nickel hydroxide. The effect on the electrode capacity may be simply a pore plugging effect by solid zinc oxide species.

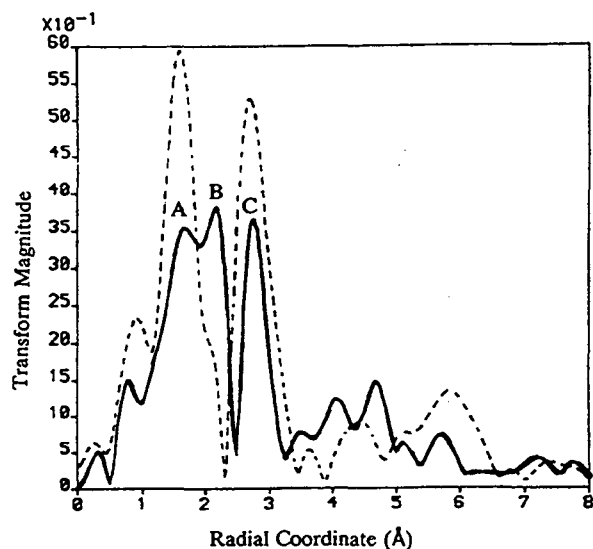


Figure 7. Fourier transforms of EXAFS for an uncycled Ni electrode (—), and a cycled electrode (- - -). Peaks A and C are the first Ni-O shell and the first Ni-Ni shell of β - Ni(OH)_2 ; peak B is the first Ni-Ni shell of Ni.

EXAFS Studies of Zincate Solutions. Several EXAFS studies were done on zincate electrolytes. These included work on ZnO dissolved in various alkali metal hydroxide electrolytes and electrochemically generated supersaturated zincate solutions in 12 M KOH with additions of silicate or sorbitol. In all cases the EXAFS spectra are identical. Typical Fourier transforms of the EXAFS are shown in Figure 8. The Fourier transform has two peaks, one at 0.15 nm and the other at 0.3 nm. Until now we have had no satisfactory explanation for the second peak. Various models based on dimers and waters of hydration were tried and none yielded a satisfactory fit for the results. Extensive analysis of the second peak indicates that it is not due to an extra coordination shell, but rather it is an artifact from a multiple scattering process. When this is included the data can be fitted to a single shell of four oxygens with a bond length of 0.196 nm. So in all cases, including supersaturated solutions, the zincate species are Zn(OH)_4^{2-} ions. Recent XANES results indicate that there may be some ion pairing between the alkali metal cation and Zn(OH)_4^{2-} . This slightly distorts the Zn(OH)_4^{2-} tetrahedra and affects the XANES. However, the interaction is too weak for detection in the EXAFS. This requires further studies since it may affect Zn deposition.

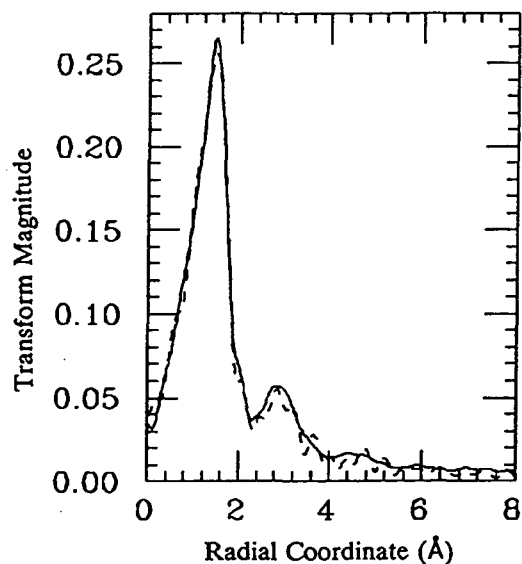


Figure 8. Fourier transform of the Zn EXAFS for a 8.4 M KOH + 0.74 M ZnO solution (—) and a supersaturated zincate solution in 12 M KOH (- - -).

PUBLICATIONS

Conway, B.E., D. Qu and J. McBreen, "In Situ and Ex Situ Spectroelectrochemical and X-ray Absorption Studies on Rechargeable, Chemically-Modified and other MnO₂ Materials," in *Synchrotron Techniques in*

Interfacial Electrochemistry, NATO ASI Series Vol. 432, C.A. Melendres and A. Tadjeddine, Eds., Kluwer Academic Publishers, Dordrecht, The Netherlands, pp. 311-334, (1994).

McBreen, J. "Nickel Zinc Batteries," *J. Power Sources* 51, 37 (1994).

Fabrication and Testing of Carbon Electrodes as Lithium Intercalation Anodes

Richard Pekala

L-322, Lawrence Livermore National Laboratory, P.O. Box 808, Livermore CA 94550

(510) 422-0152, fax: (510) 423-4897

Objectives

- Evaluate the performance of carbonaceous materials as hosts for Li intercalation negative electrodes.
- Develop reversible Li intercalation negative electrodes for advanced rechargeable Li cells.

Approach

- Fabricate electrodes from various commercial carbons and graphites and evaluate in small Li-ion cells.
- Correlate electrode performance (*i.e.*, capacity, irreversible capacity) with carbon structure and properties in collaboration with LBNL.

Accomplishments

- Electrodes fabricated from various Lonza graphites yielded Li intercalation capacities that range from 320 to 365 mAh/g (equivalent to x in Li _{x} C₆ from 0.85 to 0.95), approaching the theoretical value of 372 mAh/g corresponding to LiC₆.
- Graphite powders with particle diameter in the range of 6-44 μ m showed no Li diffusion limitation to deintercalation at rates from C/2 to C/60.

Future Direction

- Continue evaluation of commercial and chemically modified carbon materials for Li intercalation.
-

Various commercial carbons and graphites are being studied as Li intercalation compounds for anodes in Li-ion rechargeable cells. Electrode performance (*i.e.*, capacity, irreversible capacity) are obtained and related to carbon structure and properties. The non-graphitic carbons are tested in propylene carbonate-based electrolytes with a 9:1 mixture of 0.5 M lithium trifluoromethanesulfonimide (HQ115 trade name, 3M Corp.) and 0.5 M lithium hexafluoroarsenate (FMC Corp.). Graphitic materials are studied in 0.5 M HQ115/ethylene carbonate/dimethyl carbonate (50/50) electrolytes. Graphite materials are used as-received from the manufacturer without further

treatment. Cokes are ground and sieved to between 30 and 60 μ m and then pyrolyzed at various temperatures. Several polymer-based carbons were also synthesized. The electrodes were prepared using a commercial carbon fiber (Lydall Corp., 5 mil thick) as the support matrix, and PTFE (8%), PVDF (6%) or a polymer-derived carbon binder. A thick slurry containing the carbon particles, binder and acetone was spread onto the fiber support and allowed to dry. The composite was then hot-pressed at 10,000 psi. The electrode was dried in a vacuum oven at 110°C for 1 h, followed by heat treatment at 170°C (PVDF-electrodes, 1 hr) or at 350°C (PTFE-electrodes, in air for 30 min).

Electrodes with the polymer-derived carbon based binder were heated without compression to form a carbon-foam electrode. The electrochemical experiments were carried out in a 15-ml, three-electrode cylindrical cell in which the electrodes and separator are placed horizontally and stacked vertically. The geometric surface area of the working electrode is 1.12 cm².

Both the first-cycle irreversible capacity loss and the reversible Li intercalation capacity were found to be dependent on the type of binder used. Results from anodes prepared with the polymer-derived carbon binder show higher capacity (expressed here in terms of x in Li_xC_6) and lower first-cycle capacity loss than electrodes fabricated with PTFE or PVDF binders. These electrodes also show excellent mechanical and chemical integrity in the electrolytes. Therefore, the carbon-based binder is being used for electrode fabrication in subsequent studies.

The charge/discharge curves for electrodes prepared from various types of carbons and graphites as shown in Figure 9, and some performance data are summarized in Tables 1 and 2. For graphitic materials, Li intercalation/deintercalation occurs at potential less than 0.3 V vs. Li/Li^+ , and at least three voltage plateaus can be observed (associated with intercalation staging). Capacities for various Lonza graphites range from 320 to 365 mAh/g (equivalent to x in Li_xC_6 from 0.85-0.95), approaching the theoretical value of 372 mAh/g corresponding to LiC_6 . The profiles of the non-graphitic materials can vary substantially, but are smoother and are more distributed in voltage than those of graphites (Fig. 9). Among the commercial cokes studied so far, fuel green coke was found to have the highest capacity for Li (Table 2). It also has a large irreversible capacity loss ($D/C=1.71$).

The electrochemical performance of anodes made from Lonza graphite powders with particle diameter in the range of 6-44 μm were also evaluated at different charge/discharge rate ($C/2$ to $C/60$). These graphite electrodes polarized significantly in experiments at fast rates. For example, at the $C/2$ rate, the electrode potential reached the lower voltage limit of 5 mV in 90 min

in the first cycle. In the fourth cycle, when formation of the passivating layer was completed, the lower limit was reached in only 25 min indicating significant overpotentials. The characteristic (*i.e.*, equilibrium) constant-voltage plateaus associated with Li staging in the graphite structure were not apparent until $C/24$ rate or at a slower rate. Initial data indicated that the irreversible capacity loss associated with the formation of the passivated layer did not depend on the rate. Experiments with Lonza SFG6 at varying rates that included additional 4-h constant-voltage holds at 5 mV or 1.5 V were carried out. Under this condition, where the electrode is fully charged, electrode capacity did not depend on the rate. Capacities at various rates approached 350-370 mAh/g even though the charge/discharge curves differed significantly due to large overpotentials at fast rates. A constant-voltage of 0.005 V apparently facilitates Li intercalation. It is expected that this type of procedure will help to maximize intercalation kinetics.

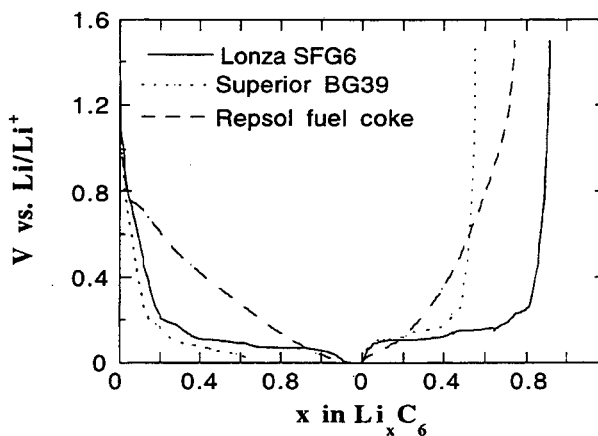


Figure 9. Charge/discharge curves for various anodes.

Table 1. Physicochemical properties and performance data^a of graphites and graphitized carbons.

Sample	Source	Type	Part. size ^b (μm)	BET area ^b (m^2/g)	L_c^b (nm)	$d(002)^b$ (nm)	x in Li_xC_6	Irr. cap. loss (mAh/g)
SFG6	Lonza	Synthetic grap.	6	15.2	>100	0.336	0.95	70
SFG15	"	"	15	8.8	>120	0.336	0.90	64
SFG44	"	"	44	4.2	<200	0.336	0.93	108
SFG75	"	"	8-96	3.5	>200	0.336	0.95	77
KS6	"	"	6	22	65	0.336	0.85	60
KS10	"	"	10	16	80	0.336	0.83	364
KS15	"	"	15	14	90	0.336	0.94	190
KS44	"	"	44	10	>100	0.336	0.93	45
KS75	"	"	8-128	8	>100	0.336	0.91	55
SG2933	Superior	purified flake natural graphite	30-40 ^c	-	>2000	0.335	0.86	76
SG4935	"	purified vein natural graphite	30-40	-	-	0.338 ^d	0.42	380
BG39	"	battery grade flake natural gra.	7	-	>2000	0.336 ^d	0.87	98
SG9400	"	graphitized pet. coke (2000°C)	30-60	-	-	0.338 ^d	0.62	68
SG9035	"	graphitized pet. coke (2700°C)	30-40	-	-	0.336 ^d	0.59	129
Sterling R2700	Cabot	graphitized C black (2700°C)	0.075	30 ^d	-	0.344 ^d	0.53	152

^a Electrolyte is 0.5M HQ115 / 50:50 EC:DMC. C/24 rate.

^b Data obtained from manufacturer information sheets unless indicated otherwise.

^c Sieved to between indicated range.

^d This study.

Table 2. Physicochemical properties and performance data^a of various cokes and carbons

Sample	Source	Type	Part. size (μm)	BET area ^b (m^2/g)	$d(002)^b$ (nm)	x in Li_xC_6	Irr. cap. loss (mAh/g)
FGC	Repsol	petroleum fuel green coke	30-60	3.3 ^c	0.349 ^c	0.69	188
LQNC	"	needle coke	30-60	6.7 ^c	0.349 ^c	0.63	104
SGC	"	sponge coke	30-60	1.2 ^c	-	0.59	90
XP30	Conoco	petroleum coke	30-60	-	0.345 ^c	0.59	55
FC250	Lonza	petroleum coke	30-60	-	-	0.62	70
PC40	"	petroleum coke	30-40	-	-	0.54	82
DB40R	Asbury	carbon black	30-40	31	-	0.88	188
Sterling R	Cabot	carbon black	0.075	25 ^c	0.352 ^c	0.93	140

^a Electrolyte is 10% 0.5M LiAsF_6 / 0.5M HQ115 / PC. C/24 rate.

^b Data obtained from manufacturer information sheets unless indicated otherwise.

^c This study

B. CORROSION PROCESSES IN HIGH-SPECIFIC-ENERGY CELLS

These projects aim to develop low-cost containers and current-collector materials for use in nonaqueous, alkali/sulfur and other molten-salt cells.

Improved Container Electrode Coatings for Na/S Battery Systems

Thomas K. Hunt

*Space Engineering and Material Science Department, Environmental Research Institute of Michigan,
4667 Freedom Drive, P.O. Box 8618, Ann Arbor MI 48108-8618
(313) 677-2113, fax: (313) 677-3377*

Objectives

- Explore sputter-deposition techniques to prepare TiN coatings.
- Develop corrosion-resistant coatings for high-temperature batteries.

Approach

- Prepare TiN coatings for corrosion studies by sputter deposition.
- Investigate ion-plating technique to prepare TiN coatings.

Accomplishment

- Two cells using TiN coatings produced by commercial reactive ion-plating have achieved over 300 cycles on accelerated charge/discharge cycles (at a rate of ~ 2/day).

Future Direction

- Project has been completed.
-

The result of the program effort has been a demonstration that TiN coatings deposited on Al electrode support structures are able to perform well during active Na/S cell tests running over 300 cycles to ~70% DOD. The cell tests have been performed at Silent Power Ltd. facilities in Salt Lake City, Utah. Three cells using TiN coatings produced by commercial reactive ion-plating were placed on accelerated cycle life tests and run through charge/discharge cycles (at a rate of ~2/day) as normally conducted on advanced cell designs by Silent Power. One of the three cells showed degraded performance after 90 cycles and it was taken off test after 180 cycles. The other two cells have performed very well through 300+ cycles as of

18 July 1995 and they are continuing under test. At present, Silent Power plans to continue these tests at least through December 1995. The observed performance is excellent and appears to indicate that the durability postulated at the program onset is likely to be achieved in practice. The issue of the cost to produce coatings by the ion-plating and sputtering methods tested has not been carefully addressed, but the use of reactive ion-plating for deposition of TiN coatings is a standard commercial operation used routinely for coating of industrial cutting tools and drill bits. It is expected that mass production methods can lead to acceptable production costs.

C. COMPONENTS FOR AMBIENT-TEMPERATURE NONAQUEOUS CELLS

Metal/electrolyte combinations that improve the rechargeability of ambient-temperature, nonaqueous cells are under investigation.

Novel Lithium/Polymer-Electrolyte/Sulfur Cells

Elton J. Cairns and Frank R. McLarnon

90-2024, Lawrence Berkeley National Laboratory, Berkeley CA 94720

(510) 486-4636; fax: (510) 486-4260

Objectives

- Investigate the behavior of S electrodes in Li/polymer electrolyte/sulfur cells and improve their lifetime and performance.
- Improve the utilization of the S electrode.

Approach

- Fabricate and test Li/polymer electrolyte/sulfur cells.

Accomplishment

- Cycling tests of small Li/polymer electrolyte/sulfur cells were initiated.

Future Directions

- Improve the utilization of the S electrode.
 - Investigate surface reactions taking place during charge/discharge cycling.
-

Variants of Li/S cells have been under investigation since the 1950's, including systems as different as high-temperature (380-500°C) LiAl/FeS₂ cells and ambient-temperature Li/Li₂S_n (lithium polysulfide) cells. Interest in the Li/S couple stems from its high theoretical specific energy (~2600 Wh/kg) as well as its environmentally benign components. In principle, this system is well-suited to EV applications, however a practical Li/S battery showing promise for EVs has not been developed. Problems have ranged from positive-electrode swelling to dissolution of partially-reduced active material (polysulfides) into the electrolyte. These problems have resulted in low utilization of active material, short cell lifetimes, and low delivered specific energy and specific power. The recent development of polymer electrolytes with acceptable ionic conductivity has created a new opportunity for the development of a solid-state Li/S cell with high specific energy and high specific power. Related research at LBNL (S.J. Visco, M.M. Doeff and L.C. De Jonghe, Materials Science Division) has led to

the development of Li/polyorganodisulfide (-(SRS)_n-) cells; however, the specific energy of the Li/SRS battery may not be sufficiently high to meet long-term USABC goals. The development of a functional positive electrode utilizing elemental sulfur should, however, provide the basis for a viable EV battery.

Our preliminary investigation of this class of cells began with the preparation of thin-film (~100s of μm) positive electrodes composed of sulfur, carbon black, polyethylene oxide complexed with a Li salt, and a carbon dispersant. Cells have been assembled with these electrodes, and galvanostatic experiments resulted in well-behaved charge and discharge cycles. Utilization of the active material has, however, been poor. Investigation of means for improving the utilization of the sulfur is currently being pursued, involving morphological studies of the electrode and the development of chemical and physical methods for improving contact between phases. Future work will include studies of surface reactions taking place during charge and discharge.

In Situ and *Ex Situ* Spectroscopic Applications to the Study of Rechargeable Lithium Batteries

Daniel A. Scherson

Department of Chemistry, Case Western Reserve University, Cleveland OH 44106
(216) 368-5186, fax: (216) 368-4874

Objective

- Gain better understanding of the nature of the passive films at the interface of Li and Li-C with nonaqueous liquid and solid polymer electrolytes (SPEs).

Approach

- Develop *in situ* and *ex situ* spectroscopic techniques to examine the reactivity of metallic Li toward these electrolytes under conditions of optimum cleanliness.
- Adapt such methodologies to gain *in situ* spectroscopic information under conditions which resemble those found in practical devices in terms of uniform current distribution and other operating parameters.

Accomplishments

- Designed and constructed a versatile, sandwich-type, variable-temperature, Li/Li⁺-based cell for conducting *in situ* attenuated total reflection-Fourier transform (ATR-FTIR) spectroscopic experiments under reduced pressure.
- Conducted the first conventional electrochemical experiments in ultrahigh vacuum (UHV) using a Li⁺-based PEO electrolyte.
- Applied *in situ* microgravimetric techniques to the study of Li deposition using *simultaneous* quartz crystal microbalance-reflectance spectroscopy techniques.

Future Directions

- Exploit electrochemistry in UHV to examine the nature of films at the Li⁺-based PEO electrolytes
- Characterize by electron-based spectroscopic techniques Li-C materials produced by spontaneous intercalation of metallic Li into carbon in UHV.
- Examine reactivity of Li-C materials toward nonaqueous solvents in the gas phase to determine whether films are responsible for loss in capacity in Li-C electrodes.

The objective of this project is to develop and implement *in situ* and *ex situ* techniques and procedures to study interfacial phenomena at the Li/electrolyte interface under charge/discharge cycling. Attention during this past year was mainly focused on two areas: *i*) application of ATR-FTIR spectroscopy for the study of the reactivity of metallic Li toward P(EO)/LiX (where X = AsF₆⁻, ClO₄⁻) electrolytes, and *ii*) development of electrochemical techniques for use in UHV to analyze electrode processes involving PEO/Li-based electrolytes relevant to Li battery technology.

***In Situ* Attenuated Total Reflection-Fourier Transform Infrared (ATR-FTIR) Spectroscopy Studies of the Reactivity of Metallic Lithium Toward PEO(LiAsF₆) Solid Polymer Electrolyte.** Changes in the structure and composition of the Au/PEO(LiAsF₆) interface induced by the deposition and stripping of metallic Li were examined *in situ* using ATR-FTIR spectroscopy. Experiments were performed with a specially designed sandwich-type cell operating at 55°C under reduced pressure (ca. 0.1 mtorr). During the measurements, the cell was placed in an environment-controlled chamber (Fig. 10) to avoid exposure to the ambient atmosphere. The working

electrode is a layer of Au (ca. 5 nm thickness) sputtered on the large face of a Ge prism internal-reflection element (IRE), the electrolyte is a film of ultrapurified PEO and LiAsF₆ or LiClO₄ solution (ca. 60 μm thick), which covers the width of the IRE, and the counter-reference electrode is a Li foil (Li[C/R]). The actual area of the Au/Ge electrode in contact with the PEO electrolyte is ca. 5.9 cm². The cell is inserted into a U-shaped holder that can be heated. The temperature can be fixed at the desired value, usually 55°C, with a controller and a thermocouple inserted into one of the plates adjacent to the cell. The entire unit is then attached *via* two pins into a Kel-F piece (not shown in this figure) attached to the bottom of an environment-controlled Al chamber (ECC), which can be evacuated to ca. 60 μm Hg. The complete cell/ECC chamber unit is fully assembled in a dry box (Vacuum Atmospheres) and then transferred to the FTIR spectrometer. A piece of freshly-cut metallic Li is often placed inside the ECC to remove gas-phase adventitious contaminants.

Figure 11 shows ATR-FTIR single-beam spectra obtained at 2.4 V *vs.* Li[C/R] before Li deposition (Curve A) and after Li stripping (Curve B) in the second voltammetric cycle at 1 mV/s. These measurements were performed at 55°C while the ECC was continuously pumped to ca. 60 μm Hg. As indicated, the electrochemical cycle leads to a broadening of some of the bands and to changes in the relative intensities of other features. Evidence for the absence of other features was obtained by normalizing the spectrum recorded after stripping by that collected before deposition. As indicated in the insert, Figure 11, this difference spectra displayed no other bands except those associated with the polymer itself. This suggests that under the experimental conditions selected for these studies, and to the level of sensitivity of this technique, PEO(LiAsF₆) does not react with metallic Li. The modifications found in the *in situ* ATR-FTIR spectrum following Li deposition and stripping are most likely caused by changes in the morphology of the polymer, including its degree of crystallinity, induced by changes in the concentration of Li ion in the electrolyte.

Electrochemistry in Ultrahigh Vacuum: Intercalation of Lithium in the Basal Plane of Highly Oriented Pyrolytic Graphite from a LiClO₄/Poly(ethylene oxide) Solid Polymer Electrolyte. Prompted by the negligible changes in the electrochemical response of the cell employed

for the *in situ* ATR-FTIR studies described in the previous section, the degassing properties of ultrapurified PEO and LiClO₄/PEO films were examined using a turbo molecular pump and ultimately an ion-pumped chamber equipped with a mass spectrometer. The presence of the PEO in the main UHV chamber caused no observable increase in the base pressure, indicating that the degassing rate was less than ca. 10⁻⁷ Pa.l/s.cm² of PEO even at temperatures of 70 ± 5°C. To take advantage of these unique properties, a series of cyclic voltammograms were performed in UHV for the intercalation of Li from PEO(LiClO₄) into the basal plane of a highly ordered pyrolytic graphite (HOPG(bp)) specimen, which had been cleaned and characterized in UHV by surface analytical techniques. A schematic diagram of the cell including the Li counter-reference electrode arrangement is shown in Figure 12.

A curve representative of the first and subsequent cycles at 80 mV/s is given in curve A, Figure 13. As shown therein, currents associated with the intercalation of Li in HOPG(bp) were observed at potentials more negative than 1.25 V *vs.* Li[C/R] with no evidence for *staging*. This behavior is characteristic of HOPG(bp) both in liquid and solid electrolytes. The prominent peak obtained in the scan in the positive direction upon reversing the cycle at 1.4 V can be attributed to the deintercalation of Li from the HOPG lattice. Essentially identical features were found in parallel experiments conducted with a sandwich-type cell involving the same constituents in the glove box (curve B, Fig. 13). This provides unambiguous evidence that the electrochemical behavior observed in UHV is indeed characteristic of the Li/LiClO₄(PEO)/HOPG(bp) system and is not affected in any discernible way by the ultralow pressures.

The ability of performing conventional electrochemical experiments in UHV using PEO-based electrolytes provides a means of examining the electrochemical characteristics of well-characterized, highly reactive surfaces under conditions of utmost cleanliness. In addition, it makes it possible to analyze surface layers formed at such interfaces with an array of powerful electron-based spectroscopies without the need of transferring specimens from high- to low-pressure environments, as is the case with virtually all liquid electrolytes.

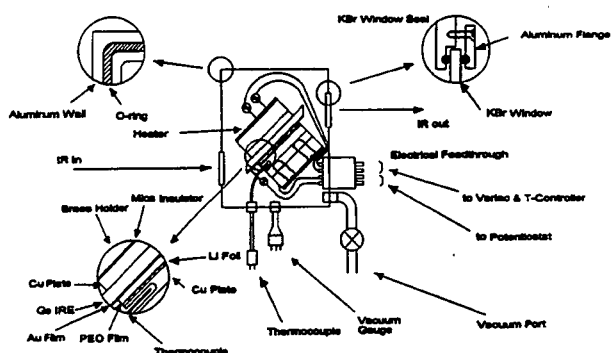


Figure 10. Schematic diagram of spectroelectrochemical cell and environment control chamber for *in situ* ATR-FTIR studies of metallic Li/SPE interfaces.

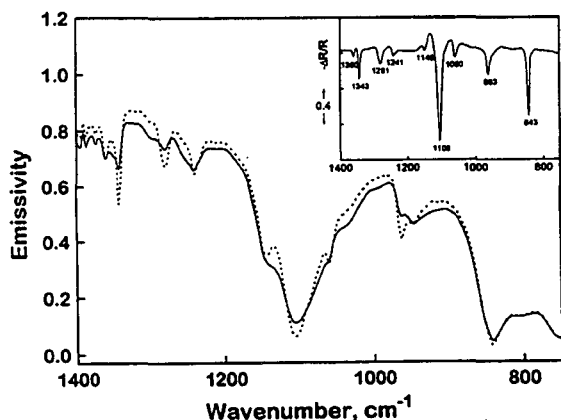


Figure 11. *In situ* ATR-FTIR single beam spectra obtained at 2.4 V vs. Li[C/R] before Li deposition (Curve A, —) and after Li stripping (Curve B, - - -) in the second voltammetric cycle at 1 mV/s.

Insert: Spectrum of the interface after Li stripping at 2.4 V vs. Li[C/R] (Curve B) normalized by the spectrum of the interface before Li deposition at 2.4 V vs. Li[C/R] (Curve A).

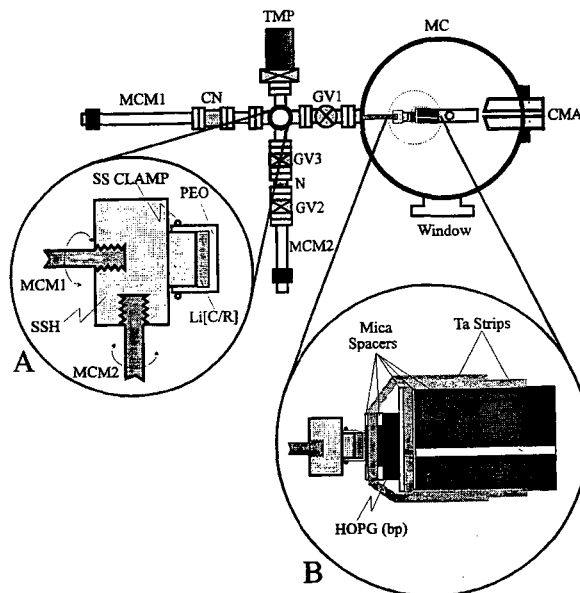


Figure 12. Schematic diagram of the electrochemical cell and UHV system for conducting electrochemical measurements in UHV.

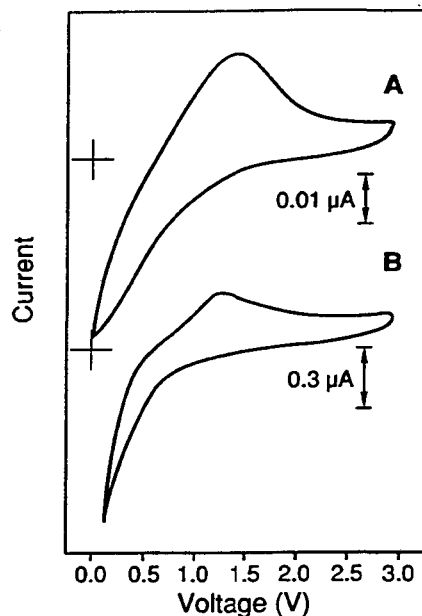


Figure 13. Representative first and subsequent cyclic voltammetry curves for the intercalation of Li into the basal plane of HOPG(bp) from PEO(LiClO₄). Measurements performed in UHV at 55°C at a scan rate of 80 mV/s (Curve A). Curve B shows the results of virtually identical measurements conducted in a high quality glove box at atmospheric pressure.

Polymer Electrolyte for Ambient Temperature Traction Batteries: Molecular Level Modeling for Conductivity Optimization

Mark A. Ratner

Department of Chemistry, Northwestern University, Evanston IL 60208-3133
(708) 491-5371, fax: (708) 491-7713

Objectives

- Analyze properties of polymer electrolytes by molecular dynamics and Monte Carlo simulations.
- Develop a microscopic understanding of the stability, structure and conduction properties of polymer electrolytes.
- Suggest modified materials with optimized conduction properties, based on mechanistic insight.

Approach

- Apply molecular dynamics and Monte Carlo simulations using high-speed computers to analyze the properties of polymer electrolytes.

Accomplishments

- Showed conclusively by molecular dynamics simulation that in polymer/salt electrolytes of the stoichiometry usually measured, there are very few free ions.
- Used hopping models to demonstrate that the conductivity is fixed both by the segmental relaxation of the polymer host (the renewal time) and by the number of effectively free ions.

Future Direction

- Continue the development of theoretical models to determine the influence of temperature, ion species, polymer chain basicity, and interionic correlations on conduction and Li transport number in polymer electrolytes.
-

Substantial progress was made towards understanding both the mechanism and the limitations for ion transport in neat polymeric materials. There are three primary results of our work to date that are significant.

i) Molecular dynamics (MD) simulation has shown conclusively that in polymer/salt electrolytes of the stoichiometry usually measured, there are very few free ions. The ions are present in pairs or larger clusters; the conductivity process is not the independent motion of free ions, or even of ion aggregates. Rather, it is a complex process involving ion motion within clusters and ion exchange among clusters. Representation in terms of the Kohlrausch relationship:

$$\sigma = \sum \mu_i n_i q_i$$

is always incorrect in this high concentration limit; here s , μ_i , n_i and q_i are respectively the conductivity, with the mobility of the i th particle,

the concentration of the i th particle and the charge of the i th particle. It has of course been known since the 1930's that this fails for concentrated solutions, but our MD simulations prove it quite clearly for polymer electrolytes.

ii) The determination that the actual conductivity, molecular dynamics simulations of the usual kind are inappropriate (the time scales are simply too long for full MD simulation). We have therefore used hopping models to demonstrate that the conductivity is fixed both by the segmental relaxation of the polymer host (the renewal time) and by the number of effectively free ions. This is shown quite clearly in Figure 14; the two straight lines for diffusion coefficient as a function of renewal rate show that increases in renewal rate will be linearly reflected in increased diffusion, as suggested by the dynamic bond percolation model. The two different lines, however, correspond to two different values of the effective temperature, which is the ratio of the

thermal energy to the coulomb pairing energy. As the coulomb energy is reduced, more effectively free ions occur and the conductivity increases.

This is an extremely important conclusion. It indicates that, as suggested by the coupling ratio arguments of Angell, polymer electrolytes are strongly coupled systems and the mobility will be limited by the polymer relaxation. There is a secondary but important effect of free ion concentration.

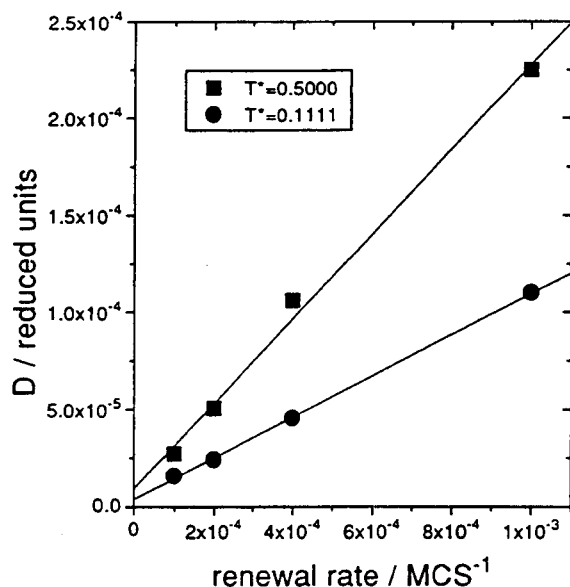


Figure 14. Tracer diffusion coefficient as a function of renewal rate for $T^* = 0.5000$, and $T^* = 0.1111$. Increased Coulomb interactions decrease the diffusion coefficient at any given value of the renewal rate, but renewal limited behavior is still preserved. This result does not hold at significantly faster renewal rates than shown in this figure.

iii) Mechanistic modeling can also be compared, and has been compared fruitfully, with experimental results. Here important work in the

D. Shriver laboratory at NWU has shown that the addition of cryptands to polymer/salt electrolytes, as well as to polyelectrolytes, will significantly increase the conductivity in poorly conductive systems. This is in exact accord with our simulations: if most of the ions are effectively free (this can be engineered by having anions of reduced basicity, such as aluminosilicates), then further increases in the number of effectively free ions will not occur on addition of the cryptand, and therefore the conductivity will be insensitive to the presence of cryptand. Conversely, with strongly basic anions (and relatively poor conductors), addition of the cryptand increases the number of effectively free carriers, thus increasing the conductivity.

These three results (strongly clustered polymer electrolytes at high concentrations, conductivity dependent on renewal rate and free ion number, effectiveness of increasing free ions in the situation where complexing is dominant) are important in understanding the current set of polymer/salt electrolytes. They also suggest that there is a rate limitation caused by the coupling of the relaxation time of the host to the ionic diffusion. This in turn suggests that to increase the conductivity of polymer electrolytes, it is necessary to go away from the simple paradigm of the uni-univalent salt complexed with a basic polymer. Several directions are suggested by our modeling, and will be pursued (both theoretically in this project, and experimentally by Shriver) in the course of the next year.

PUBLICATIONS

Nitzan, A. and M.A. Ratner, "Conduction in Polymers: Dynamic Disorder Transport," *J. Phys. Chem.* **98**, 1765 (1994).

Loneragan, M.C., A. Nitzan and M.A. Ratner, "Ionic Diffusion in Dynamically-Disordered Materials: Motion on a Renewing, Percolative Lattice," *J. Mol. Liq.* **60**, 269 (1994).

The Performance of New Materials for Polymer Electrolyte Batteries

Duward F. Shriver

Department of Chemistry, Northwestern University, Evanston IL 60201-3133

(708) 491-5655, fax: (708) 491-7713

Objectives

- Synthesize polymer electrolytes based on aluminosilicate-polyether hybrid polyelectrolyte with improved low-temperature performance and higher cation transport number.
- Develop improved polymer electrolytes for rechargeable Li/polymer batteries.

Approach

- Synthesize polymer electrolytes based on aluminosilicate-polyether hybrid electrolytes and evaluate in electrochemical cells.

Accomplishment

- Synthesized polymer electrolytes based on aluminosilicate-polyether hybrid electrolytes, (amorphous PEO)₂₅LiTf and (amorphous PEO)₃₈Li[Al(OSiEt₃)₄], which yielded 135 mAh/g active cathode material in Li/Li_xMn₂O₄ cells.

Future Directions

- Cycle cells containing polymer electrolytes and polyelectrolytes.
 - Evaluate the performance of cells containing cryptands in the polymer electrolyte.
-

The objective of this research project is to synthesize polymer electrolytes with improved low-temperature performance, higher cation transport number and useful performance in rechargeable Li/polymer batteries.

Initial cell testing was performed with cells containing simple polymer-salt electrolytes, such as (amorphous PEO)₂₅LiTf and (amorphous PEO)₃₈Li[Al(OSiEt₃)₄]. The test cells contained Li-metal anodes and composite cathodes (70% Li_xMn₂O₄, 15% carbon, and 15% of the respective electrolyte). Cells were charged/discharged at different rates. The typical discharge curves for cells with (amorphous PEO)₃₈Li[Al(OSiEt₃)₄] complex polymer electrolyte are depicted in Figure 15. It is evident that high cell capacity (135 mAh/g active cathode material) can be achieved at low discharge current. The utilization of the cathode material drops significantly when the discharge current increases. Cell capacity degrades with cycling (Fig. 16). Symmetrical cells, such as Li/(a-PEO)₃₈Li[Al(OSiEt₃)₄]/Li and (composite cathode)/(a-PEO)₃₈Li[Al(OSiEt₃)₄]/(composite cathode), are being constructed and tested to determine if the

electrolyte is degraded at the positive or negative electrode, or both.

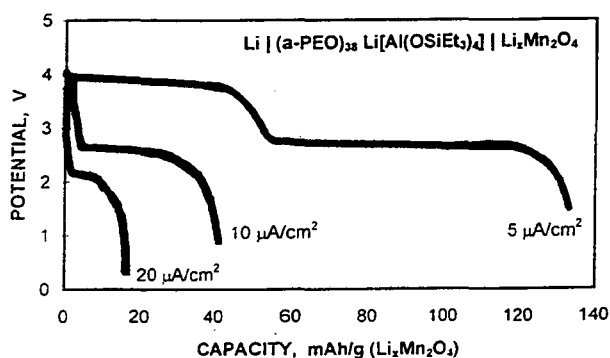


Figure 15. Discharge of Li/(a-PEO)₃₈Li[Al(OSiEt₃)₄]/Li_xMn₂O₄ cell at different current rates.

This project will continue to focus on the synthesis of polymer electrolytes and polyelectrolytes, fabrication and evaluation of cells containing polymer electrolytes and polyelectrolytes. New cell tests of aluminosilicate polyelectrolytes and modified clays, where the

aluminosilicate anion is covalently bonded to the polymer and therefore less exposed to the electrodes, will be performed.

New composites of V_2O_5 and polymers will be explored as positive electrodes in test cells, and cryptands as mobilizing agents will be tested.

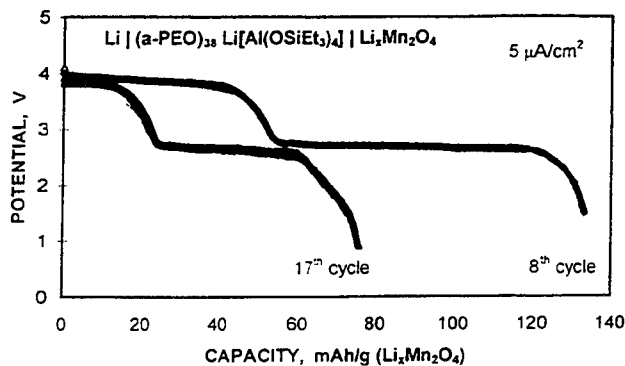


Figure 16. Degradation of cell capacity with cycling for $\text{Li}/(\text{a-PEO})_{38}\text{Li}[\text{Al}(\text{OSiEt}_3)_4]/\text{Li}_x\text{Mn}_2\text{O}_4$ cell.

Novel Polymer Electrolytes for Rechargeable Lithium Batteries

Morton Litt

*Department of Macromolecular Science, Case Western Reserve University, Cleveland OH 44106
(216) 368-4174, fax: (216) 368-4202*

Objectives

- Synthesize and characterize polybenzimidazole-base (PBI) materials for polymer electrolytes.
- Develop advanced SPEs for rechargeable Li batteries.

Approach

- Prepare sulfonated and phosphonated PBI polymers, phosphonated poly(2,5-dimethyl phenylene ether) (PPE) polymers and poly(4,5-dimethylene imidazole and hydroxy imidazole) polymers for electrochemical studies.

Accomplishments

- PBI was successfully sulfonated by heating with sulfuric acid to yield a maximum of 0.95 $-\text{SO}_3\text{H}$ groups per PBI unit. When PBI was dissolved in H_2SO_4 containing either SO_3 or P_2O_5 and heated to 150°C , it reached 2.1 to 2.2 sulfonic acid groups/per PBI unit.
- Two point conductivities of 7.1×10^{-8} and 2.3×10^{-8} S/cm, respectively, were measured at 150°C for PBI/PEO films with weight ratios of 1/1 and 2/1.

Future Directions

- Methods to increase the degree of sulfonation to higher than 2.2 sulfonic acids per PBI unit will be investigated and the products will be evaluated in electrochemical tests.
 - Project will be completed in 1996.
-

The objective of this research is to develop advanced novel polymer electrolytes for rechargeable Li batteries. Thin polymeric films will be cast and characterized by spectroscopic, nuclear magnetic resonance (NMR), thermal and electrochemical techniques. Three types of polymer materials are under investigation:

i) Sulfonated PBI polymers – the labile protons will be replaced by Li to make a salt that should be stable to Li metal and should conduct well since it would have many ions per repeat unit. The Li transference number should be 1, since the anions are fixed on the polymer.

ii) Novel poly(4,5-dimethyleneimidazole and hydroxy imidazole) polymers – these are acidic and can have a very low equivalent weight per Li.
iii) Phosphonated poly(phenylene ethers) – if complete phosphonation can be obtained, they will have an equivalent weight of 76.

Polybenzimidazoles. PBI (Hoechst Celanese) was dissolved in concentrated sulfuric acid and a dehydrating agent (P_2O_5 and SO_3) was added and the solutions were heated for five hours at either 150 or 200°C. Sulfonation using P_2O_5 was cleaner, based on FTIR spectra. The polymers only dissolved in water if enough LiOH was added to ionize the benzimidazole NH groups. The cast films had reasonable strength and conductivity measurements could be made, however, the polymer conductivity was too low for our normal four point probes. Therefore, a two-point probe was used at various frequencies. The conductivity reported were taken in the frequency range where θ is near 0.

Polyimidazoles. Two approaches are being used in the synthesis of polyimidazoles. In the first approach, the precursor monomer, 4,5-dimethylene ethylene carbonate was synthesized and polymerized. The monomer yield was about 30%. Polymerization, using azo(bis) iso butyryl nitrile (AIBN) initiator, was quantitative. The corresponding model compound, 4,5-dimethyl vinylene carbonate, was synthesized and reactions were attempted on this to generate imidazole derivatives. However, reaction conditions that

could transform the model compound to imidazole derivatives could not be found. Therefore, this approach was abandoned in favor of the direct synthesis of imidazole monomer precursors.

Based on a literature report of the synthesis of poly(N-methyl4,5-dimethylene imidazole), we decided to make an analogous precursor using an unmethylated imidazole derivative, 4-methyl, 5-hydroxymethyl imidazole. The methyl xanthate ester was in 35% yield and pyrolyzed at temperatures from 160 to 240°C. The xanthate cleaved from the precursor, removing a proton, and the resulting monomer polymerized *in situ*. A polymer was obtained, but NMR showed that it was not the desired material.

Phosphonated PPE. Reports in the literature indicate that 100% bromomethylated PPE can be obtained. When we tried to duplicate this, the maximum obtained was 70%, accompanied with some dibromomethyl substitution. With more than 5% dibromomethyl present, the polymer gelled during the phosphonation reaction. Since bromination efficiency depended on the rate of addition of bromine, the reactor volume and the temperature, it took many experiments to determine reaction conditions that gave high monobromomethyl substitution and low dibromomethyl substitution. Phosphonation went to completion, however, hydrolysis of the methyl esters has proved to be difficult, which was also reported earlier.

Novel Solid Polymer Electrolytes for Advanced Secondary Batteries

D. Gerald Glasgow

Materials Engineering Division, The University of Dayton, 300 College Park, Dayton OH 45469-0130
(513) 229-2517, fax: (513) 229-3433

Objectives

- Synthesize and characterize new polymer electrolytes that contain crown ethers to provide improved Li-ion transport.
- Develop advanced SPEs with high conductivity and better dimensional stability for rechargeable Li batteries.

Approach

- Synthesize and characterize new doped polymer electrolytes with side chains having the ability to form liquid crystalline mesophases which are terminated with crown ether groups.

Accomplishment

- A novel liquid crystalline monomer, 4-[11-acryloylundecan-1yl)oxy]-4'-(4'-carboxybenzo-15-crown-5)biphenyl, ACB, was synthesized by a four-step synthetic route.

Future Directions

- Complete synthesis of polymer electrolytes with attached crown ethers, and optimize the electric field alignment and photopolymerization parameters.
 - Conduct characterization studies of the polymers with respect to ionic conductivity, dimensional stability and interfacial stability.
-

The objective of this research program is to develop new polymer electrolytes which will have a fundamentally different mode of ion transport than those currently under investigation. The systems under investigation are doped polymers with side chains that have the ability to form liquid crystalline mesophases. The side chains are terminated with crown ether groups which can complex with the Li salt dopant. It is hypothesized that these materials will create highly ordered liquid crystalline structures, thereby forming paths through which ions can easily move. Consequently, the polymer will conduct ions through a different mechanism which will not rely on the segmental motion of large portions of the polymer chains for ion transport as the current systems do.

A novel liquid crystalline monomer, 4-[11-acryloylundecan-1yl)oxy]-4'-(4'-carboxybenzo-15-crown-5)biphenyl (ACB) was prepared by a four-step synthetic route. This method produces ACB in an overall yield of 60% that is five times higher than yields previously reported. ACB was found to be a monotropic nematic liquid crystal based on differential scanning calorimetry (DSC) and hot-stage cross-polarized microscopy. It is crystalline at RT and melts to the isotropic state at 113°C. Upon cooling (15°C/min) from its isotropic state it forms a nematic mesophase between 113 and 92°C. The addition of 1.5% photoinitiator, 2,2-dimethoxy-2-phenyl-acetophenone, and lithium triflate (14 wt%, molar ratio O/Li=8/1) shifted the nematic mesophase to 89 and 105°C. The 16°C nematic range is a very convenient working range

for carrying out the alignment and photopolymerization studies.

ACB and ACB/lithium triflate were readily photopolymerized at 350 nm in the photoDSC cell. The photopolymerization was over within 6 min with no evidence of residual reactivity. Photopolymerization was also performed by using a mercury vapor lamp to yield a clear, colorless film.

Studies were carried out to prepare aligned, doped polymeric films that will be used for measuring the ionic conductivity. This technique entails the use of an ac electric field for aligning the side chain of ACB. An assembly which allows *in situ* alignment, photopolymerization and conductivity tests of doped polymerized ACB was built and tested. This assembly takes advantage of the good conductivity of indium-tin oxide coated glass. In particular, the fine powder mixture comprising the final monoacrylate monomer, ACB, photoinitiator and Li salt, was placed between two indium-tin oxide coated glass slides with a silicone spacer having a thickness of 125 μm . The assembled sample cell was heated above the monomer clearing temperature (about 140°C) under vacuum and cooled slowly to the nematic mesophase (100°C). The monomer film inside the assembled cell was UV-cured at 100°C under vacuum for 20 min. One conductivity test showed that the doped polymer of ACB has room-temperature conductivity of 10^{-9} S/cm. Note that this value is low and does not reflect the ultimate ionic conductivity of this system since the liquid crystalline monomer was not aligned before it photopolymerized. Studies to align ACB in an electric field are underway.

Sol-Gel Electrolytes in Lithium Batteries

Lisa C. Klein

College of Engineering, Rutgers University, P.O. Box 909, Piscataway NJ 08855-0909
(908)445-2096, fax (908) 445-3258

Objectives

- Investigate solid electrolyte compositions that can be applied directly to electrode materials by the sol-gel process.
- Design oxide substitutions for silica in Li silicates that improve electrochemical performance relative to Li metal, and that increase ionic conductivity.

Approach

- Identify suitable oxide components for Li-ion conductor by thermodynamic analysis.
- Prepare sol-gel formulations and evaluate in electrochemical cells.

Accomplishments

- Identified alumina-containing formulations that showed improved thermodynamic stability. A formulation containing 14 mol% alumina had the highest ionic conductivity at 250°C - 4.7×10^{-6} S/cm.
- Fabricated thin-film and bulk samples of the same composition that had similar ionic conductivities and the same temperature dependence.

Future Direction

- Project was completed.
-

The objective of this program is to investigate solid electrolyte compositions that can be applied directly to electrode materials by the sol-gel process. Lithium silicates with 15 mol% lithia have stable ionic conductivities on the order of 10^{-6} S/cm at 200°C. Starting from this composition, various oxide additions were made to Li silicates, designed to improve their electrochemical performance, and possibly, their ionic conductivity. Using simple thermodynamic calculations, it was found that alumina and zirconia additions to lithium silicates would lessen their reactivity with respect to Li metal. Substitutions of 3, 5, 10 and 14 mol% of alumina and zirconia for silica were incorporated into Li silicate formulations.

Tetraethyl-orthosilicate (TEOS) was used as the silica precursor and lithium nitrate was the source for lithia. When adding alumina or zirconia to the solution, aluminum nitrate and zirconium nitrate, respectively, were used. Table 3 lists the formulations for lithium aluminosilicate. R is the

molar ratio of water to TEOS. Solutions were clear, with no precipitates. The time-to-gel (t_{gel}) is given in days. Bulk samples were prepared so that dried pellets could be used to measure bulk conductivity with complex impedance spectroscopy. Thin films were deposited by spinning solutions directly onto commercial devices, Microsensor System SAW (surface acoustic wave) 302, that have 50 interdigitated pairs of electrodes with a width of 15 μ and a spacing of 15 μ . The electrode geometry provided the large ratio of electrode perimeter to electrode spacing that was necessary to measure weakly conducting materials.

The results of the conductivity measurements are listed in Table 3, giving conductivity at 250°C ($\sigma_{250^\circ C}$) and the activation energy (E_a). There is no evidence of proton conduction, nor is there evidence for lithium nitrate melting at 265°C in samples with alumina. The conductivities appear high and stable from room temperature to 300°C. The

highest conductivities are those for the 14% alumina sample.

When the results of ionic conductivity measurements on a film were compared to those from a bulk sample, the thin film showed a slight increase in conductivity following heating, due to some relaxation of the gel film. Overall, the conductivities of the two samples were very close and showed the same temperature dependence.

Table 3. Properties of Lithium Aluminosilicate Formulations

Al ₂ O ₃ (mol%)	R	t _{gel} (days)	σ _{250°C} (S/cm)	E _a (eV)
3	8	~5	3.6x10 ⁻⁷	0.82
5	10	~9	7.1x10 ⁻⁷	0.76
10	20	~15	1.8x10 ⁻⁶	0.66
14	30	~22	4.7x10 ⁻⁶	0.58

According to classical glass structure models, there is a compensating effect between Al³⁺ and Li⁺ equivalent to Si⁴⁺. This effect appears to contribute to increasing conductivities from 3 to 14% alumina.

In summary, when the alumina content was increased from 3 to 14 mol% in a lithium silicate solid electrolyte, both the calculated thermodynamic stability of the electrolyte improved relative to Li metal, and the ionic conductivity exceeded 10⁻⁶ S/cm at 250°C.

PUBLICATION

Mouchon, E., L.C. Klein, V. Picard and M. Greenblatt, "Sol-Gel Lithium Silicate Electrolyte Thin Films," *Materials Research Soc.* 346, 189 (1994).

New Cathode Materials

M. Stanley Whittingham

Chemistry and Materials Research Center, State University of New York at Binghamton

Binghamton, NY 13902-6000

(607) 777-4623, fax: (607) 777-4623

Objectives

- Synthesize and evaluate oxides of W, Mo, and first-row transition metals for alkali-metal intercalation electrodes.
- Identify new intercalation compounds for positive electrodes in advanced nonaqueous secondary batteries.

Approach

- Synthesize metal oxides that have crystallographic structure to permit facile intercalation of Li ions.
- Characterize the metal oxide structures by X-ray diffraction analysis and evaluate materials in electrochemical cells.

Accomplishments

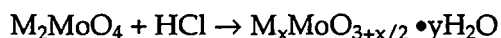
- Produced hexagonal Mo oxides by a hydrothermal method at 150-200°C which has a greater capacity for Li intercalation than the normal MoO₃ phase.
- Obtained layered structures which should allow for rapid diffusion of Li ions

Future Direction

- Expand synthesis and electrochemical studies to vanadium and manganese oxides.
-

The objective of this project is to synthesize and evaluate oxides of W, Mo, and first-row transition metals for alkali-metal intercalation electrodes in advanced nonaqueous rechargeable batteries. Mild hydrothermal techniques are being used for the synthesis of molybdenum oxides or, in cases where the hydrothermal technique does not lead to compounds in the highest oxidation states, electrochemical oxidation will be used to drive the transition metal to its highest oxidation state.

The feasibility of preparing molybdenum oxides by the hydrothermal method has now been proven. A number of phases have been formed at 150-200°C according to the following equation:



where M is a cationic specie and M_2MoO_4 is synthesized *in situ*. The synthesis conditions of three materials, which have open crystal structures and are therefore of potential electrochemical interest, are shown in Figure 17.

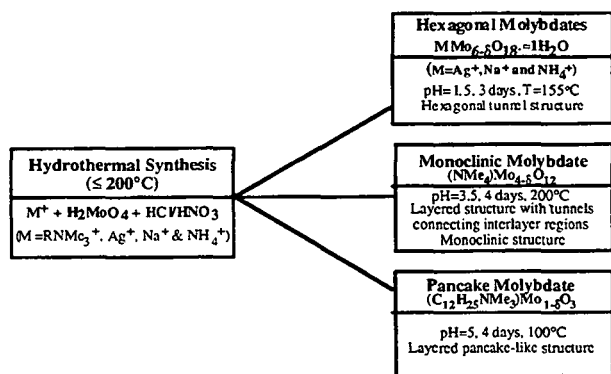


Figure 17. Synthesis conditions of new molybdenum oxides.

In the case of Na the resulting pale yellow crystallites consisted of hexagonal rods as shown in Figure 18. The Na ions can be readily ion-exchanged for hydrogen ions by immersion in nitric acid. These hydrogen ions can subsequently be removed on gentle heating leaving a hexagonal "MoO₃".

When the tetramethyl ammonium ion, TMA, was used in the synthesis, a layered structure with the chemical formula $(NMe_4)Mo_4O_{12}$ was formed. When still larger species such as long-chain quaternary ammonium ions are used, large pancake like crystals were formed.

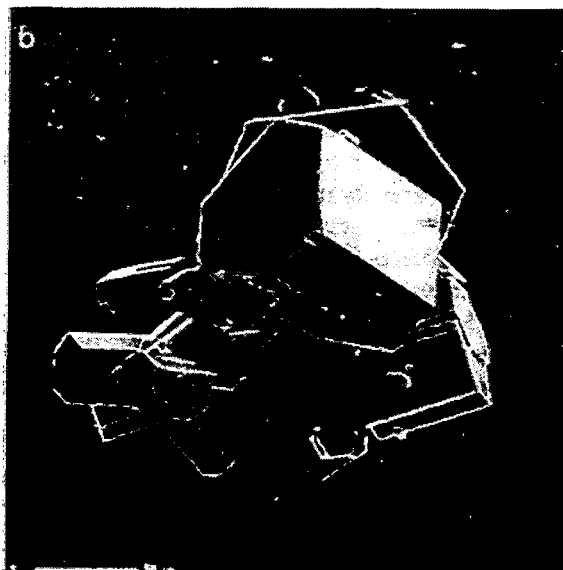


Figure 18. Hexagonal molybdenum oxide phase.

Rietveld analysis has been performed on the first two molybdenum oxide phases. The hexagonal phase contains a large tunnel along the c-axis. The chemical composition can be represented by the formula:



The structure of this phase is shown in Figure 19, where the large tunnels are very apparent, and the Na resides in the tunnels together with the water molecules.

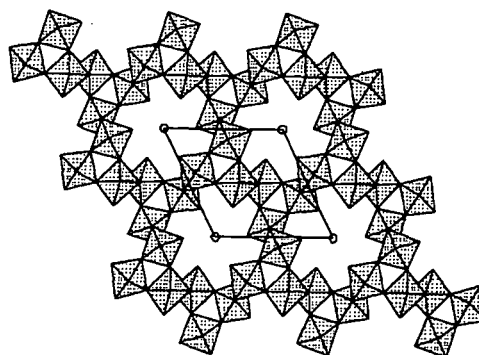


Figure 19. Crystal structure of hexagonal molybdenum oxide phase, shown along the 001 axis.

When the NMe_4 ion was present, a layered structure was formed. The structural and chemical analyses of this compound have been completed and it has the chemical formula $(\text{NMe}_4)\text{Mo}_4\delta\text{O}_{12}$. Its structure should allow for ready diffusion of Li ions in the interlayer regions and from one interlayer to the next. The molybdenum oxide formed using the long-chain alkyl ammonium species has a layered structure, with a spacing around 2.2 nm. Its exact structure is being determined.

Chemical lithiation of the above two classes of molybdenum oxides using n-butyl Li indicates that all these phases readily react with Li. Moreover, little change is seen in the lattice volume (<4%), suggesting that changes in structure should not be a cause of loss of charge on cycling (Table 4); in comparison TiS_2 expands 10% on reaction with Li.

Table 4. Cell volume of hexagonal oxides.

As Synthesized Oxide	Dehydrated Oxide	After Lithiation	% Vol. Change
Sodium 364.19\AA^3	350.5\AA^3	0.7Li/Mo 362.7\AA^3	+3.36
Hydrogen 361.63\AA^3	" MoO_3 " 362.2\AA^3	0.7Li/Mo 359.7\AA^3	-0.70
Ammonium 359.59\AA^3	359.96\AA^3	0.95Li/Mo 362.53\AA^3	+0.71
Silver 362.7\AA^3	362.49\AA^3	1.7Li/Mo Amorphous	?

Early tests in electrochemical cells, shown in Figure 20, are confirming the greater capacity for this phase over the normal MoO_3 phase. The initial EMF of the hexagonal is higher, exceeding $3\text{ Mo}_4\delta\text{O}_{12}$. Although the n-butyl Li indicated a higher reactivity with the Ag phase than with the others, electrochemical tests do not. In the second cycle the voltage profile has changed slightly, suggesting that there might be changes to the crystal structure on cycling Li in and out.

To ascertain whether any changes had occurred in the structure of the molybdenum oxide cathodes during cycling, a cross-section of the cathodes was X-rayed. In all cases studied so far, sharp X-ray lines were found. However, these did not

correspond to the original hexagonal phase, nor do they correspond to the regular MoO_3 structure.

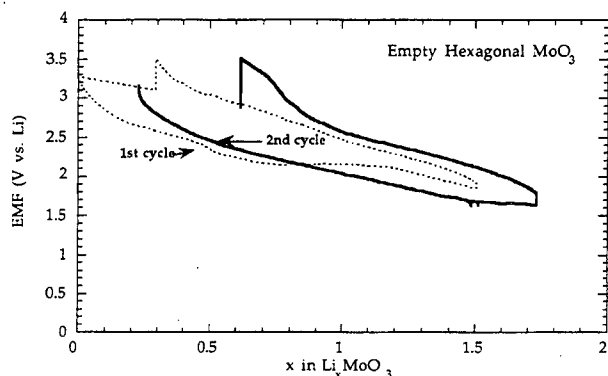


Figure 20. First and second cycles of hexagonal MoO_3 .

A number of layered vanadium oxides have been formed using the hydrothermal method. In each case the NMe_4^+ cation had to be present in the reaction medium, but was not found in the final reaction product. Several structures are particularly promising as Li ions should be able to easily intercalate the layered structure. Large quantities of pure material have been successfully formed. These compounds will undergo electrochemical evaluation in the next six months; comparison will be made with crystalline and amorphous V_2O_5 .

PUBLICATIONS

- Guo, J., P. Zavalij and M.S. Whittingham, "Preparation and Characterization of a MoO_3 with Hexagonal Structure," *Eur. J. Solid State Chem.* **31**, 833 (1994).
- Guo, J., P. Zavalij and M.S. Whittingham, "Hydrothermal Synthesis of a New Molybdate with a Layered Structure," *Chem. of Materials* **6**, 357 (1994).
- Guo, J., "Novel Tungsten Oxides and Molybdenum Oxides: Low Temperature Synthesis, Characterization and their Applications in the Energy Area," *Ph.D. Thesis*, October 17, 1994.

Development of High Energy Density Cathodes for Sodium/Polymer Cells

Stuart Smedley

SRI International, 333 Ravenswood Avenue, Menlo Park, CA 94025

(415) 859-6173, fax: (415) 326-3678

Objectives

- Synthesize and test hexathiobenzene-based compounds and their derivatives for use as positive electrodes in Na polymer cells.
- Develop high-performance organic polydisulfide positive electrodes for low-temperature (ambient to 100°C) Na/polymer batteries.

Approach

- Synthesize polydisulfides based on hexathiobenzene (C_6S_6 , HTB) which has up to six reducible S centers and an equivalent weight of 44 g/eq.
- Evaluate electrode performance using standard electrochemical techniques, including dc charge/discharge cycling, CV, and EIS to screen potential materials to identify those with the highest sustainable current densities and practical energy densities.

Accomplishments

- Achieved a cathode utilization of 164 mAh/g, with an energy density of 260 Wh/kg, for polyHTB cathodes discharged at the C/10 rate, at 95°C.
- Prepared HTB-based electrodes for evaluation in Na/PEO/polyorgano-disulfide cells.
- Developed a rapid screening procedure for evaluation of candidate cathode materials in Na/PEO/polyorganodisulfide cells.

Future Directions

- Continue to synthesize and optimize new cathode materials with improved cycling performance.
 - Develop an electrolyte with improved Na-ion conductivity.
-

The major objective of this research is to develop high-energy-density organic polydisulfide positive electrodes for use in low-temperature (ambient to 100°C) Na/polymer cells. This will be achieved by synthesizing and characterizing hexathiobenzene-based (HTB) compounds and their derivatives for positive electrodes. Specific parameters of investigation include the nature of any heteroatoms or side chains added to the base polymer, the structure of the polymer, the cathode thickness, the voltage stability window of the cathode, the degree of loading of the positive electrode material, the electrode construction technique, and the cell operating temperature.

Polydisulfides based on HTB (C_6S_6) were examined. HTB has six reducible sulfur centers per molecule, which corresponds to a theoretical

specific capacity of 608 mAh/g or a specific energy of 1200 mWh/g, assuming an electrode potential of ≈ 2 V *vs.* Na. Other candidate materials examined included polymers of difluorotetrathiobenzene, $C_6F_2S_4$ (DFTTB), tetrafluorodithiobenzene, $C_6F_4S_2$ (TFDTB), and pentathiopyridine, C_5NS_5 (PTP).

Cyclic voltammetry was used to screen candidate materials and various model compounds in acetonitrile solvent to establish a structure-function relationship. The cyclic voltammogram of the $[Bu_4N^+]_6$ salt of HTB exhibited poorly defined oxidation peaks at -0.6 V *vs.* Ag/Ag⁺ (0.01 M AgNO₃) and 0.0 V *vs.* Ag/Ag⁺, whereas a large oxidation peak is observed at +0.8 V *vs.* Ag/Ag⁺. If the voltage sweep is interrupted at the top of the peak, the current falls precipitously to zero rather than the expected exponential decay, behavior similar to electrophoretic painting. A reduction

peak at -1.9 V, absent at the clean electrode, forms upon repeated cycling to positive potentials. These results suggest the formation of a polymer that blocks further access to the electrode surface. The voltammogram of the $[\text{Bu}_4\text{N}^+]_2$ salt of TFDTB revealed a reversible couple at around +0.6 V, indicating that, as expected, the electron-withdrawing fluorine substituents shifted the potentials in a positive direction and also improved the kinetics of electron transfer. A three-electrode sandwich-type cell was designed which contains an organic polydisulfide positive electrode, a Na foil negative electrode, and two layers of polyethylene oxide-sodium triflate (PEO_8NaTf) electrolyte. The reference electrode, a piece of Na attached to a thin strip of Ni foil, was placed between the layers of the electrolyte. Nickel current collectors were used for both electrodes. Positive electrodes were cast directly onto the current collector from a slurry (in acetonitrile) comprising 30 wt% of the polydisulfide polymer, 10 wt% carbon black, 3 wt% surfactant and balance polyethylene-oxide/sodium triflate ($\text{PEO}_{20}\text{NaTf}$). Cells were cycled galvanostatically, typically at 0.05 mA/cm^2 , between 4.5 V *vs.* Na/Na⁺ and 1.0 V *vs.* Na/Na⁺. This corresponds to a C/10 charge/discharge rate at the cathode loading used (0.5 mA/cm^2). Cells were cycled at 85 to 95°C. Cells built using polyHTB as cathode showed that cathode utilization was a strong function of operating temperature, although even at 95°C cathode utilization was poor. The best result achieved for polyHTB was 27% cathode utilization after the first cycle, using a current density 0.05 mA/cm^2 . This corresponds to a specific

capacity of 168 mAh/g for polyHTB. This result, equivalent to 1.6 electron per HTB unit, is encouraging given that the cathode formulation was not optimized.

AC impedance spectroscopy showed that the impedance of the Na/electrolyte interface could be attributed to charge transfer and the diffusion of Na ions within the electrolyte film, the latter being twice as large. The high charge-transfer impedance probably arises from electrochemical instability of the Na/electrolyte interface possibly due to reaction of Na with impurities in the electrolyte such as trace water or residual solvent, or simply reaction with the electrolyte itself. This illustrates the possible beneficial effects of a single ion conductor, which has a Na⁺ transport number of unity and therefore, in principle, would exhibit no diffusional impedance. The impedance of the cathode is two orders of magnitude higher than that of the anode, suggesting that the major factor limiting cell performance is related to the cathode impedance. The cathode impedance included contributions from the uncompensated electrolyte resistance and charge transfer impedance at high frequencies and a process which could be characterized by the combination of a resistor and capacitor in parallel at low frequencies. The low-frequency process accounted for 90% of the cell impedance. We ascribe this feature to poor electronic and ionic continuity in the cathode. Optimization of the cathode formulation should significantly improve the cathode behavior to allow a proper evaluation of the molecular structure.

Synchrotron Radiation Studies of Structure, Rechargeability and Corrosion in Li/SPE/FeS₂ Battery System

Rambabu Bobba

Department of Physics, Southern University A&M College, Baton Rouge LA 70813

(504)-771-4130, fax: (504)-771-2495

Objectives

- Investigate the relationship between the structure and rechargeability of FeS₂ electrodes by utilizing using synchrotron radiation based XAS and EXAFS and other *in situ* methods.
- Evaluate the performance of Li/FeS₂ cells.

Approach

- Utilize the synchrotron radiation source at the Center for Advanced Microstructures and Devices (CAMD) for *in situ* EXAFS studies of structure and electronic properties of Li/FeS₂ battery system.

Accomplishment

- EXAFS system has been built for electrochemical studies using the double-crystal monochromator beam line (port 5B) at CAMD.

Future Directions

- Initiate *in situ* EXAFS studies of Li/FeS₂ cells.
-

The objective of this project is to understand the structural integrity and rechargeability of FeS₂ electrodes in Li/FeS₂ cells using EXAFS. An electrochemical cell for *in situ* EXAFS measurements of the FeS₂ electrode was designed. The cell consists of a pyrite electrode, three layers of filter paper as an electrolyte separator and a thick carbon (Grafoil) electrode. The design configuration for the test cell is Al (0.25 μm), Mylar (1.5 μm), pyrite (10 μm), PEO (6 μm), Li (250 μm) layers sandwiched between support screens. It is a prismatic cell with the cathode/electrolyte interface exposed to the X-ray radiation to study the absorption as a function of energy at both the Fe edge and S edge. An allotment of synchrotron beamtime to perform EXAFS is reserved for the experiments.

The EXAFS system for electrochemical studies was installed on the beam line (port 5A) at the Center for Advanced Microstructures and Devices (CAMD), Baton Rouge, LA. This beam line will be used for a number of experimental techniques: EXAFS, NEXAFS, diffraction, fluorescence X-ray analysis and photoelectron spectroscopy. A Nicolet FTIR spectrometer has been installed in our laboratory. Dr. D. Scherson, a consultant for this project, has visited CAMD to provide direction and information to conduct the EXAFS measurements, and both a student and a research associate spent a week in Dr. Scherson's laboratory learning techniques for making rechargeable Li batteries. Software and the source used to analyze EXAFS data were obtained. A glove box and a portable trace oxygen analyzer for *in situ* measurements were ordered.

D. CROSS-CUTTING RESEARCH

Cross-cutting research is carried out to address fundamental problems in electrocatalysis, current-density distribution and gas evolution, solution of which will lead to improved electrode structures and performance in batteries and fuel cells.

Analysis and Simulation of Electrochemical Systems

*John Newman (Lawrence Berkeley National Laboratory)
201 Gilman Hall, University of California, Berkeley CA 94720
(510) 642-4063, fax: (510) 642-4778*

Objectives

- Improve the performance of electrochemical cells used in the interconversion of electrical energy and chemical energy by identifying the phenomena that control the performance of a system.
- Identify important parameters which are crucial to the optimization of an advanced secondary battery.

Approach

- Utilize electrochemical engineering principles and advanced computer techniques to develop mathematical models

Accomplishments

- A model which describes the impedance response of a rechargeable Li battery at open circuit has been developed. Some analytic solutions in limiting cases have also been developed.
- The metal hydride/NiOOH battery has been modeled in both one-dimensional and full two-dimensional form.
- A model has been developed which predicts the behavior of electrochemical double layer capacitors during operating conditions. The effect of side reactions, which have a pronounced impact on the cycling behavior, was included in the model.

Future Directions

- Salt precipitation in the separator will be considered in the basic Li battery model.
 - Transport of protons in NiOOH, which may be nonuniformly oxidized, will be considered as an extension of the present model.
 - The capacitor model will be extended to include thermal and concentration effects on the double layer, and the model will be used for the design of large-scale energy storage devices.
-

The Li battery has been modeled in both the Li foil and "rocking chair" configurations. The "rocking chair" system is based upon two materials which insert Li at different potentials. Experiments were conducted to verify the model, in particular by examining the Na analog of the lithium/cobalt dioxide cell. Transport properties and thermodynamic data were gathered over a wide range of salt concentrations for the polymer

electrolyte, polyethylene oxide/sodium trifluoromethane-sulfonate. Further experimental verification was obtained by collaboration with Bellcore by examining the behavior of their lithium/carbon/Mn₂O₄ spinel cell with a gelled electrolyte.

Several experimental techniques were reviewed and refined, including the steady-state current method of transport property measurements

and transition time experiments. Study has continued on limiting and simplified cases of Li battery design, and particular attention has been paid to capacity-rate behavior.

A model which describes the impedance response of the Li battery at open circuit has been developed. This will provide insights into the measurement of important physical properties which govern the behavior of the system. Some analytic solutions in limiting cases have also been developed, which should prove useful in the analysis of this type of experimental data.

The metal-hydride/NiOOH battery has been modeled in both one-dimensional and full two-dimensional models. In conjunction with the project, a technique has been developed to determine an appropriate diffusion coefficient for use in mathematical simulations in some cases where the diffusion coefficient depends strongly upon the state of charge.

The important phenomena related to electrochemical double-layer capacitors and so-called "supercapacitors" have been identified, and a model has been developed to predict the behavior of these devices under projected operating conditions. The model includes the effect of side reactions, which have been shown to have a pronounced effect on the cycling behavior of these devices.

Thermodynamic and transport properties of several systems are currently under study. Work is under way to measure the properties of LiMn_2O_4 . The transference number of aqueous KCl is being determined by using the potentiostatic polarization technique, as a means of verifying the technique. Solid-phase diffusion in NiO intercalation electrodes, prepared by sol-gel techniques, has been studied and measured.

PUBLICATIONS

Fuller, T.F. and J. Newman, "Electrochemical Processing (Introduction)," in *Kirk-Othmer Encyclopedia of Chemical Technology*, John Wiley and Sons, Inc., NY, Vol. 8, 111-123 (1994).

Fuller, T.F., M. Doyle and J. Newman, "Simulation and Optimization of the Dual Lithium Ion Insertion Cell," *J. Electrochem. Soc.* **141**, 1 (1994).

Mao, Z., R.E. White and J. Newman, "Theoretical Analysis of the Discharge Performance of a

H_2/NiOOH Cell," *J. Electrochem. Soc.* **141**, 54 (1994).

Battaglia, V.S. and J. Newman, "Magnetic Field Effects in High-Power Batteries I. The Penetration of an Electric Field into a Cylindrical Conductor," *J. Electrochem. Soc.* **141**, 703 (1994).

Battaglia, V.S. and J. Newman, "Magnetic Field Effects in High-Power Batteries II. Time Constant of a Radial Circuit Terminated by a Cylindrical Cell with Inductance," *J. Electrochem. Soc.* **141**, 708 (1994).

Fuller, T.F., M. Doyle and J. Newman, "Relaxation Phenomena in Lithium-Ion-Insertion Cells," *J. Electrochem. Soc.* **141**, 982 (1994).

Doyle, M., T. F. Fuller and J. Newman, "The Importance of the Lithium Ion Transference Number in Lithium/Polymer Cells," *Electrochim. Acta* **39**, 2073 (1994).

Newman, J., "Optimization of Porosity and Electrode Thickness with a Reaction-Zone Model," Proceedings of the Douglas N. Bennion Memorial Symposium, *Topics in Electrochemical Engineering*, PV 94-22, pp. 264-275, The Electrochemical Society, Inc., Pennington, NJ (1994).

Pals, C.R., M.M. Doyle, T.F. Fuller and J. Newman, "Modeling of Adiabatic and Isothermal Galvanostatic Discharge Behavior of the Lithium/Polymer/Insertion Cell," Proceedings of the Douglas N. Bennion Memorial Symposium, *Topics in Electrochemical Engineering*, PV 94-22, pp. 248-263, The Electrochemical Society, Inc., Pennington, NJ (1994).

Pals, C.R. and J. Newman, "Thermal Modeling of the Lithium/Polymer Battery. I. Discharge Behavior of a Single Cell," LBL-36294, November 1994.

Pals, C.R. and J. Newman, "Thermal Modeling of the Lithium/Polymer Battery. II. Temperature Profiles in a Cell Stack," LBL-36295, November 1994.

Doyle, M. and J. Newman, "The Use of Mathematical Modeling in the Design of Lithium/Polymer Battery Systems," LBL-35713, June 1994.

Heat Transport and Thermal Management in Advanced Batteries

James W. Evans (Lawrence Berkeley National Laboratory)
585 Evans Hall, University of California, Berkeley CA 94720
(510) 642-3807, fax: (510) 642-9164

Objectives

- Investigate by mathematical modeling and experimental measurement, heat generation and transport in advanced secondary batteries for EV applications.
- Evaluate the management of the temperature of Li/polymer batteries for optimum performance and to avoid temperature excursions that could damage the battery.

Approach

- Utilize mathematical models to analyze the thermal conduction properties of Li/polymer batteries.

Accomplishment

- A two-dimensional mathematical model revealed that the major resistance to heat transport in a Li/polymer-electrolyte battery is the polymer electrolyte.

Future Direction

- Determine the thermal conductivities of polymer electrolytes and other cell components.
-

The objectives of this project are to evaluate the management of the temperature of the battery for optimum performance and avoiding temperature excursions damaging to the battery. The initial investigation is on Li/polymer batteries that are under development to operate in the temperature range of ~60 to 140°C which is needed to obtain sufficient polymer conductivity and to avoid overheating.

Research has continued on the thermal behavior of large batteries suitable for use in EVs. These batteries are not 100% efficient which means that not all of the chemical energy stored in the battery is converted into electrical energy on discharge. The difference appears as thermal energy within the battery and must be managed if overheating and degradation of battery performance are to be avoided. Conversely, on charging the battery, a portion of the input electrical energy is consumed in the generation of heat. A second important consideration for batteries operating above ambient temperature is the provision of suitable insulation to prevent heat loss during periods of standby or low discharge rate.

These issues have been addressed using mathematical models for the unsteady state heat transport in multicell stacks. Most of the effort was directed towards mathematical modeling of Li-

polymer cells in two and three dimensions. Thermal analysis of Li-polymer batteries was used to examine the relationship between thermal behavior and design parameters. By studying the effect of stack size and cooling/insulating conditions on battery temperature under different discharge rates, information was obtained as to how to maintain the operating temperature by designing proper cell stacks and choosing the appropriate cooling/insulating systems. Moreover, temperature distributions within cell stacks for different cell designs, including different thicknesses of cell components and different current materials were calculated so as to carry out cell structure optimization from a heat transfer point of view. Finally, thermal characteristics of Li-polymer electrolyte batteries based on different positive electrodes (*e.g.*, V_6O_{13} , TiS_2 and redox polymer) were discussed.

The material within the battery that presents the major resistance to heat transport is the polymer electrolyte. The thermal conductivities of the polymer materials are not reported in the literature, and therefore an apparatus was obtained to measure conductivities. Conductivities for two polyethylene oxide-Li salt combinations were measured over a range of temperature.

PUBLICATION

Chen, Y. and J.W. Evans, "Thermal Analysis of Lithium Polymer Electrolyte Batteries by a Two-Dimensional Model - Thermal Behaviour and Design Optimization," *Electrochim. Acta* 39, 517 (1994).

Electrode Surface Layers

Frank R. McLarnon

90-2024, Lawrence Berkeley National Laboratory, Berkeley CA 94720
(510) 486-4636, fax: (510) 486-4260

Objectives

- Apply advanced *in situ* and *ex situ* characterization techniques to study the structure, composition and mode of formation of surface layers on electrodes used in rechargeable batteries.
- Identify film properties that improve the rechargeability, cycle-life performance, specific power, specific energy, stability and energy efficiency of electrochemical cells.

Approach

- Apply sensitive techniques such as ellipsometry, Raman spectroscopy and scanning electron microscopy to monitor the formation of surface layers on secondary battery electrodes.
- Incorporate foreign ions in porous nickel oxide electrodes to improve cycle performance in alkaline electrolytes.

Accomplishment

- A newly developed technique for low-energy ion implantation, MPIII, was used to implant Au, Pb, Ta, Ti, W and Ti_4O_7 in nickel oxide electrodes. Tests showed that the overpotential for O_2 evolution at the surface of a Ti_4O_7 -implanted Ni electrode is increased by 50-105 mV, compared with electrodes implanted with other elements.

Future Direction

- Continue studies of the effect of ion-implantation on the performance of nickel oxide electrodes and the use of ellipsometry and Raman spectroscopy.
-

Advanced *in situ* and *ex situ* characterization techniques are being used to study the structure, composition and mode of formation of surface layers on electrodes used in rechargeable batteries. The primary objective of this research is to identify film properties that improve the rechargeability, cycle-life performance, specific power, specific energy, stability and energy efficiency of electrochemical cells. Prior work on the evaluation of ion implantation as a means to improve the corrosion resistance of Pb battery electrode current-collector materials has been completed, and the present research seeks to characterize the

transformation of surface phases that accompanies the charging and discharging of Ni electrodes in alkaline electrolytes.

We have evaluated Au, Pb, Ta, Ti, W and Ti_4O_7 as dopants to the Ni electrode because of their relatively poor surface catalytic behavior with respect to O_2 evolution, however the effects of these species on electrochemical inter-conversions in Ni electrodes have not been well studied. A low-energy ion implantation technique known as Metal Plasma Immersion Ion Implantation (MPIII) was selected to change the chemical character of the Ni electrode surface and thereby alter the

O₂-evolution reaction. The MPIII electrode bias potential and the duty cycle of the substrate bias pulser were controlled at -2 kV (the beam energy varies from 3.2 to 6.2 keV depending on the mean ion charge for individual elements) and 25%, respectively, to produce an ion-penetration depth of ~2-3 nm. The dose levels of implanted ions were estimated to be 4×10^{15} - 2×10^{16} /cm², which implies that the atomic fraction of foreign atoms at the Ni electrode surface is ~30%. Preliminary tests showed that the overpotential for O₂ evolution at the surface of a Ti₄O₇-implanted Ni electrode is increased by 50-105 mV, compared with electrodes implanted with other elements. However this suppression of O₂ evolution did not result in a better electrode performance. Of the doping materials investigated thus far, Au, W, and Pb performed the best with respect to overall charge/discharge characteristics.

Deconvolution of the measured *in-situ* ellipsometric spectra allowed us to quantitatively analyze the interconversion between Ni(OH)₂ and NiOOH. We estimated the initial charge efficiency of an Au-implanted electrode to be ~90%, but it dropped to ~30% during the charging process. These values are significantly lower than those obtained in the electrode with Co additives by high-energy ion implantation techniques. This fact suggests that the bulk effects rather than surface effects may play a more important role in porous Ni battery electrodes.

PUBLICATION

Zhang, S.T., F.P. Kong and R.H. Muller, "Effect of Ion Implantation on the Corrosion Behavior of Lead and a Lead-Antimony Alloy," *J. Electrochem. Soc.* **141**, 2677 (1994).

Electrode Kinetics And Electrocatalysis

Philip N. Ross, Jr.

2-100, Lawrence Berkeley National Laboratory, Berkeley CA 94720
(510) 486-6226, fax: (510) 486-5530

Objectives

- Develop an atomic level understanding of the processes taking place in complex electrochemical reactions at electrode surfaces.
- Determine the relationship between the kinetics of electrode processes and the atomic structure of the electrode surface by using a variety of surface- or bulk-sensitive techniques.

Approach

- Employ LEED to study single crystals, HREM in the case of carbon electrode materials, and EXAFS for organometallic catalysts.
- Utilize LEIS and AES to study the composition of sputtered and UHV-annealed polycrystalline Pt-Ru bulk alloys for methanol electrocatalysis.

Accomplishment

- It was found that the property of Ru atoms to nucleate oxygen-containing species at low potentials produced a strong enhancement in the catalytic activity of sputter-cleaned Pt-Ru alloy electrodes compared to pure Pt, thereby supporting the concept of the bifunctional character of the oxidation process of these alloys.

Future Direction

- Continue the study of CO tolerance in low-temperature acid fuel cells and in parallel begin the examination of methanol oxidation on one or more new Pt alloy systems.
-

The objective of this project is to develop an atomic-level understanding of the processes taking place in complex electrochemical reactions at electrode surfaces. Physically meaningful mechanistic models are essential for the interpretation of electrode behavior and are useful in directing the research on new classes of materials for electrochemical energy conversion and storage devices.

The electrocatalytic activity of well-characterized Pt-Ru alloy electrodes towards the electrooxidation of CO in acidic electrolyte at room temperature was measured on alloy surfaces prepared in UHV. A clearly defined surface composition was determined *via* low energy ion scattering (LEIS). Electrocatalytic activities were measured by CO stripping voltammetry as well as by potentiostatic oxidation of adsorbed CO. It was found that the property of Ru atoms to nucleate oxygen-containing species at low potentials produced a strong enhancement in the catalytic activity of sputter-cleaned Pt-Ru alloy electrodes compared to pure Pt, thereby supporting the concept of the bifunctional character of the oxidation process of these alloys. A further synergistic effect of the alloy with a Ru surface composition of ca. 50 at% Ru was observed, with a catalytic shift in the CO electrooxidation current of -0.25 and -0.15 V compared to pure Pt and pure Ru surfaces, respectively. This synergism was attributed to a uniquely active state of OH_{ads} on Pt-Ru pair sites. The different electrocatalytic activities of sputter-cleaned *vs.* annealed Pt-Ru alloy electrodes with essentially identical Ru surface compositions are attributed to Ru clustering during annealing.

Voltammetry combined with single-potential alteration infrared spectroscopy (SPAIRS) was used to study the extent of adsorbed CO produced at Pt, Ru and Pt-Ru alloy electrodes during methanol and formic acid oxidation in acidic supporting electrolyte. The addition of even small atomic fractions of Ru to Pt surfaces caused a decrease in the quasi-steady-state level of CO on the surface for both reactions. This result is consistent with the bifunctional mechanism proposed previously: Ru sites nucleate oxygen-containing species at ca. 0.2-0.3 V lower potential than on the pure Pt surface, and the adsorption of methanol occurs on Pt ensembles producing adsorbed CO. In the case of formic acid, adsorption is equally facile at Pt-Pt, Pt-Ru and Ru-Ru sites, with dehydration producing adsorbed CO. The further electrooxidation of CO is catalyzed by oxygen-containing species nucleated on nearby Ru atoms. The improved efficiency of the alloy surfaces for oxidation of adsorbed CO at low

potential shifts the rate-limiting step to the adsorption step, which results in very low coverages of the surfaces by adsorbed CO.

High-resolution electron microscopy (HREM) and X-ray microchemical analysis were used to characterize composition, size, distribution and morphology of Pt-Ru particles with nominal Pt:Ru ratios 1:1 and 3:1, supported on carbon black. The particles are predominantly single nanocrystals with diameters in the order of 2.0 to 2.5 nm. Occasionally, twinned particles are also observed. All investigated particles represent solid solutions of Pt and Ru with compositions very close to the nominal one. Based on two-dimensional projection in high-resolution images, it is suggested that the well-resolved particles are of cubooctahedral shape. In addition to {200} and {111} facets, {113} facets are also observed.

The electrochemical oxidation of hydrogen, carbon monoxide and dilute mixtures of carbon monoxide in hydrogen on a well-characterized Pt₃Sn alloy electrode was examined using the rotating disk electrode technique in 0.5 M sulfuric acid at 62°C. A non-equilibrium surface of the alloy produced by sputter-etching was found to be much more active than the annealed surface and this surface was studied. The potential for the onset of carbon monoxide oxidation on this surface was nearly 600 mV lower than for pure Pt and approximately 150 mV lower than pure Ru or any Pt-Ru alloy. The potential for the onset of the oxidation of hydrogen in the presence of 0.1-2% CO coincides with the potential for the onset of CO oxidation on the alloy surface. The polarization curve for the oxidation of these gas mixtures is shifted cathodically by more than 400 mV with respect to that for pure Pt. The shift is attributed to the bifunctional action of the two metals on the alloy surface, with the Sn sites nucleating oxygenated species at low potential enabling oxidation of CO adsorbed on neighboring Pt sites to occur at low potential; oxidation of the adsorbed CO frees up Pt sites for hydrogen oxidation.

PUBLICATIONS

Gasteiger, H., N. Markovic, P. Ross and E. Cairns, "CO Oxidation on Well-Characterized Pt-Ru Alloys," *J. Phys. Chem.* **98**, 617 (1994).

Gasteiger, H., N. Markovic, P. Ross and E. Cairns, "Temperature-Dependent Methanol Electro-oxidation on Well-Characterized Pt-Ru Alloys," *J. Electrochem. Soc.* **141**, 1795 (1994).

Gasteiger, H., N. Markovic, P. Ross and E. Cairns, "Electrooxidation of Small Organic Molecules on Well-Characterized Pt-Ru Alloy Surfaces," *Electrochim. Acta* 39, 1825 (1994).

Markovic, N. and P. Ross, "Study of Bismuth Ruthenate as an Electrocatalyst for Bifunctional Air Electrodes," *J. Electrochem. Soc.* 141, 2590 (1994).

Poisoning of Fuel Cell Electrocatalyst Surfaces: NMR Spectroscopic Studies

Elton J. Cairns

90-3026, Lawrence Berkeley National Laboratory, Berkeley CA 94720

(510) 486-5028, fax: (510) 486-5454

Objective

- Obtain information on the nature of the poisoning intermediate(s) in CH₃OH electrooxidation on Pt-based electrocatalysts by NMR and PDS.

Approach

- Apply NMR and PDS to obtain information about surface poisoning on Pt supported on graphite and Pt anodes in electrolytes containing methanol.

Accomplishment

- Experiments are underway to detect and characterize surface species on Pt by NMR and PDS.

Future Direction

- Establish the feasibility of NMR and PDS to detect surface poisons during methanol electrooxidation.
-

Platinum is the most active single-component catalyst for CH₃OH electro-oxidation in direct methanol fuel cells (DMFCs); however, poisoning reactions at the surface render the anode ineffective under target operating conditions. Recently, a number of *in-situ*, on-line, and *ex-situ* techniques have been utilized to obtain information on the nature of the poisoning intermediate(s) in this system. Significant advances have been made towards this end, although no present technique can yield information on practical (supported, dispersed) electrocatalysts *via in-situ* analysis. In this project, two spectroscopic techniques, nuclear magnetic resonance (NMR) and photothermal deflection spectroscopy (PDS), are utilized to study the presence of surface species which are formed during the electrooxidation of CH₃OH on the electrocatalyst surface.

Nuclear Magnetic Resonance Spectroscopy. NMR is a quantitative, non-destructive, bulk method of probing the chemical environment of a specific nucleus. In the last two decades the technique has been used successfully in the field of gas-phase catalysis as a tool for identifying and characterizing chemisorbed species on practical catalysts. Our research seeks to extend the application of NMR spectroscopy to studies of

surface poisoning of carbon-supported Pt and Pt-alloy DMFC anodes.

For these experiments, we have designed and constructed a glass three-electrode electrochemical cell for use in a narrow-bore (5 cm) spectrometer operating at a proton frequency of 270 MHz (illustrated on p. 6 of the *Energy Conversion & Storage Program 1993 Annual Report*, LBL-35242). The working electrode material is commercially obtained and is composed of 20 wt% Pt on Vulcan XC-72 carbon. These catalyst particles are further supported on a thin carbon cloth. This cloth is rolled tightly to form a cylindrical porous plug, filling the working electrode chamber inside of the NMR transmitter/receiver coil with an active catalyst surface area of ~3 m².

We have carried out preliminary studies on a model system of adsorbed CO. Lending justification to this choice are results of *in situ* infrared studies of smooth Pt electrodes which have suggested CO as the main poisoning adsorbate in the CH₃OH reaction. We have set up a flow system for adsorption of ¹³C-enriched CO from CO-saturated aqueous H₂SO₄. Because CO is irreversibly adsorbed on the Pt surface, we are able to monitor adsorption indirectly by voltammetrically observing the suppression of H adsorption (Fig. 21).

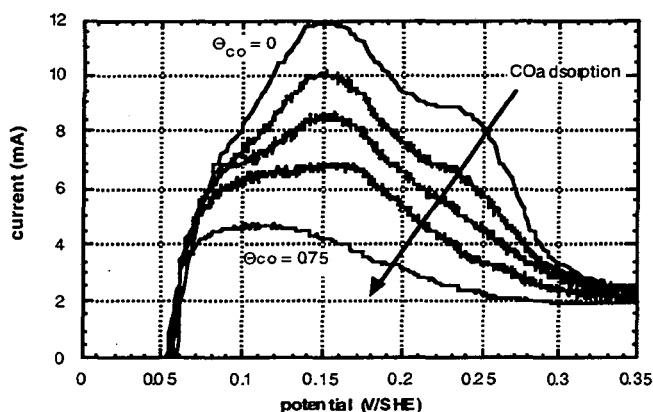


Figure 21. Electrochemical monitoring of CO adsorption onto carbon-supported Pt electrocatalysts. Sweep rate = 0.2 mV/s, electrolyte is 3 M H₂SO₄.

Our current efforts are focused on the detection and isolation of the ¹³C NMR signal arising from ¹³CO adsorbed on the electrodes described above under open-circuit conditions. With these initial studies we hope to establish the feasibility of NMR for providing *in situ* information on species adsorption at the electrode-electrolyte interface. We will

then have a firm base for studying surface poisoning in the CH₃OH electrooxidation reaction.

Photothermal Deflection Spectroscopy. The purpose of this work is to use *in situ* PDS to study CH₃OH electrooxidation on a Pt electrode surface. With PDS, we can measure the absorption spectrum of the electrode surface and simultaneously detect concentration gradients in the electrolyte, thus allowing us to better understand the mechanism of the electrooxidation reaction. We have carried out initial experiments using probe beam deflection to detect the electrolyte concentration gradients that accompany the formation and removal of platinum oxide films. We have found that the deflectograms (graphical output from the probe beam deflection signal) for three acidic media (H₃PO₄, H₂SO₄ and HClO₄) show slight differences due to specific anion adsorption on the electrode surface. However, we discovered that the deflectogram changes its shape remarkably for an electrolyte contaminated by trace amounts of metal ions (Figure 22). In comparing PDS results to those obtained with cyclic voltammetry, we found PDS to be more sensitive to metallic ion contamination on the Pt electrode; metal-ion concentrations of about 10⁻⁷ M can be detected by PDS.

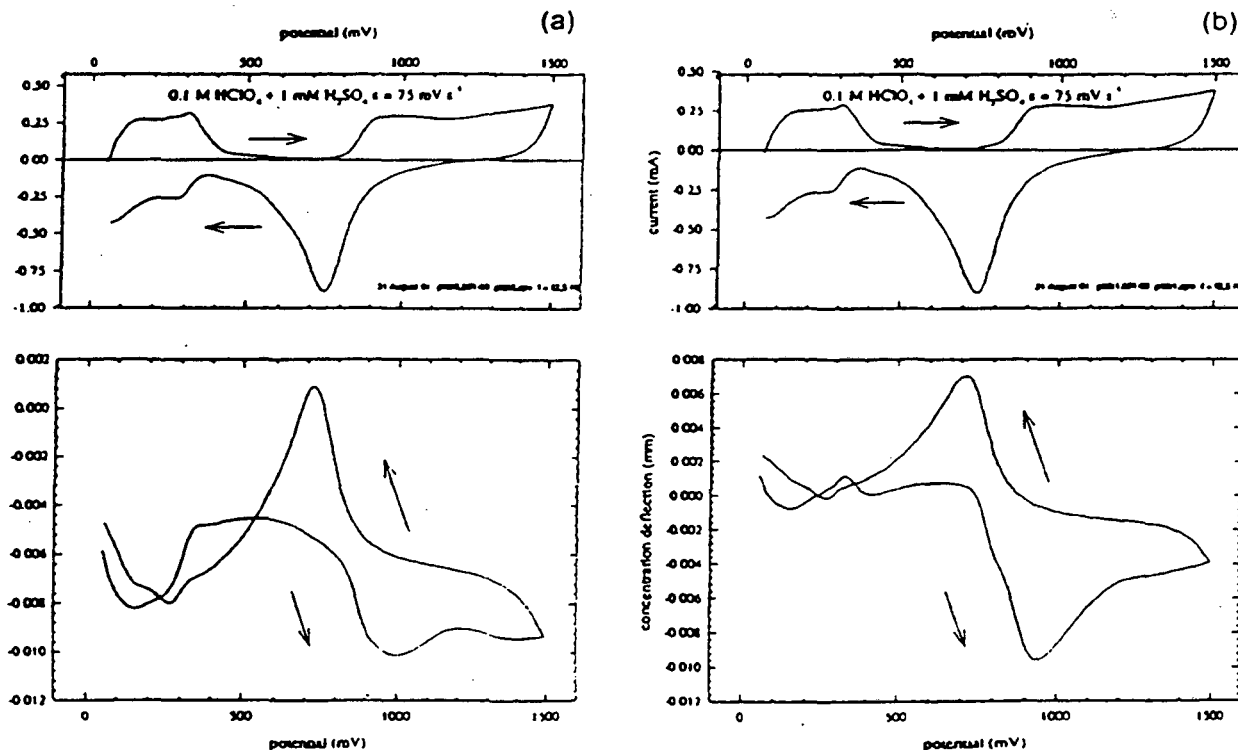


Figure 22. Voltammogram (upper panel) and corresponding deflection (lower panel) recorded on Pt at 24°C in 0.1 M HClO₄ + 0.001 M H₂SO₄ electrolyte: (a) without contamination and (b) contaminated by metallic ions.

Before PDS can be used to study the CH₃OH electrooxidation reaction on Pt electrodes, it is necessary to develop physically meaningful mechanistic models which are essential for the interpretation of electrode behavior. For this purpose, mathematical models which solve the

diffusion equations for the time-varying flux boundary conditions at the electrode will be used to predict the concentration gradients and the corresponding electrolyte refractive-index gradients.

Effect of Electrocatalyst and Electrolyte on Direct Hydrocarbon and Methanol/Air Fuel Cell Performance

Elton J. Cairns and Frank R. McLarnon

90-2024, Lawrence Berkeley National Laboratory, Berkeley CA 94720

(510) 486-4636, fax: (510) 486-4260

Objectives

- Demonstrate in a realistic system that the electrooxidation of methanol is efficient and produces only H₂O and CO₂ as reaction products.
- Explore the feasibility of a direct-hydrocarbon solid-polymer-electrolyte fuel cell (SPEFC).

Approach

- Fabricate model fuel cell and analyze the exit gases from the electrooxidation of methanol.
- Design and fabricate a model fuel cell and investigate the electrochemical performance with a variety of hydrocarbon fuels.

Accomplishment

- Fuel cells with 20-cm² electrodes were designed and fabricated. Studies of the direct electrochemical oxidation of methanol and hydrocarbon fuels in liquid alkali carbonate and SPEs, respectively, are underway.

Future Directions

- Optimize DMFC performance by varying the composition of the electrode and electrolyte, and adjusting the operating temperature (80-140°C).
 - Analyze the exit gases from a fuel cell utilizing hydrocarbon fuels.
-

Fuel cells offer the promise of higher energy conversion efficiency and greatly reduced emissions, compared to combustion engines, and they are being developed for use in EVs. However, present-day fuel cells operate on H₂, so either a H₂-storage device or a reformer must be carried on-board the vehicle. Each of these H₂-delivery options results in a heavy, bulky, costly, slow-reacting, and complex fuel-cell power plant. There is a strong need to develop a fuel cell that can electrochemically oxidize liquid fuels, and the successful development of a DMFC would represent a major advance for fuel-cell-powered vehicles. However, some major obstacles must be addressed

before acceptable performance can be attained with DMFCs. The oxidation rate of CH₃OH is several orders of magnitude lower than that of H₂ on a Pt catalyst, and oxidation products other than the expected H₂O and CO₂ were observed in some cases. The problem of the slow oxidation rate of CH₃OH has been partially addressed by utilizing bimetallic catalysts. Previous work in this laboratory has confirmed that a Pt/Ru catalyst supported on graphitized carbon has a significantly higher catalytic activity for the oxidation of CH₃OH than supported Pt alone. Other options involving hydrocarbon fuels and SPEFCs are also being considered in this project.

Liquid Electrolyte. Cathode deactivation and the formation of CH_2O in acidic electrolytes, and the unwanted formation of carbonates in hydroxide electrolytes, have prompted previous researchers to study buffered electrolytes. Aqueous Cs_2CO_3 appears to be an electrolyte that does not suffer from the shortcomings of acidic and other alkaline electrolytes. The major goal of this research project is to demonstrate in a realistic system that the electrooxidation of CH_3OH is efficient and produces only H_2O and CO_2 as reaction products. A model fuel cell was designed and fabricated to accommodate 20-cm^2 electrodes. Electrodes of various catalyst loadings and polytetrafluoroethylene (PTFE) content have been prepared and tested in both half-cell and full-cell configurations, utilizing both H_2SO_4 and Cs_2CO_3 electrolytes and H_2 and CH_3OH feeds. The electrodes have a bi-layered structure, consisting of a semi-hydrophilic reaction layer which is pressed onto a hydrophobic gas diffusion layer. The active surface area is $18\text{-}20\text{ cm}^2$ with a metal loading of 0.3 to 0.5 mg/cm^2 . Recent efforts have addressed various problems including electrolyte seepage through the electrodes, inadequate catalyst wetting and possible catalyst poisoning. Future experiments will seek to optimize DMFC performance by varying the composition of the electrode and electrolyte, and adjusting the operating temperature ($80\text{-}140^\circ\text{C}$). Analyses of the exit gases will be performed to determine if CH_3OH oxidizes completely to benign reaction products. An examination of an optimized system will be performed to ascertain its suitability for EVs and other applications.

Polymer Electrolyte. SPEFC appear to be one of the most-promising systems for transportation applications due to their high power and energy density and low-temperature operation. Many researchers are investigating the possibility of a direct-methanol SPEFC because of problems such as on-board storage of H_2 or in-vehicle reforming of fuels such as CH_3OH . Although CH_3OH is one of the most electroactive organic fuels its performance in SPEFCs is significantly degraded by the undesirable crossover of fuel from the anode to the cathode. The crossover rate is substantial because of the affinity of the perfluorinated sulfonic acid (PFSA) membrane electrolyte for CH_3OH as well

as water. Because CH_3OH and water are similar polar molecules, the prospect for developing a separator that can discriminate between them is not very promising.

The goal of this research project is to explore the possibility of a direct-hydrocarbon SPEFC. Because of the slow anodic oxidation rate of hydrocarbons, especially at low temperatures, such systems have not been examined in recent years. However, the same factors which have produced a significant improvement of fuel cell reaction kinetics with PFSA electrolytes, compared to other acids, may also significantly enhance the electrochemical oxidation rate of hydrocarbons. PFSA is a superacid and the anions are strongly hydrated in addition to being essentially immobilized by the membrane structure; this results in minimal anion adsorption on the electrocatalyst surface. Although the direct electrochemical oxidation rate of hydrocarbons will likely be substantially slower than that of H_2 or CH_3OH , the overall performance of a direct-hydrocarbon SPEFC may be justified by the convenience and low cost of using these fuels. Also, because hydrocarbons are non-polar, crossover should not be a significant problem in this system.

A model SPEFC was designed and fabricated to accommodate 20-cm^2 electrodes. Polarization tests utilizing H_2 fuel are underway to calibrate the cell performance. These results will be used as a comparison for future experiments with a variety of hydrocarbon fuels. The performance of alkanes and alkenes as well as mixtures of these fuels, such as natural gas, will be investigated. Analyses of the exit gases will be performed to determine if these fuels oxidize completely to benign reaction products. Experiments using electrocatalysts other than Pt will also be conducted with these fuels. An examination of the results will be performed to ascertain the feasibility of direct-hydrocarbon SPEFCs for EVs and other applications.

PUBLICATION

Kinoshita, K. and E.J. Cairns, "Fuel Cells,"
Encyclopedia of Chemical Technology **11**, 1098
(1994).

IV. AIR SYSTEMS RESEARCH

The objectives of this program element are to identify, characterize, and improve materials for air electrodes; and to identify, evaluate, and initiate development of metal/air battery systems and fuel-cell technology for transportation applications.

A. METAL/AIR CELL RESEARCH

Metal/air cell research addresses O₂ electrocatalysis; bifunctional air electrodes, which are needed for electrically rechargeable Zn/air cells; and novel alkaline Zn electrode structures.

Novel Concepts for an Oxygen Electrode in Secondary Metal-Air Batteries

Eric J. Rudd

*Eltech Research Corporation, 625 East Street, Fairport Harbor OH 44077
(216) 357-4073, fax: (216) 357-4077*

Objectives

- Investigate the electrochemical stability of graphitized carbons and metal oxides in bifunctional air electrodes.
- Provide improved bifunctional air electrodes for electrically rechargeable metal/air batteries.

Approach

- Fabricate bifunctional air electrodes using graphitized carbon and selected metal oxide electrode catalysts and evaluate their performance in half-cell tests.
- Determine the cycle life of these electrodes in Zn/air cells.

Accomplishment

- Achieved 145 cycles with electrodes containing graphitized carbon black (Monarch 120) for the support and La_{0.6}Ca_{0.4}CoO₃ as electrocatalysts in 35 wt% KOH at room temperature.

Future Direction

- Project was completed.
-

The objective of this research is to develop improved bifunctional air electrodes for electrically rechargeable Zn/air cells. The successful development of bifunctional air electrodes depends on selecting electro-chemically stable support materials and electrocatalysts for O₂ reduction and evolution, and the fabrication of suitable porous structures that are capable of extended operation. In this program, the properties of corrosion-resistant substrates such as semi-graphitic carbon, graphite or non-carbon materials were investigated. For the electrocatalyst, stability in a strongly alkaline environment and

over the range of potentials from -300 to +700 mV vs. Hg/HgO was considered. The structure must provide the three-phase boundary necessary for the electroreduction of oxygen and yet be suitably hydrophobic to prevent flooding of the electrode by the electrolyte.

In the early phase of this project, either graphitized Shawinigan Black or graphitized Cabot Monarch 120 was used as the substrate in the active layer of the electrode and selected metal oxides were evaluated as catalysts. The second phase of the program, initiated in May 1993, included a "bicatalyst" approach as well as

investigating the activity and stability of two perovskite catalysts, lanthanum nickelate and lanthanum calcium cobalt oxide.

The performance of eight electrodes was determined in both half cells and single zinc/air cells, the latter effort being completed at MATSI Inc. (R. Putt). It had been determined earlier with a single Zn/air cell that the performance can be regarded as "unacceptable" when the discharge voltage is less than 0.8 V (at 10 mA/cm²) and the charge voltage is more than 2.15 V (at 5 mA/cm²). It is calculated that these criteria correspond to oxygen electrode potentials of -0.3 V and +0.8 V vs. Hg/HgO.

A comparison of the performance of the eight electrodes is shown as Table 5, the "end of life" being determined as stated above. The half cell and single cell tests were carried out at room temperature, using 35 wt% KOH as the electrolyte and the cycle was as follows:

Discharge (or polarize the oxygen electrode cathodically) at 10 mA/cm² for four hours,

Charge (or polarize the oxygen electrode anodically) at 5 mA/cm² for eight hours.

The performances in the single cell and half cell correlate reasonably well for electrodes A2, B1 and B2; unfortunately the tests with electrodes A1 and A4 were compromised. The results with electrodes A3 and B3 were widely different suggesting non-uniformity in the parent 8" x 8" electrode.

The data raise a number of questions and certainly some conflicting trends are evident. However, the data are largely based on single tests. It would be important to repeat the studies, at least with the more promising catalyst/substrate combinations. It is also evident that consumer applications will likely require current densities of 20-30 mA/cm², particularly for the charge cycle and it would therefore be of interest to explore the effect of a charge/discharge cycle using higher current densities.

Table 5

I.D.	Composition of Active Layer	No. of Cycles Completed	
		Half Cell	Single Cell
A1	SB2700 + CoTMPP + NiCo ₂ O ₄	125*	80**
A2	SB2700 + La _{0.6} Ca _{0.4} CoO ₃	97	105
A3	SB2700 + LaNiO ₃	152	23
A4	SB2700 + CoTMPP + La _{0.6} Ca _{0.4} CoO ₃	125*	60**
B1	SR2700 + CoTMPP + NiCo ₂ O ₄	65	35
B2	SR2700 + La _{0.6} Ca _{0.4} CoO ₃	120+	145
B3	SR2700 + LaNiO ₃	100+	23
B4	SR2700 + CoTMPP + La _{0.6} Ca _{0.4} CoO ₃	65	15
* cell test was interrupted			
** electrode damaged during cell maintenance			
+ initial polarization characteristics were poor			

B. FUEL CELL RESEARCH

Fuel cell research includes projects in several areas of electrochemistry: fuel-cell testing, fuel processing, fuel-cell component characterization and theoretical studies.

Fuel Cells for Renewable Applications

Shimshon Gottesfeld

Los Alamos National Laboratory, MS D429, P.O. Box 1663, Los Alamos NM 87545

(505) 667-0853, fax: (505) 665-4292

Objectives

- Identify, evaluate and initiate development of fuel cell technology for transportation applications.
- Conduct basic research in electrochemistry to explore and improve the potential of fuel cell systems for use in transportation applications.

Approach

- Apply electrocatalysis and heterogeneous catalysis principles to develop improved electrode materials for PEFCs.
- Utilize experimental techniques to determine the transport properties of polymer electrolyte membranes.
- Test laboratory-scale fuel cells to obtain information on the performance of cell components.

Accomplishments

- For the first time, "limiting currents" significantly in excess of 2 A/cm² were obtained for H₂/air PEM fuel cells under ordinary operating conditions.
- Experiments established that with a cathode of low Pt loading (0.4 mg/cm²), the cathode loss caused by methanol cross-over could easily reach 100 mV.
- The diffusion coefficient of methanol measured by NMR in Nafion membranes is only a factor of 2-3 smaller than in aqueous solutions, which is an important factor contributing to the sizable cross-over rates observed.

Future Directions

- Continue tasks to improve the performance and life of PEM fuel cells, and to identify new low-cost components for these fuel cells.
 - Continue efforts to improve the performance of DMFCs.
-

The primary focus of this program is to develop efficient and cost-effective polymer electrolyte fuel cells (PEFC) for transportation applications. The specific goals of the program are to: *i*) reduce the cost of the Pt catalyst and ionomeric membrane, *ii*) increase the efficiency and power density of the PEFC, *iii*) optimize the system for operation on reformed organic fuels and air, *iv*) achieve stable, efficient, long-term operation, and *v*) solve key

technical issues that impede the development of the DMFC.

Thin-Film Catalyst Technology. Electrode structures containing low Pt loadings are needed for commercialization of PEFCs. The electrode structures developed at LANL are based on utilizing the ionomer as a binding agent for the catalyst layer and on application of the catalyst layer to the membrane. These are described as "thin-film" catalyst layers because the high

performance is obtained with a very low catalyst loading (0.12-0.16 mg Pt/cm²) in a very thin layer (< 10 μm thick). PEM fuel cell performances obtained this year with M&Es based on four different ionomeric membranes are shown in Figures 23 and 24 for operation on pressurized H₂/O₂ and on pressurized H₂/O₂, respectively. These performances can be obtained with very high fuel utilizations and with the utilization in the air electrode ranging between 25 and 50%.

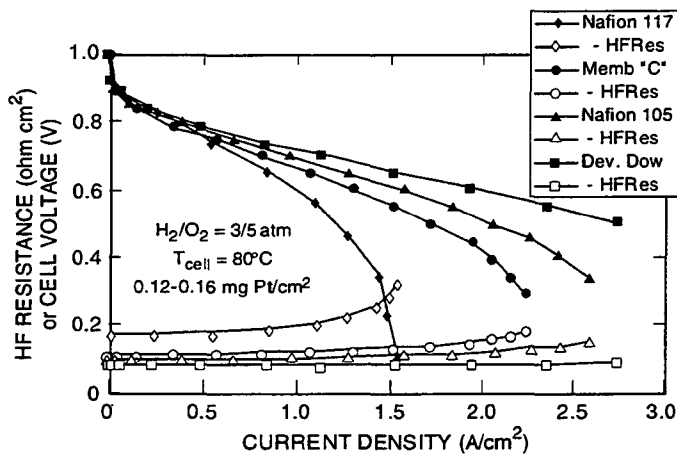


Figure 23. PEM H₂/O₂ fuel cell polarization curves obtained with the LANL membrane/electrode assemblies based on thin-film catalyst layer applied directly to four types of ionomeric membranes. Operation conditions are specified in the figure.

Several life tests of single cells with M&Es based on such thin-film catalysts were completed. The iR-corrected polarization curves exhibited negligible change with time after 3000-4000 h, indicating a highly stable catalyst structure. Indications are available that this mode of fabrication of M&Es would also enable use of thinner membranes and provide higher cell performance, as demonstrated by the long life (over 2000 h) obtained in a cell with a Nafion[®] 112 (50 μm thick) membrane.

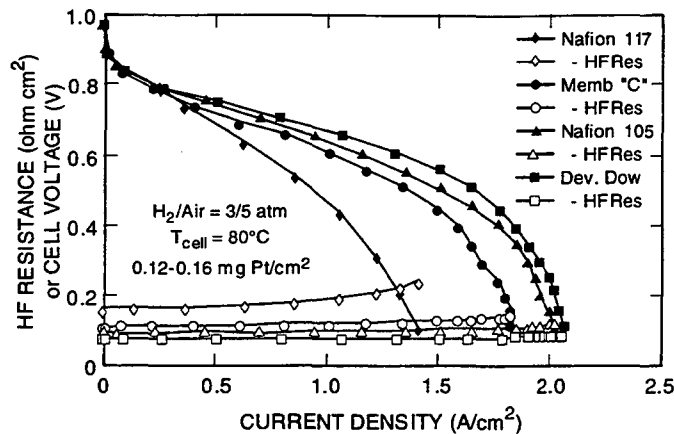


Figure 24. Same as Figure 23, for operation on H₂/air.

Membrane Characterization. Investigations of the dependence of transport properties in poly-PFSA membranes on membrane pretreatment conditions are continuing. Specifically, studies of the conductivity of Nafion 117 membranes swollen in glycerol at elevated temperatures were completed. Figure 25 shows that PFSA membranes treated in glycerol at elevated temperature are capable of imbibing very large amounts of water if the treatment temperature is above the glass transition temperature of the membrane. Previous work showed that the water content in Nafion 117 reaches 22 H₂O/H⁺ for membranes equilibrated with boiling water and that the membrane conductivity increased monotonically with water content in Nafion 117 up to the level of 22 H₂O/H⁺. It was concluded that the increase in water content seemed to proportionately enhance the mobility of protons in the membrane. However, at even higher degrees of membrane swelling, as obtained by the treatment in glycerol at T > 100°C, the protonic conductivity in the super-swollen membrane actually *decreases with increased water content*, as shown for a Nafion 117 membrane in Figure 26. This interesting decrease in conductivity is apparently brought about by spreading apart of the polymer side chains terminated in sulfonate anions. As this distance increases, it becomes more difficult for the protons to hop along the pore wall from side chain to side chain in the highly swollen polymer.

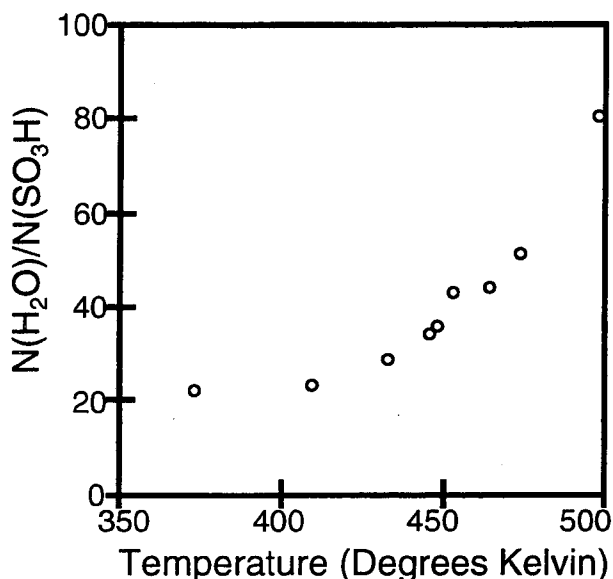


Figure 25. Room temperature water uptake by Nafion 117 membranes pre-swollen in glycerol at temperatures well above the boiling point of water.

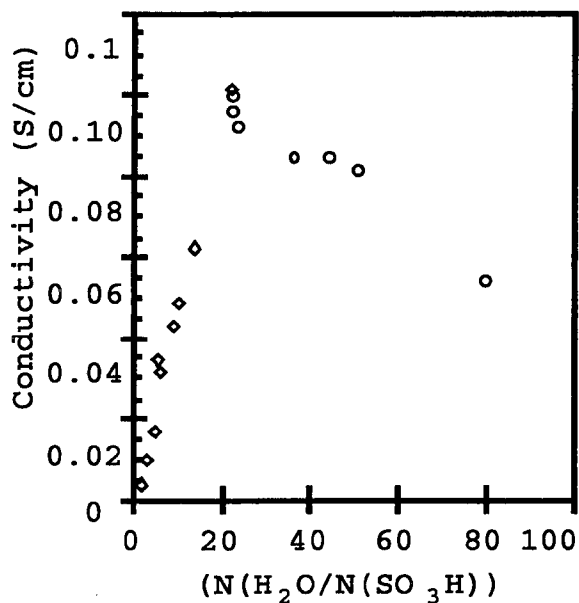


Figure 26. Conductivity of Nafion 117 at room temperature as a function of water content including super-swollen membrane data.

Backing And Flow Field Optimization. To ensure an optimized level of liquid water in the cathode catalyst layer without excessive "flooding", the thin-film catalyst requires a partly hydrophobic, microporous layer for the catalyst substrate. Recent experiments with a machine-

made product which is much thinner than the hand-made uncatalyzed gas-diffusion electrode used previously were conducted. The improvements obtained for air operation of the PEFC have been substantial. For the first time, "limiting currents" significantly in excess of 2 A/cm² were obtained for H₂/air PEM fuel cells under ordinary operating conditions, using membrane electrolytes of ordinary thickness. Comparison of iR-corrected polarization curves for single PEM fuel cells with standard and with improved backing layers are shown in Figure 27. Additional important advantages here are: *i*) the replacement of a hand-prepared element by a machine-made product, and *ii*) the reduction in unit cell width achieved by employing much thinner backing layers (25 μm now *vs.* 300 μm before).

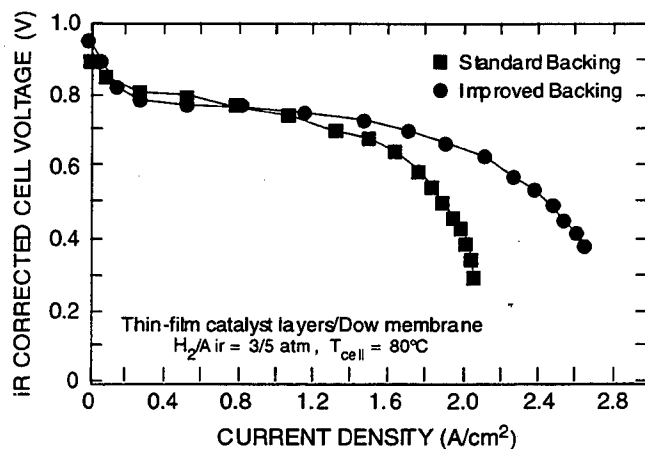


Figure 27. Comparison of cell performance with standard and with new, thin cathode backing layer

PEM Fuel Cell Modeling. A comprehensive analysis of the ac impedance spectra of polymer electrolyte fuel cell cathodes measured under various experimental conditions was completed using a dynamic version of an LANL model. The measurements were carried out using a novel combination of instruments enabling the determination of the impedance spectrum in the presence of large dc currents. Normally, individual impedance spectra recorded at one potential are fitted separately and an evaluation of parameters at each separate potential is made. The fitting code was modified to allow *simultaneous fitting of many spectra at once*. This provides a strong test of the model. Figure 28 shows measured and model-fitted impedance spectra simultaneously fitted for six (air) cathode potentials.

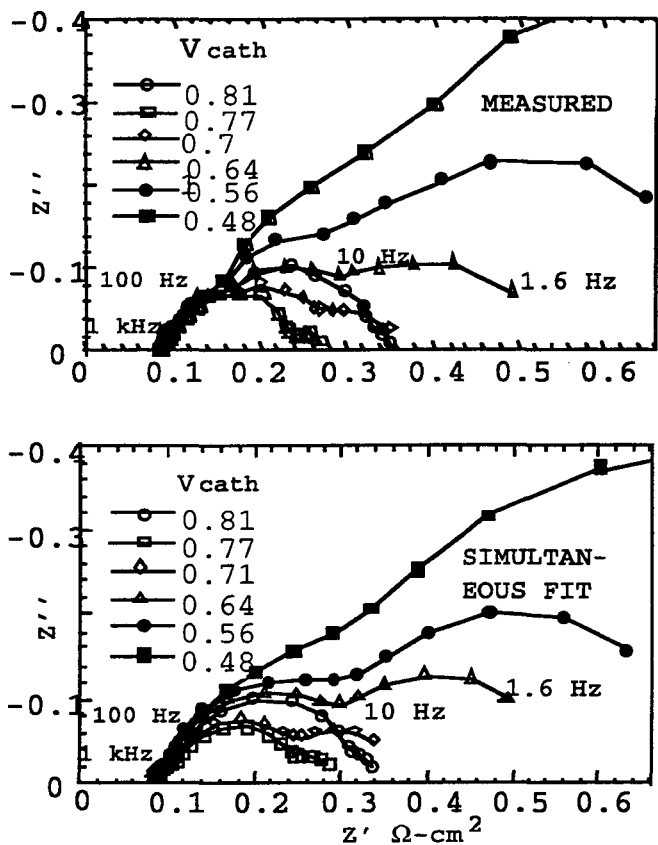


Figure 28. Experimental (top) and simultaneously fitted impedance spectra (bottom) for an air cathode in a PEFC at six cathode potentials. Fit parameters are summarized in Table 6.

The impedance spectrum of the air cathode is seen to contain two features: a higher-frequency loop determined by interfacial charge transfer resistance and catalyst layer properties and a lower-frequency loop determined by gas-phase transport limitations in the backing. The lower-frequency loop is completely absent from the spectrum of cathodes operating on neat oxygen.

The low-frequency loop which reflects limitations in the gas diffusion layer could be interpreted only by consideration of significant tortuosity in the backing. A tortuosity, $t^{1/2}$, of 2.5-3.0 in this layer has been revealed by matching of the dynamic model for the backing layer with the experimental ac impedance data. These tortuosity effects cannot be resolved from cell steady state polarization measurements alone. Also, three different types of losses caused by insufficient cell hydration, to interfacial kinetics, proton conductivity in the catalyst layer and conductivity in the membrane, could be clearly resolved from

effects on the high-frequency loop of such impedance spectra.

Table 6 shows fuel cell air cathode parameters evaluated from the simultaneous fit to the model of six impedance spectra recorded at six potentials.

Table 6. Protonic resistivity and oxygen permeability of the catalyst layer, electrocatalytic activity at 0.9 V, backing tortuosity factor and double layer capacitance for a cathode in an operating PEM fuel cell, as evaluated from a simultaneous fit of impedance spectra measured at six potentials.

RCL	C*D	Ar i*	t	CDL
$\Omega \text{ cm}^2 \times 10^{10}$		$\text{mA/cm}^2\text{-atm}$		mF/cm^2
0.106	12.30	32.80	7.716	13.70

Direct Methanol Fuel Cell. A key part of our effort this year has been devoted to the PEM DMFC. Fabrication of M&Es, *i.e.*, thin-film catalysts bonded directly to the membrane, was used in the DMFCs. Significant performances and high catalyst utilization were obtained in DMFCs with thin-film catalysts and operated at temperatures above 100°C. The ability to operate cells based on ionomeric membranes at such high temperature is significant. We have shown that the temperature of the DMFC can be increased to 130°C in the presence of liquid in direct contact with the anode side of the membrane. To further facilitate this contact, the anode backing layer was eliminated from the DMFC structures. Experiments at higher cell temperatures and with high loadings of unsupported catalysts (typically 4 mg/cm²) in wet-proofed electrode structures were conducted. While the catalyst utilizations in such structures are not particularly high, cell performances are significantly improved. The current density achieved at this high loadings of Pt-Ru anode catalysts and Pt cathode catalysts approaches 300 mA/cm² at 0.5 V for oxygen cathodes (60 psi) and 150 mA/cm² at 0.5 V for air cathodes (60 psi).

Another important issue in DMFCs is methanol cross-over, which was investigated by experiments with membrane treatments that lowered the flux of methanol. In some cases, improved cell performance was obtained. A technique for estimation of cathode losses caused by methanol cross-over was established. This method is based on operation of the cell in the H₂ + methanol/oxygen mode. Under these conditions, the loss in cell voltage following introduction of a given concentration of methanol at the anode is

exclusively caused by losses related to cross-over at the cathode. Figure 29 shows that, for a cathode of low Pt loading (0.4 mg/cm^2), the cathode loss caused by methanol cross-over could easily reach 100 mV.

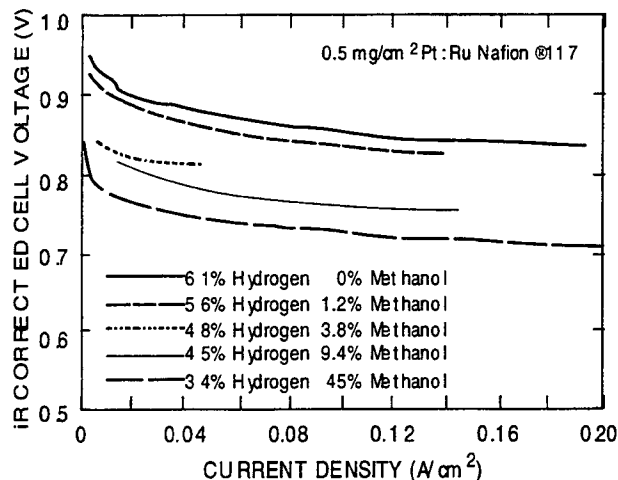


Figure 29. Direct measurements of DMFC cathode losses caused by methanol cross-over, using a cell operated on hydrogen + methanol anode and an oxygen cathode.

The uptake and transport rates of methanol and water in the ionomeric membranes and the conductivity of the membrane equilibrated with methanol + water mixtures have been measured in detail to provide a data base for DMFC modeling and for further development of membranes for DMFCs. Results of NMR measurements for membranes equilibrated with different mixtures of methanol and water showed that methanol does not selectively partition into an immersed membrane. However, even the apparent "internal aqueous solution of methanol", of concentration similar to that of the external bath, is a very significant problem in terms of resulting cross-over rates. Figure 30 shows diffusion coefficients, measured by NMR techniques, for water and methanol in aqueous solutions and in Nafion membranes. It can be seen that the diffusion coefficient of methanol in such membranes is only a factor of 2-3 smaller than in aqueous solutions. This is obviously an important factor contributing to the sizable cross-over rates observed. Finally, the effect of methanol taken up by the membrane on the conductivity of the membrane was found to be negligible, as indeed verified by high-frequency resistance measurements in operating DMFCs.

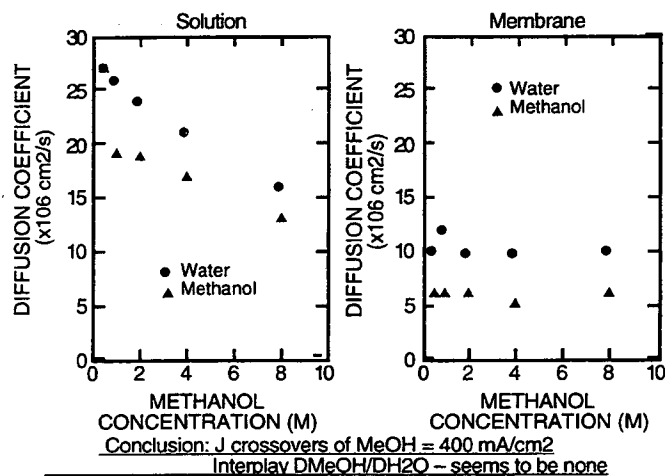


Figure 30. Results of NMR measurements of self-diffusion coefficients for methanol and water in aqueous solutions of methanol and in membranes equilibrated with such solutions.

PUBLICATIONS

- Wilson, M.S., J.A. Valerio and S. Gottesfeld, "Endurance Testing of Low Pt Loading Polymer Electrolyte Fuel Cell," Paper No. 607, 185th Meeting of the Electrochemical Society, San Francisco, CA, May 1994.
- Gottesfeld, S., T.E. Springer and M.S. Wilson, "Modeling and Experimental Diagnostics in Polymer Electrolyte Fuel Cells," Paper No. 620, 185th Meeting of the Electrochemical Society, San Francisco, CA, May 1994.
- Wilson, M.S., J.A. Bett, T.A. Zawodzinski and S. Gottesfeld, "Development of Direct Methanol Fuel Cell at LANL," Paper No. 626, 185th Meeting of the Electrochemical Society, San Francisco, CA, May 1994.
- Landgrebe, A. and S. Gottesfeld, "Proton Exchange Membrane Fuel Cell - Potential Applications in Power Generation, Paper No. 604, 186th Meeting of the Electrochemical Society, Miami, FL, October 1994.
- Zawodzinski, T.A., T.E. Springer, M.S. Wilson and S. Gottesfeld, "Methanol Cross Over in DMFCs: Development of Strategies for Minimization," Paper No. 613, 186th Meeting of the Electrochemical Society, Miami, FL, October 1994.
- Neutzler, J.K., B.D. Wood, M.S. Wilson and S. Gottesfeld, "Development of a Portable Air-Breathing Polymer Electrolyte Fuel Cell Stack," Paper No. 614, 186th Meeting of the Electrochemical Society, Miami, FL, Oct. 1994.

LAWRENCE BERKELEY LABORATORY
UNIVERSITY OF CALIFORNIA
TECHNICAL INFORMATION DEPARTMENT
BERKELEY, CALIFORNIA 94720